Univerzita Karlova v Praze
Přírodovědecká fakulta

Studijní program: Fyzická geografie a geoekologie

RNDr. Jana Bernsteinová

MODELING OF MASS TRANSPORT CAUSAL CONDITIONS

MODELOVÁNÍ PŘÍČINNÝCH PODMÍNEK LÁTKOVÉHO TRANSPORTU

Disertační práce

Vedoucí závěrečné práce/Školitel: Doc. RNDr. Jakub Langhammer, Ph.D.

Praha, 2015

Prohlášení:

Prohlašuji, že jsem závěrečnou práci zpracoval/a samostatně a že jsem uvedl/a všechny použité informační zdroje a literaturu. Tato práce ani její podstatná část nebyla předložena k získání jiného nebo stejného akademického titulu.

V Praze, 30.04.2015

……..……..

Podpis

Modeling of Mass Transport Causal Conditions

ACKNOWLEDGEMENTS

Institutional support was provided by Charles University in Prague (Project 244-260078 1 SVV). Special thanks goes to my supervisor Doc. Jakub Langhammer, Ph.D. for leading this thesis and his co-authorship. The research presented in this thesis was supported by the Czech Science Foundation project GAČR P209/12/0997: "The impact of landscape disturbance on the dynamics of fluvial processes". Part of the study was prepared with the support of research project MSM 0021620831, "Geographical Systems and Risk Processes in the Context of Global Changes and European Integration". Part of the study was conducted within the framework of the project "SedBiLa" and "SedLa", in the framework of the international initiative ELSA (Schadstoffsanierung Elbsedimente), provided by the Hamburg Department for Urban Development and the Environment (Freie und Hansenstadt Hamburg – Behörde für Stadtentwicklung und Umwelt) and agreed upon by the International Commission for the Protection of the Elbe River (ICPER). Other support was obtained from DBU MOE Stipentium Project 2014, "Changing runoff dynamics as a response on extended vegetation changes in the Bavarian Forest and the Šumava National Parks". Special thanks go to Dipl.-Geoökol. Burkhard Beudert, NP Bayerischer Wald for his professional leadership, consulting, and on-going cooperation, and to NP Bayerischer Wald-Sachgebiet III. for all the support. The author thanks DHI a. s. for providing the software support and special thanks go to DHI a.s. staff, namely Ing. Petr Jiřinec, Ing. Pavel Tachecí, Ph.D., Ing. Vitor Hrnčíř, Ing. Jan Špatka Ph.D., and my husband, Ing. Maxim Bernstein for valuable professional and personal support.

ABSTRACT

The evidence of a flood wave passing through a catchment remains visible even for a long time after it occurs. The morphological update in the channel and floodplains, together with the processes related to the mass transport within the aquatic environment, can be regarded as flood event evidence. The advancement in hydroinformatics brought the development of numerical modeling as a tool for the solution of broad hydrological tasks. Thanks to the scenario modeling, flood events with interconnected processes can be explored in detail. This thesis is broadly focused on the mass transport initialization issue both in the polluted and clear Central-European water environments. The aim of the thesis is the evaluation of the principal issues connected with the mass transport initialization based on complex and integrated numerical modeling.

The thesis brings original datasets resulting from several case studies. The aim of the thesis is also to bring a comparative study of methodological approaches evaluating the possibilities and limits regarding the accuracy of inputs vs. outputs and computational time requirements. This thesis also brings several useful comparisons and innovative solutions design.

The mass transport initialization issue is solved in both balance and event-scale processed-based models. The partial outputs are the general water quality improvement measures designed to fulfill the European legislative requirements. The particular site-specific threshold values of the flow parameters necessary for the mass transport initialization are evaluated. Those values vary from 0.12 – 7.8 $N \cdot m^{-2}$ in the case of the middle and the lower river reaches to 16.3 ± 8.2 $N \cdot m^{-2}$ regarding the coarser gravels of the upper river reach.

In order to relate the causal hydrological conditions, the results were relativized by the statistical evaluation of the event return period (Q_N, Q_m). Even though the causal conditions for the mass transport initialization are site-specific, the thesis aims to find regularities and link the different geographical sites regarding the mass transport initialization tendency.

The return period is used as the results' interconnecting parameter rather than a prognostic tool. Nevertheless, regarding hydrological non-stationarity, the influence of the trend behavior of the hydrological system due to the abiotic and biotic factors must be considered. The trend behavior can be representatively studied in the catchments without structural changes or where those changes are well-known. In the case of this thesis, the influence of the climate change and natural disturbances' effects on the hydrological process was studied. Even though the study did not prove any significant influence of the drivers on the high-flow events' magnitude, the increment of flooding frequency is obvious. From this statement, there is a clear underestimation of the remobilization frequency if the results will be used in a prognostic sense.

KEY WORDS:

Modeling · hydrology · mass transport · particle remobilization · pollution · balance · flood event

OUTLINE

1 INTRODUCTION

The evidence of the high-flow event remains within the catchment in the form of qualitative changes of the fluvial morphology. Haddadchi et al. (2013a) states that 70–85 % of sediment transported as a suspended load originates from surface erosion, while coarse sediment originates mostly from bank erosion processes. The majority of the material is transported during high-flow river activity. Sediments are mobilized and accumulated accordingly to the local flow conditions, once they exceed the threshold values, e.g. critical shear stress for erosion τ_c and deposition τ_{cd}. According to Buzek (2000), the Moravian high-flow event observed in 1997, which had a return period of 100 years (further used as RP), transported 51 % of the total suspended material within the recorded period of 23 years. Similar findings result from the studies on the Middle Elbe (Schwartz 2006; Büttner et al. 2006). Lair et al. (2009) prove the findings by long-term evaluation of the sediment balance of the main European rivers, giving an example of 222 t of fine-grained material eroded and transported from the 32 km-long river reach of Danube River in the year 2002, with a flood event with an RP of 100 years. As the opposite aspect of the process and as a consequence, there are many calm water zones along the middle and lower reaches that serve as a reservoir for the particle-mass bound complexes representing various ecological threads. Documentation of such deposits can be found in studies of the Middle Elbe (Büttner et al. 2006; Krüger et al. 2006; Schwartz 2006) and Upper Rhine (Jacoub & Westrich 2006).

The knowledge of the triggering conditions for the mass transport occurrence is crucial for the understanding of hydrological process and adequate consequences. Many engineering studies have been performed in order to measure the initial hydrodynamic conditions for sediment movement (e.g. El Kadi Abderrezzak et al. 2014; Wilcock & Crowe. 2003) or the influence of soil properties on erosion (Bryan 2000) in fully- or semi-artificial channels. Those studies bring knowledge about the reconstruction process under ideal conditions and often steady-state hydrodynamic conditions. Those conditions are hardly experienced in nature, and can lead to process generalization and conceptualization into mostly empirical mass transport formulae. Useful reviews can be found in Yang (1973) discussing the disadvantages of the Shields diagram or Wu et al. (2008), comparing the conventional theories in order to test the predictability of highly-concentrated flow in the Yellow River. Other comparisons of broadly-used theoretical concepts of the total load calculation can be found in Haddadchi et al. (2013b), advantaging the usage of the Engelund-Hansen formula for a broad scale of river reaches. Eder et al. (2014) experiments with a 64 ha catchment, acquiring an original dataset of the flow velocities at the sediment remobilization site. The innovation process in hydroinformatics enabled the

incorporation of the theoretical knowledge base into fully-integrated modeling systems, once they were well-designed and properly verified as suitable for numerous solutions within scenario-based modeling.

Scenario modeling often uses the concept of hydrological stationarity (Matalas 1998). An example of the utilization of the hydrological stationarity concept is the return period assessment. This broadly-used relativization of hydrological conditions is based on the statistical evaluation of the long-termed historical time series. Thus, the information obtained by the last epoch evaluation tends to serve as the prediction tool (Li & Duffy 2011). However, the non-stationary hydrologic behavior is discussed within the topics of long-term observation of runoff changes (Dettinger & Cayan 1995; Hannaford & Marsh 2006; Wilby et al. 1997; Zampieri et al. 2015) and the role of landscape disturbances and climatic trends in the hydrological cycle (Alila et al. 2009; Kuraś et al. 2012; Zeng et al. 2013). It is therefore necessary to understand the nature of the results obtained by scenario modeling within the non-stationary hydrological regime (Van De Wiel et al. 2011) and to use the return period assessment as a tool for actual state results comparison more than a prediction tool.

2 MOTIVATION AND THESIS STRUCTURE

The main aim and motivation for the study was to contribute to the understanding of the causal conditions of the mass transport initialization and to discuss the possible consequences of this process regarding the environmental impact on the aquatic ecosystems and human society. Several partial goals were fulfilled in order to gain the necessary knowledge base. Those partial goals were namely:

(1) to detect and analyze risk processes connected with mass transport in various geographical conditions of the Czech Republic;

(2) to use and critically discuss the available software packages and their combination in order to design highly complex modeling systems with the ability of the mass transport description regarding the causes and consequences. To discuss the possibilities of these systems and limiting factors of the process generalization, conceptualization and schematization;

(3) to process the regional case studies based on the mass transport phenomena and create valuable data for international literature.

In order to fulfill these goals, three case studies were designed and processed. The methodological design was mostly based on the modeling tools. The methods cover the simple conceptual WQ balance model at the catchment scale, 1D models of the flow description up to highly complex models of the sediment transport induced by the 2D or quasi-3D unsteady flow or the 3D model of the entire hydrological cycle. Specific issues were resolved through other methods, such as statistical evaluation of the runoff conditions in the non-stationary hydrological regime.

The presented doctoral thesis is divided into 3 blocks. In the first block (Chapter 3), there is an introduction with the theoretical framework and brief review of the current state of the art. The second block (Chapter 4-6) is focused on the resolution of the issues. Chapter 4 includes a brief description of the design of the case studies. The methods used for the issue solution are introduced with the accentuation of the key factors significantly influencing the success of the study. The synthesis and discussion of the results obtained is presented in Chapters 5 and 6. The aim of the synthetic chapter is to conclude and discuss the contribution of the thesis to the current state of the art in the mass transport modeling research and point some lessons learned. The last block (Chapter 7) includes reprints of the original scientific papers summarizing the main findings of the partial case studies. The papers are joined into three thematic chapters.

3 THEORETICAL FRAMEWORK

The theoretical framework of the mass transport problem is worked out through numerous reviews and case studies. The general mass transport concepts can be found in former sources, e.g. Colby (1963), Rose (1993), Haan et al. (1994). Vanoni (1984) brought a review on the sediment transport equations available in the 1990s. These equations are still the most utilized in the modeling praxis as seen and discussed in the comparison of the results obtained by conventional formulae brought by Wu et al. (2008).

Sediment properties are generally described in Allen (1964). Grabowski et al. (2011) brings a comprehensive review on fine-grained sediment properties and transport assessment methods. Knapen et al. (2007) summarizes the current knowledge base about soil resistance to concentrated flow and points out the remobilization assessment approaches including modeling tools.

The regional-simplified models of sediment transport from the catchment are discussed in (de Vente et al. 2013). Tayfur & Singh (2012) review non-cohesive transport capacity models using the stream power, excess shear stress or slope energy concepts. A comprehensive review of mass transport modeling approaches, tools, and limitations can be found in Merrit et al. (2003), dealing with catchment erosion balance modeling as well as process-based models of catchment sediment load. A similar review can be found in Aksoy & Kavvas (2005), extending the topic of physically-based models and pollutant particle-bends transport. The monograph of van Rijn (1993) summarizes the state of the art of the in-stream sediment transport modeling. Hardy (2013) and Papanicolaou et al. (2008) enhance the review by supplementing modern knowledge of numerical modeling approaches to sediment transport problems. The water quality (WQ) modeling as a tool for non-point pollution sources detection is outlined in Ritter & Shirmohammadi (2001), Aksoy & Kavvas (2005).

Enumerating on other interesting papers on mass transport modeling, Van De Wiel et al. (2011) reviews the available approaches to the paleo-evolution of the fluvial morphology by summarizing numerous case studies on the paleo-reconstruction of the relief and landscape evolution. The most interesting examples of such landscape evolution modeling are the theoretic studies on numerical modeling of river morphology evolution in Quarter, covering tremendous time periods (Bogaart & van Balen 2000) or theoretical concepts of landscape evolution, e.g. Davis cycle (Tucker & Hancock 2010), even though those models express a high degree of simplification.

3.1 MASS TRANSPORT FROM THE CATCHMENT

For almost one century, the engineering society has been strongly interezsted in the mass transport problem. The key driver of the research on mass transport topics is the environmental impact as a consequence of the transport process. With the development of eco-hydrology and implementation of ecological goals within European legislatives, the interest in the mass transport topic has been strengthened. The thesis is aimed to study the *in-situ* process of updating channel morphology and the process of remobilization of dissolved matters (chiefly pollutants) or particle-pollutant complexes transport. Those mass transport issues were regarded as the most significant threads expected in the fluvial environment of Central Europe.

For simplification purposes, the process of mass transport as understood in the thesis (Tab 1) can be divided into three parts, even though it is continuous: Initialization (erosion, remobilization), Transport (load), and Sedimentation (accumulation). The thesis is mostly aimed on the problems of the mass transport initialization.

Table 1: General classification of the mass transport from the catchment based on the thesis scope. Note that parts of the process examined in the study are bold highlighted.

Mass transport from the catchment			
Transported media	**Dissolved matters**	**Particle-matter bound complex**	**Solids**
Mode of transport	**Solute transport**	**Suspended load**	**Bed load**
Phase	**Initialization**	Transport	Sedimentation

Sediment is eroded, transported, and accumulated within the river network according to the flow, bed, and individual grain characteristics (e.g. Hjulström 1935; Shields 1936; Wilcock 2004). During a high-flood event, the majority of sediment transported within the channel can originate from in-stream erosion within the actual channel (Merritt et al. 2003). Meanwhile, the total load is within the natural environment mostly unknown, and sediment transport initialization is still visible within the landscape in the form of altered morphology as a consequence of a flood event. The conceptualization of the morphological alteration caused by runoff influenced by long- and short-termed variations of the causal factors is given by Fig 1, adopted from Armaş et al. (2013).

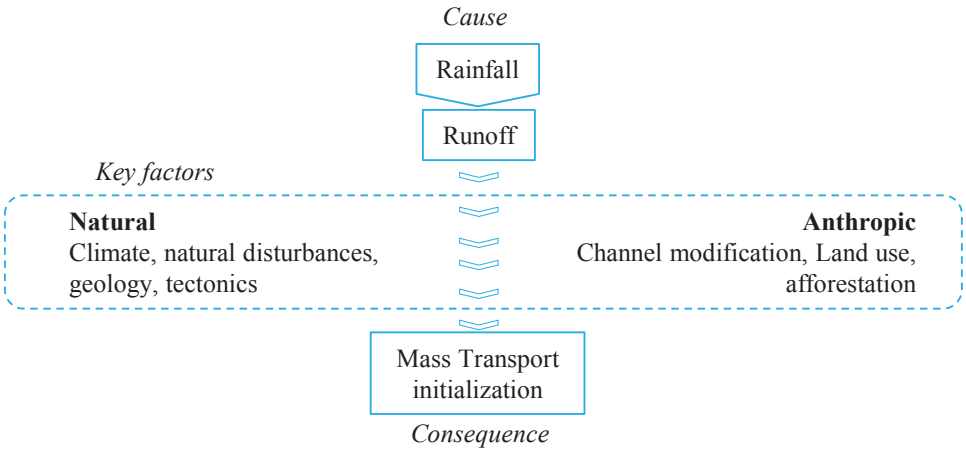

Figure 1: Conceptualization of the mass transport initialization as a response to the flow conditions and the effect of the alteration of key causal factors. Modified according Armaş et al. (2013).

Kondolf et al. (2002) have studied the influence of the key factors of alteration due to landscape disturbances – both natural (deforestation due to conflagration), and anthropogenic (mining, construction) – on mass transport from the catchment. As a response on those disturbances, the channel instability occurred and resulted in severe morphological processes, chiefly the channel extension by 50 % in numerous reaches and the mass transport increment. According to Recking et al. (2012), who have studied the step-pool morphology in Alpine streams, large floods with a return period Q_{50} trigger the remobilization of the whole step-pool pattern, but the channel morphology is progressively reworked by much smaller floods. An example of the channel morphology alteration downstream from anthropogenic disturbances can be found in Heitmuller (2014).

Many studies have been focused on the qualitative and quantitative mass transport theoretical concepts, and with the rapid development in the hydroinformatic field, the numerical models are also improved by using this knowledge. The problem of mass transport within the river network is not solved completely even on the basic level (Silva, 2014, personal communication), and all the approaches are far from the physics being based on empirical observations. The transport formulae incorporated within the models were designed in the 1930s (Shields 1936; Meyer-Peter & Müller 1948) to 1980s (Engelund & Hansen 1967; Vanoni 1984). Numerous studies discuss the crucial differences of the results obtained by various concepts (e.g. Horritt & Bates 2002).

There is an increasing need to model scenarios of mass transport from the catchment, as well as on large topographical scales, to measure the influence of different measures together with climate change (White et al. 1992). The evaluation of non-point pollution sources is very difficult and unclear in comparison with point sources (Ritter & Shirmohammadi 2001). The group of non-point sources aggregates the pollution emitted from diverse, spatially-distributed sources with unclear localizations and quantifications (Leon et al. 2000). Several studies were focused on the quantification of non-point mass transport sources in the Czech Republic (e.g. Langhammer 2005; Nesměrák 2009; Rosendorf & Prchalová 1998). The separation and function of individual sources still remains an open question for the numerical modeling praxis. Numerical modeling tools enable the solution of the non-point mass transport by the generalization of the problem at the basic topographical scale. These models bring results that are highly dependent on the spatial and temporal density of input data. The general presumption of the appropriate model design is the selection of the basic topographical unit (spatial scale). This unit should be sufficiently homogenous from the physical and socio-economical point of view in order to describe the key process representatively. According to Kouwen et al. (1993), the main factor for topographical unit definition is land use, because the boundary condition at various land use types differ most dramatically. The mass transport from the topographical unit is very variable and differs moreover by micro-climate conditions, morphology, soil properties and lithology.

Which model is appropriate? Which theoretical concepts should it include? What kind of schematization should be used? What is the level of uncertainty and complexity of the problem? Such questions still remain unclear and represent a scope of interest in this thesis.

3.2 MODELING IN HYDROLOGY

Current hydrological and hydrodynamic modeling (Tab 2) covers the entire perspective of small hydrological cycle processes. Causes of the hydrological event are described in the form of precipitation-driven runoff dynamics (R-R models). Water drained within the river system is described by the hydrodynamic models. Consequences of hydrological events are described by morphological, water quality (WQ), and ecological models.

Table 2: Various conventional classifications of hydrological models, based on the purposes of the thesis. Note that types of models used for the study task solution are bolded.

Hydrological models				
Interest	**R-R**	**Hydrodynamics**	**Morphology**	**WQ**
Conceptualization	Neuron nets	**Empirical**	**Conceptual**	**Physical**
Time scale	**Long termed balance**	**Short termed event**		
Variables description	Stochastic	**Deterministic**		
Differentials	**0D**	**1D**	**2D**	**3D**
Spatial distribution	**Lumped**	**Semi-distributed**	**Distributed**	

Theoretical concepts and practical tools of the numerical modeling are developed and used in the operative and prognostic hydrology from the 1960s. Numerical modeling is based on the solution of partial (physically-based models) or ordinary (empirical models) differential equations (Aksoy & Kavvas 2005) in various dimensions within a numerical scheme. It was the development of computational technologies that has always been the main limiting factor of the evolution of numerical modeling tools. Nevertheless, being the limiting factor, the relatively low computational speed encouraged researchers to focus on the optimization of numerical schemes and process simplification. Thanks to this fact, a broad selection of various modeling tools of different data and CPU requirements exist, even though of different levels of accuracy. Nowadays, numerical models usually simulate much more extended tasks within substantially smaller computational time.

3.2.1 MODELING THE FLOW CONDITIONS

One of the general water resources management issues is to evaluate flow dynamics within a river reach and the surrounding floodplain. For decades, hydraulic engineers have improved the knowledge base of physical laws governing fluid mechanics; chiefly the Navier-Stokes (N-S) equations. Those equations are derived from Euler's equations, designed for the ideal fluid according the Newton's second law by incorporating the viscosity term, and it represents the headstone of hydraulic modeling tools. The description of the physical process by complex partial differential equations requires a solution with a certain level of discretization of the space and time continuum (Tab 3). Due to the computational ambitiousness, the tremendous difficulties in describing the turbulence within unsteady conditions, and the issue of numerical instabilities, the physical description requires simplification. Nevertheless, according to Lane (1998), despite the simplification of the unpredictable turbulence term, Reynolds-averaged N-S eq. are not yet solvable without empirical or semi-empirical concepts: Saint-Venant eq. (so-called "shallow water"), Businesque eq., or even more simplified forms are often used for steady-state simulations. The general assumptions are primarily the incompressible and homogeneous fluid and relatively small longitudinal variations of the channel-bottom geometry (According to DHI 2014), the bottom slope should not exceed 1%). The partial differential equations for the unsteady flow, shallow-water equations, mostly used in the hydroinformatics, can be separated into the expression of the conservation of mass (eq. 1) described below in the one-dimensional form, the "Continuity Equation" and momentum (eq. 2), the "Momentum Equation":

$$\frac{\partial Q}{\partial x} - B\frac{\partial h}{\partial t} - q = 0 \tag{1}$$

$$\frac{\partial Q}{\partial t} + \frac{\partial\left(\alpha\frac{Q^2}{A}\right)}{\partial x} + gA\frac{\partial h}{\partial x} + \frac{gQ|Q|}{C^2AR} \tag{2}$$

Where Q is discharge, x is the one-dimensional axial direction, B is the cross-sectional width, h is the water surface elevation, t is time, q is the lateral inflow, α is the momentum distribution coefficient, A is flow area, g is the acceleration due to gravity, R is the hydraulic radius, and C is the Chezy roughness coefficient.

Table 3: Conventional classifications of hydraulic models purposely chosen and simplified to fit the thesis scope. Note that types of models used for the study task resolution are bolded

Hydrodynamic models				
Horizontal plan schematization	**1D**	**2D**	**3D**	
Navier-Stokes eq.	**Routing** ***None***	**Kinematic Wave** ***Suppressed***	Diffusive Wave *Suppressed*	**Fully Dynamic** ***Solved***

A differential relationship expressing physical laws requires a solution with a certain level of discretization of the space-time continuum. It was the progress in informatics technologies that enabled the development of numerical solution methods such as finite differences (FDM), finite elements (FEM), or finite volumes (FVM) method. The former simplified techniques of flow characteristic calculations based on the Chezy-Manning formulae can currently be replaced by more sophisticated iterative solutions of the N-S law and the simplified forms of Saint-Venant equations. In fact, there are two ways to solve the Saint-Venant equation:

1) by approximation: only the mass conservation is solved and the momentum conservation problem is dramatically simplified (e.g. Muskingum, Kinematic Wave, Diffusion Wave)

2) complex numerical methods tend to solve the whole scheme of the Saint-Venant equations (e.g. above mentioned FDM, FEM, or FVM).

The general differences within hydro-dynamical models lie in the descriptions of the flow environment. The solution of a 1D model is based on the mean cross-sectional average flow parameter calculation in the axial direction. With an increasing number of dimensions comes the description along the cross section in the transverse (2D) and vertical (3D) directions. This improvement of the channel schematization is crucial, especially while modeling complex fluvial environments where the transversal direction is important (e.g. for sediment transport modeling).

With the increase of computational speed and possibilities of multi-core CPU or even GPU allocation (MIKE 21 FM), the trend is to create complex descriptions of the natural environment by using a fine computational network or "mesh". The goal is to improve techniques in research in remote sensing technologies that can provide detailed terrain resolution up to 1 cm or even less. There is also an increasing need to solve the fully-dynamic equations instead of the conceptualization within highly generalized models (hydrological routing methods, Businesque equations, steady-state approach) and use the unsteady flow description of the full N-S laws with the simultaneous integration of the morphological update or mass transport resolution (Hervouet, 2014, personal communication). Nevertheless, some kind of generalization can be very useful,

especially in dealing with the lack of data for setting up and parameterizing the complex modeling system. The example is given by the work of Hrissanthou (2005), who brought a comparison study of several empirical, conceptual, or stochastic approaches to model the mass transport balance without any sediment data. Another example is given by the large-scale hydrodynamic model proposed by (Paiva et al. 2011), including only globally-available datasets. It is better to implement a generalization than to mislead the problem resolution by detailed, but incorrect, process descriptions caused by wrong or insufficient data utilization. Thus, for most tasks, the fine schematization does not necessarily improve the results when the scope of the problem is of a much larger scale.

The discussion about the discrepancy between the possibilities for modeling data acquiring, pre- and post-processing, and the required results resolution leads to the decision of which schematization approach is suitable, and finally to an adequate modeling software selection.

3.2.2 MODELING THE MASS TRANSPORT

A broad scale of modeling tools (classified in Tab 4) with different levels of simplification is available for expert selection across the engineering and scientific praxis. The selection process plays an important, key role for the success of the final solution. Empirical models (AGNPS, USLE and its modifications, RUSLE and MUSLE) usually oversimplify the process (Aksoy & Kavvas 2005). Conceptual models (LASCAM) use the non-physical process conceptualization as extension of a simple empirical relationship. Physically-based models (MIKE ST, KINEROS, WESP, SHESED, EUROSEM) use the transport equations based on the concept of mass conservation law. There are also numerous purposely-built models (e.g. Basile et al. 2010) that are successful in the local issue solution, but the transfer of the parameters and discretization routine must be critically evaluated before application elsewhere.

Table 4: Conventional classifications of mass transport models purposely chosen and simplified to fit the thesis scope. Note that types of models used for the study task solution are bolded.

Mass transport models			
ST concept	**Stream power**	**Vertical concentration profile**	
Grain properties	**Cohesive** ***Clay, Silt***	**Non-cohesive** ***Sand, gravel***	
Mode of ST	**Bed load**	**Suspended load**	**Solute load**
Solution transport	**First order Decay** ***Conceptualized***	**Advection-Dispersion** ***Conservative***	WQ process included *Non-conservative*

Fluvial morphology and its variability in real sites can be studied by several approaches: fieldwork (e.g. Eder et al. 2014; Yu et al. 2009), physical experimental models – flumes (e.g. Abderrezzak et.al 2013; Ghoshal et al. 2013; Silva et al. 2014), or numerical modeling based on the theoretical or conceptual description of real-case processes (e.g. Fang et al. 2008; Gourgue et al. 2013; Huybrechts et al. 2011; Jacoub & Westrich 2006; Kombiadou & Krestenitis 2012; Li et al. 2008).

Honored examples of the theoretical approaches can be found in the works of e.g. Le Hir et al. (2011, 2014), Li & Duffy (2011), Vested et al. (2013, 2014), and Tassi (2007), who are recently focused on the numerical simulation of non-real case studies based on the fully experimental horizontal plan purpose design.

The majority of the real case studies uses a 1D hydrodynamic description within the integrated HD-ST modeling system (e.g. Armaş et al. 2013; Fang et al. 2008; Kiat et al. 2008) due to the simplicity of the construction and the fact that inaccuracies of flow description are caused by the lack of topographical data rather than by a less-precise model. Such statements are supported by several comparative modeling studies (Cook & Merwade 2009; Horritt & Bates 2002). However, the more demanding 2D models give substantially more accurate results (Li et al. 2008; Li & Duffy 2011; Liu et al. 2002; Simpson & Castelltort 2006). The most accurate 3D models (Jun et al. 2012; Meselhe et al. 2012) are not often presented in the literature due to the tremendous data requirements.

Once the hydrodynamic model is selected, set up, and calibrated to be able to give an accurate flow description, it can be used as a basis for in-stream sediment transport calculation. Broadly-used equations are primarily dependent on the evaluation of flow dynamics acting together with the sediment characteristics. The flow dynamics can be generalized within the parameter of bed shear stress τ, or more precisely, "excess shear stress τ_e" that exceeds the friction forces and the endurance of the river bed material (e.g. Wilcock 2004). The value of τ is calculated in the modeling software MIKE 21 by DHI (2014) according (eq 3)

$$\tau = \rho g h I_R \qquad \text{Where} \qquad I_R = \frac{v^2}{M^2 h^{\frac{4}{3}}} \qquad (3)$$

Where ρ is the water density, h is water column depth, I_R is the dimensionless slope, v is the velocity and M is the Manning's friction coefficient. Often, the bed shear stress is replaced by a dimensionless Shield parameter (first mentioned in Shields (1936)), incorporating both the flow and sediment properties.

In non-uniform channels, the bed load is heavily influenced by turbulence events. According to Solari (2001), τ_e can be regarded as a suitable measure of turbulence activity or so called entrainment activity of the stream and was incorporated to numerous classical (Basile et al. 2010; Naik et al. 2009) or experimental (Le Hir et al. 2011) studies. The suitability of τ_e is critically discussed in (Buffington & Montgomery 1997; Schmelter et al. 2011). According to Solari (2001), on a sufficiently sloping bed, the motion of the particle is significantly influenced by the vertical component of gravity, thus, the particle needs less momentum then the stream to be remobilized and the value of τ_e is exaggerated.

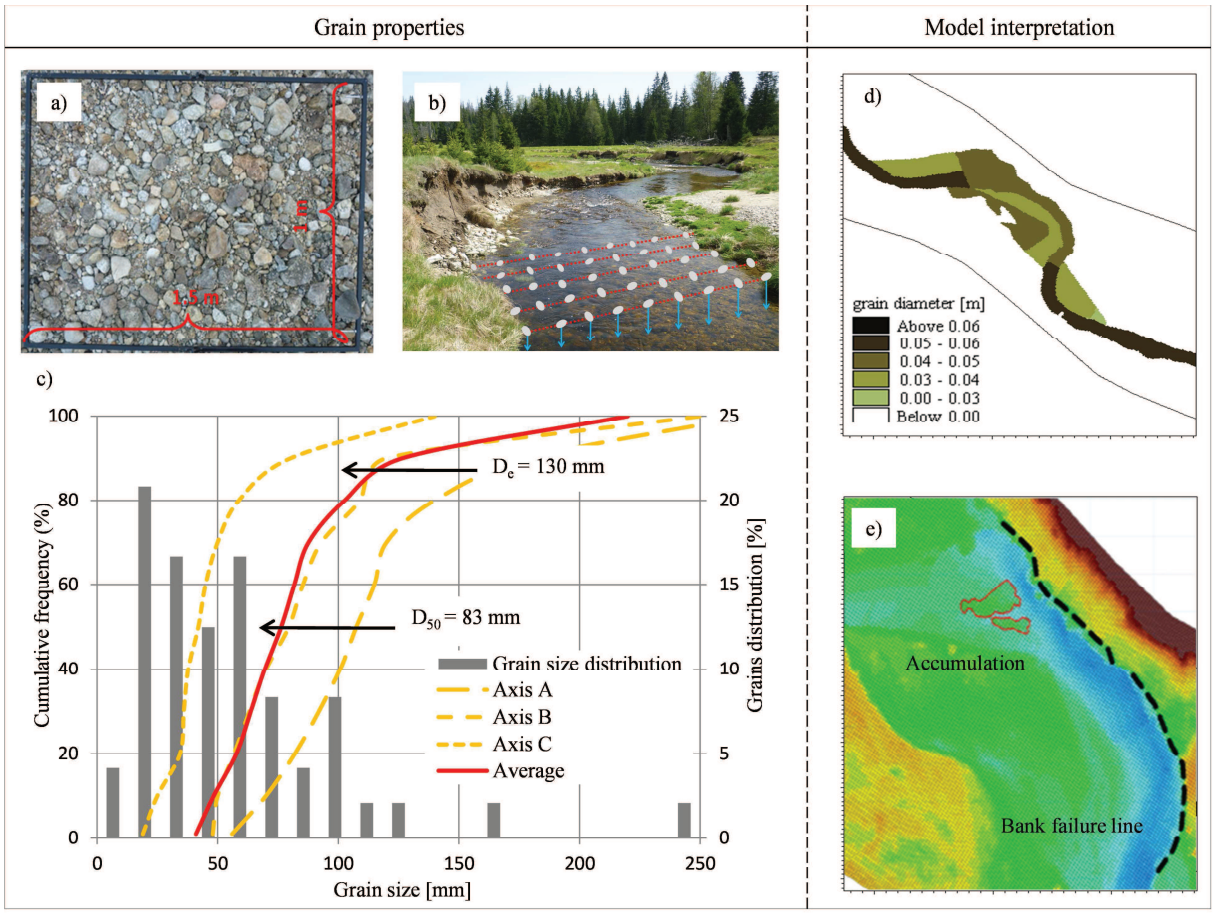

Figure 2: Sediment and morphological characteristics and definition within the modeling interface. On the left are the physical characteristics: a) grain sampling by an optical granulometry method, based on raster clustering, b) manual sampling of submerged sediment, c) elaborated granulometric curve of bed sediment with typical grain characteristic values. On the right, the model interpretation: d) spatial distribution of point samples, e) definition of erodible sites.

The most important sediment characteristics for the model description are grain size (median – D_{50}, effective grain – D_e), density, and porosity of the bed material (Fig 2). Sediments with unimodal distribution (as Fig 2) behave uniformly as the D_{50} fraction. It is caused by the hiding of smaller grains, and exposing of the larger fractions (Wilcock 1993), thus, the D_{50} grain parameter can be successfully used. The grain size plays a key role in the understanding of the transport dynamics and sediment distribution within a catchment. It influences the erodibility, mean of transport, and settling velocity (e.g. Stone & Walling 1997; Walling et al. 2000). The form of sediment transport has to be considered as well. The process can be simplified into a bed load (τ_e cannot exceed the settling velocity and the particle is dragged on the bed; traditionally mentioned in Peter & Müller (1948)) and suspended load (result of advection, diffusion, and settling mechanisms – see e.g. Galapatti (1983)). The sediment transport problem is often

regarded in the form of sediment transport capacity, defined as the state of equilibrium established at the channel bottom (Vanoni 1984). Numerous scientific approaches to the sediment transport problem can be distinguished by the complexity and the versatility of use (Table 5).

Table 5: Selected modeling approaches and brief description of the complexity, versatility, and typical usage

Theory	Key parameters and concepts	Complexity	Versatility	Typical application
Meyer-Peter Müller (1948)	· Semi-empirical formula · Critical Shield stress (θ_c) compared with the skin Shield stress (θ') · Sediment volumetric discharge per unit width [-]	Low (Only Bed Load)	Low (Only selected problems)	Fine sorted gravels, dominated bed load and slopes of 0.4 - 20‰
Smart & Jaeggi (1983)	· Modification of Meyer-Peter Müller · Implementation of grain distribution term · Adjustment of the Shield parameter as a function of slope	Medium (Only Bed Load, even in steep reaches)	Medium (Upper reaches)	Gravels with less sorting, bed load dominated reaches, steep slopes
Engelund-Hansen (1967)	· Critical shear stress not used · Shield stress (θ) · Friction factor (M)	Medium (Total load can be divided by factors into Bed and suspended load)	Medium (Lower reaches)	Sand (all ranges)
Engelund & Fredsøe (1976)	· Probability of moving sediment grain · Friction velocity (u'f) related to θ' based on the logarithmic vertical velocity profile · Empirical expression of reference concentration near the bed · Lateral bed slope	High (Bed and suspended load separate)	High	Straight alluvial channels
Van Rijn (1993)	· Non-dimensional particle diameter (D^*) · Critical shear stress is varying with D^* · Critical friction velocity (u_c)	High (Bed and suspended load separate)	High	Lower courses, estuaries, and marine environments
Wilcock & Crowe (2003)	· Critical shear stress for each grain size · Hiding function (small grains trapped behind large grains)	Low (Bed load of multiple grain sizes)	High	Sand and gravel sediments (wide range of sizes)

3.2.3 MODELING THE QUALITATIVE ASPECT OF MASS TRANSPORT

Two of the problems related to mass transport in the water ecosystem were selected as the key problems of the Central European rivers:

(1) The extensive nutrient load from non-point source pollution.
(2) The secondary pollution caused by the remobilization of the riparian sediment accumulations, polluted by toxic matters.

(1) Nutrients representing the threat of eutrophication in the aquatic environment usually reach the water course through direct discharge, accompanied by an erosion-driven wash load (Ritter & Shirmohammmdi 2001; Lair et al. 2009). The work of Kroiss et al. (2006) focused on the basin of the Western Black Sea shows that the rate of eutrophication in central Europe acts as a direct response from the strategy of using of mineral fertilizer. According to (Hein et al. 2005), it was the surface water connectivity caused by the floodplain inundation that led to the eutrophication caused by the increased nutrient concentration in the water environment. According to Lair et al. (2009) and Nilsson & Malm-Renöfält (2008), there is a strong connection between the hydrological regime and the aquatic ecosystem pollution, thus the changing hydrological patterns have a significant impact on the quality of those ecosystems. Not only hydrological conditions govern the final pollution. Adsorption of the matter to particles and their consequent release in the aquatic ecosystem depends on very broad scales of the local factors, even on the micro-scale of individual particles' geometry (discussed by Fang et al. 2013). This scale was not considered in the study.

(2) Organic pollutants that are released to the aquatic environment can seriously harm the biota downstream from the pollution source (Jurajda et al. 2010; Langhammer 2010). The primary source of toxic pollution is located as a point input directly in the channel bank or riparian zone, or can be deposited atmospherically through precipitation or as a consequence of free or accidental emitting of chemicals during industrial production (Lair et al. 2009). Although the primary pollution of central European rivers has decreased substantially since the 1990s (van der Veen et al. 2006), a thread of secondary pollution still remains high due to the toxic-bound sediment depositions that persist for a long time, accumulated in calm, slack waters or in flood plains (Büttner et al. 2006; Droppo et al. 2009; Grabowski et al. 2011; Pores 2009). Such deposits, after exceeding the threshold of hydrodynamic conditions, can be remobilized in the form of wash load routed downstream. Thus, according to Jacoub & Westrich (2006), secondary pollution from the desorption of pollutants bound on bed particles plays a key role regarding the qualitative aspect of the anthropogenically-modified aquatic environments or those water courses located downstream from any emission source.

In order to be able to design the mitigation measure that is appropriately targeted to the main problem at the catchment scale, there is a need to distinguish between several factors and processes governing at the local scale. The information is enclosed within the final concentration on the monitoring profile and modeling tools can help with the inverse detection of the pollution source by pollution tracking from the known or expected source further downstream. Once the mass degradation and self-purification capability of the river course is considered within the WQ model parameterization, the comprehensive information on the character and amount of pollution can be obtained in the entire river network. While there is some information about the point sources of pollution, even though they are not complete, the non-point sources of pollution are estimated with inverse balance modeling or directly by additive methods based on land use and municipal information processing.

The topic of modeling mass transport causal conditions was worked out through several case studies focused on the variable perspectives of the problem. The aim of the study design was to cover the mass transport initialization topics focused on Central European watersheds. The example modeling tasks thus include the broad complexity of the transport processes faced in both clean and polluted water environments. The study focuses on the interpretation of the deterministic nature of the results obtained and the role of hydrological non-stationarity as well.

4.1 CASE STUDY DESIGN AND SITE SELECTION

Case studies were focused on the 4 river reaches of various scales (micro-mezzo-macro) located within different physical and socio-geographical regions with different consequences of mass transport on the natural and socio-economic environment (Fig 3).

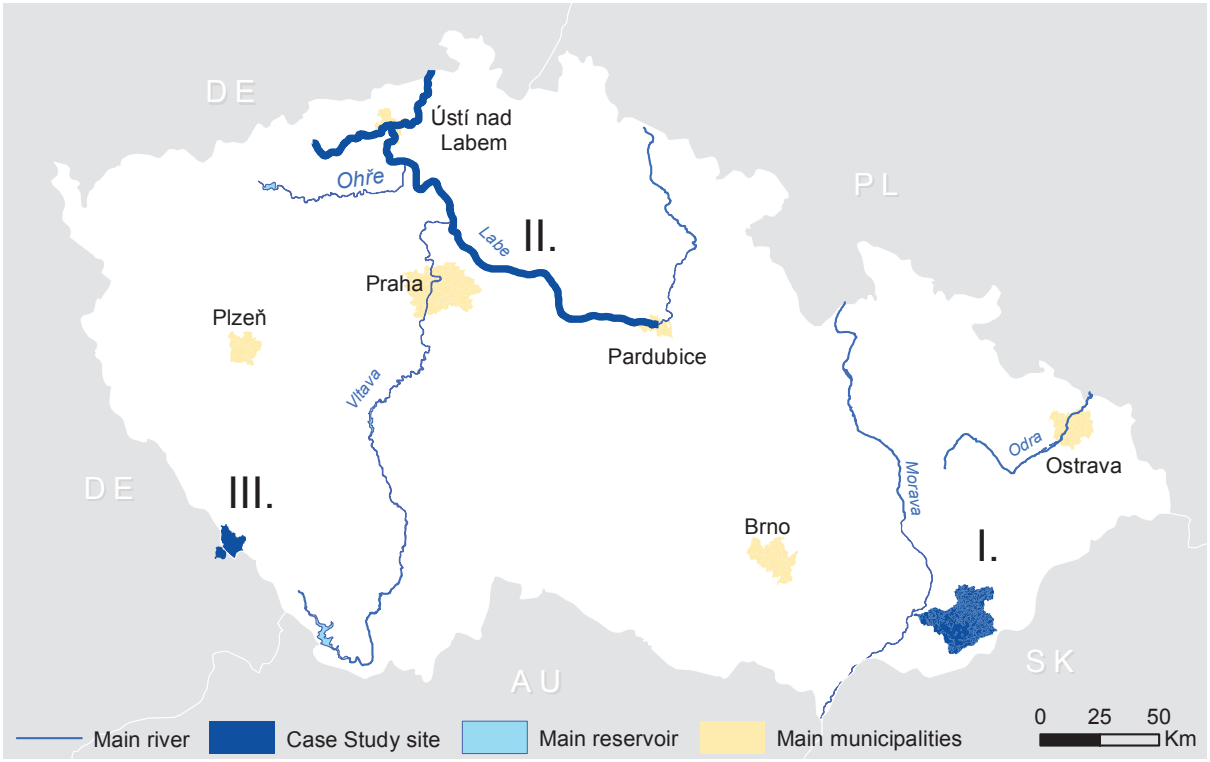

Fig 3: Localization of the case study sites, covering various regions of the Czech Republic.

Case Study I

Non-point pollution mostly derives from arable land wash. The particles, bound with nutrients, are transported downstream the catchment. The catchment of the Olšava River belongs to a typical rural peripheral area of the Czech Republic. The WQ, although improved significantly in last two decades, still expresses high levels of pollution by both point and non-point sources. In order to analyze the causes of extended mass transport, the basin scale model was set up, parameterized, and further used for the scenario modeling under land use variation and waste water treatment intensification. The consequences of such possible changes were discussed regarding the impact on the riparian settlement and overall good ecological status defined by the European legislative, chiefly the Water Framework Directive, WFD (2000/60/EC).

The issue is resolved in Kaiglová, J., Langhammer, J., 2014. Analysis of efficiency of pollution reduction measures in rural basin using MIKE Basin model. Case study: Olšava river basin. Journal of Hydrology and Hydromechanics, 62 (1), pp. 43-54.

Case Study II

The industrial and highly-urbanized areas that are often placed near or within the river floodplain represent a significant source of non-point pollution of a toxic character. The dissolved mass transport in the catchment of the Elbe River from the 1950s – 90s was regarded as one of the most polluted in Europe (van der Veen 2006) and has decreased substantially. Nevertheless, the fine-grained sediments that have accumulated in areas of low flow velocity (Schwartz 2006) show an extreme concentration of heavy metals and specific organic matters. The remobilization of those sediments and consequent release in aquatic environments could represent a significant environmental threat (Förstner et al. 2004; van der Veen 2006). In order to qualify the probability of the remobilization, 4 hydrodynamic models integrated with sediment mass conservation equations were constructed (in Upper Elbe and the most polluted tributary Bílina). The models were parameterized and simulated by using a set of synthetic boundaries. Finally, the results were evaluated by the return period assessment.

The topic is resolved in Kaiglová, J., Langhammer, J., Jiřinec, P., Janský, B., Chalupová, D., 2015. Numerical simulation of heavily polluted fine-grained sediments remobilization using 1D, 1D+ and 2D channel schematization. Environmental Monitoring and Assessment, 187 (3). In press, avaliable online; Kaiglová, J., Langhammer, J., Jiřinec, P., Janský, B., Chalupová, D., Ferenčík, M., 2015. Numerical modelling of the heavily polluted fine-grained sediments remobilization in the northern Czech Republic. Ecohydrology & Hydrobiology. In press, avaliable online.

Case Study III

The results of the previous studies are predetermined by the actual and historical flow conditions within a stationary hydrological system. Currently, there is no doubt on the non-stationarity of the hydrological processes that are caused by a combination of several factors. Among others, climate and land use changes play the key roles. For analysis of those factors, the mountainous, fully natural catchments of the Upper Vydra and Upper Grosse Ohe served as a unique record for understanding the actual influence of climate and vegetation cover change. Javoří Brook, located in the Bohemian Forest plateau, with a moderate slope and fully-natural channel served as a micro-scale case study of the extended morphological changes as the consequences of floods with a one-year return period. The morphological changes, although not representing the direct threat for human environments, remain as a footprint of historical flood events. In order to qualify the probability of mass-transport triggering, the hydrodynamic model was integrated with the bank erosion and non-cohesive sediment transport module and coupled with the detailed hydrological model of the wider locality of National Park Šumava. The causes of morphological changes were explored and further analyzed within the non-stationary hydrological system in order to evaluate the possible impact of the ongoing changes of the hydrological processes that were experienced and expected. The acceleration of mass load could involve the downstream settlement significantly, as well as the increment in the dynamic of flood events. The catchment of Volyňka River represents an intersection with highly-dynamic mountainous processes and dense settlement near the river reach (Vimperk). Bank erosion processes caused the destruction of several holdings and infrastructure, thus the experimental nature of the results obtained in the 3rd case study give a socio-economical aspect and greater importance.

The topic is resolved in Bernsteinová, J., Bässler, C., Zimmermann, L., Langhammer, J., Beudert, B., 2015. Changes in runoff of two neighbored catchments in the Bohemian Forest related to climate and land cover changes. Journal of Hydrology and Hydromechanics. In Review; Langhammer, J., Ye, S., Bernsteinová, J., 2015. Runoff response to climate warming and forest disturbance in a mid-mountain basin, Water. In Review; Kaiglová, J., Langhammer, J., 2014. Numerical modelling of gravel remobilization competence in mountain stream. In: Hudec, M., Csáky, A., 2014. Sciencia Iuvenis, UKF, Nitra, pp. 208-216.

4.2 DESIGN OF COMPLEX MODELING SYSTEM

Motto: *"Everything should be made as simple as possible, but not simpler." (Einstein, A., 1950)*

The most important task is to decide which process to include in the model (Van De Wiel et al. 2011). The modeler has always to hold a reasonable balance within the objectives of the modeling process: (1) requirement of accuracy in the results; (2) level of ambitiousness in the data of the solution and (3) computational time (Fig 4). The lack of data for real process description and parameterization or model calibration and verification is always one of the most limiting factors for complex modeling studies. The data requirements of any model dramatically increases with complexity (Aksoy & Kavvas 2005).

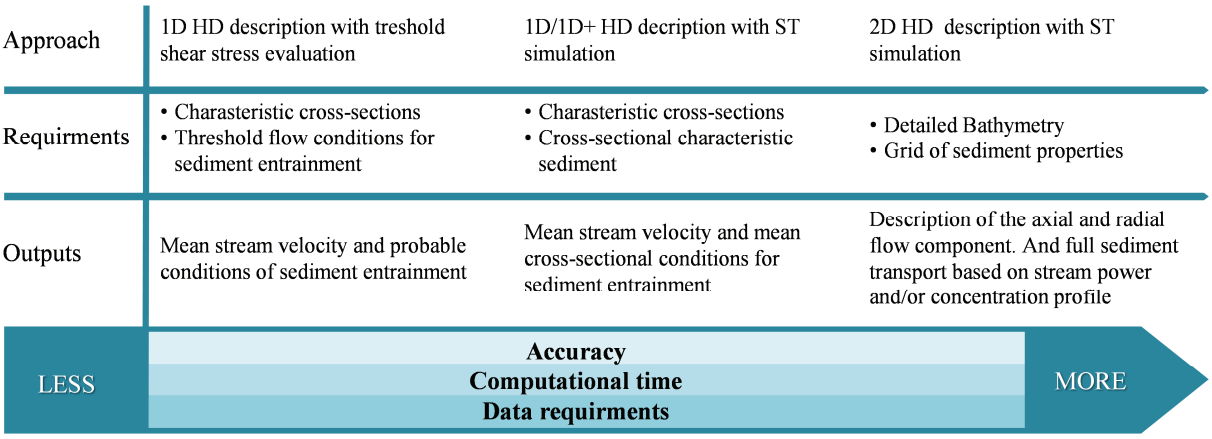

Figure 4: An example of the methodological approach selection process. Further described in Kaiglová et al. (2015). Methods of evaluation of sediment remobilization according the data requirements, computational time, and accuracy of results obtained.

Often, the more suitable model is the less detailed one, especially while dealing with large geographical scales. By including a higher degree of fragmentation, the inaccuracies caused by an insufficient process description at the local scale can cause superposition in errors, resulting in completely misleading final results. The computational time is often another limiting factor, as the 1D simulation of a similar reach extent can be finished 2-3 orders faster.

The thesis is mainly aimed at the resolution of the problem of mass transport initialization. There is a dramatic increment of the input data requirement for the resolution of consequent transport tasks.

The process of mass transport induced by flow activity can be understood as a "*morphological cycle loop"* (According Vested 2014), a fully-dynamic and integrated numerical modeling of morphological processes and mass transport (Fig 5).

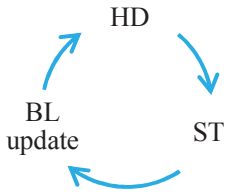

Figure 5: The representation of the morphological cycle loop in the numerical modeling scheme. Adapted according to Vested (2014). Note: HD is hydrodynamic calculation, BL is bed level (Bathymetry), and ST is sediment transport simulation.

Within the morphological cycle loop, the flow characteristic variables resulting from the hydrodynamic model are instantaneously used in every time step as main variables of sediment transport equations. The planform and bathymetry changes resulting from the sediment source and sink evaluation (sediment conservation laws) are used as the inner boundary conditions for the hydrodynamic simulation in the following time step. By extending the concept of the morphological cycle loop, other parts of the hydrological process can be added. This model should describe the entire process from the precipitation occurrence until the morphological change as a consequence of exceeded flow transport capacity.

The flow chart of the modeling scheme used for the purpose of this thesis is presented in Fig 6. In the center of the system, there is a hydrodynamic simulation of the flow parameters for the fully-dynamic, process-based event modeling that can be substituted by simple flow balance modeling in the case of yearly mass transport balance studies. The simulation is based on the results of the hydrologic modeling study (Aksoy & Kavvas 2005) entering the hydrodynamic model in the form of initial and boundary conditions. The hydrologic situation, resulting in stream shear stress, represents the cause of the mass transport initialization in the model. The consequence of the process is simulated in the morphological part of the scheme, within the WQ, sediment transport, and bank erosion model. Thus, the tools configuration dynamically processes the results of the flow modeling (hydrodynamic or flow balance) by introducing the mass transport differential equations at every computational point.

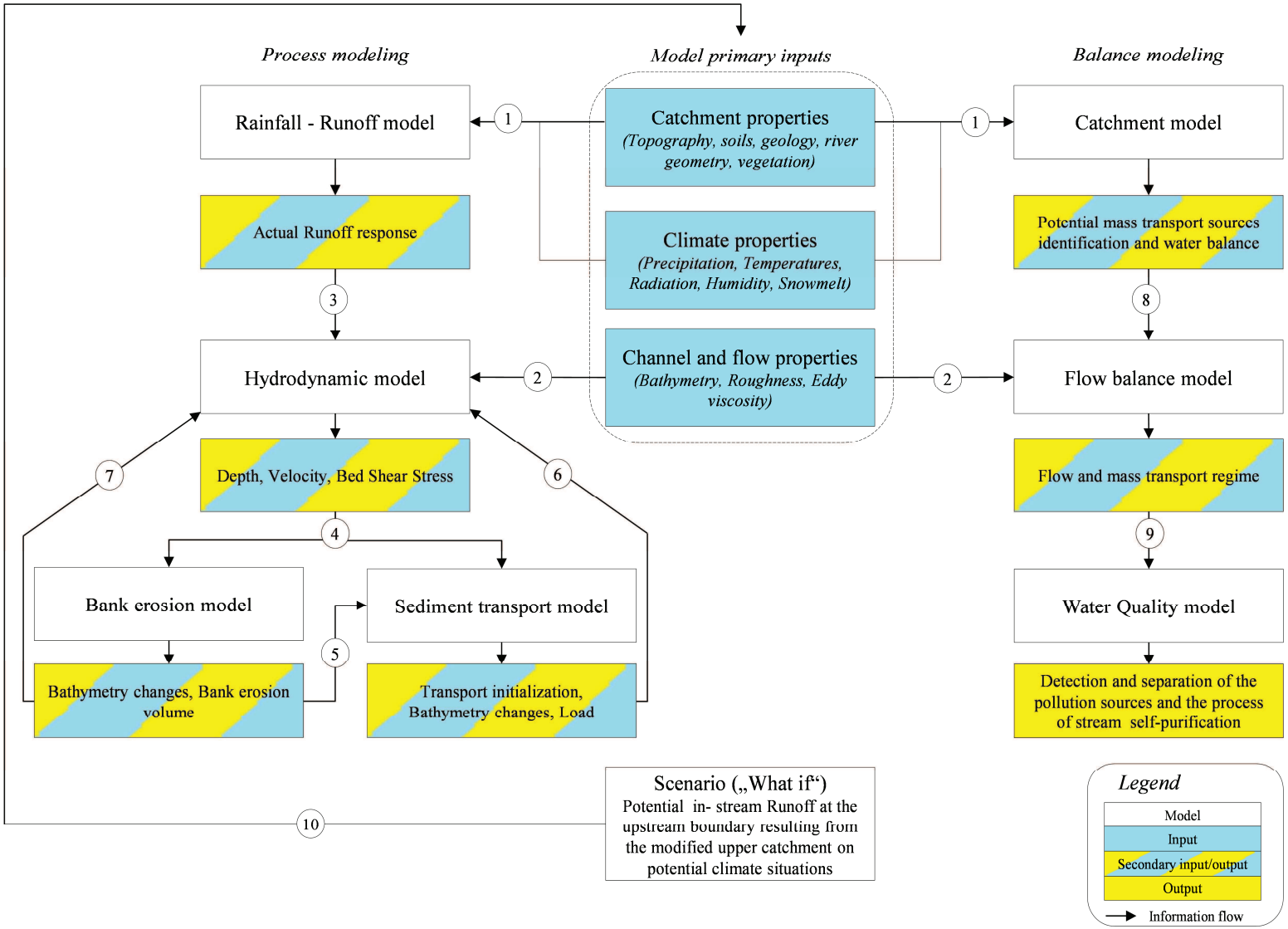

Fig 6: Design of the complex modeling system of mass transport causal conditions. Note that some information flows (numbered 1-10) are explained in the text.

Although several processes are connected only with a one-way flow of information, the importance of simultaneous runs is accentuated in the modeling of morphological consequences, since there is a feedback loop (morphological cycle loop). The bed level change directly influences the bathymetry that is the main domain of the hydrodynamic model (e.g. Kiat et al. 2008; Simpson & Castelltort 2006; Yang et al. 2004).

Detailed description of individual information flows displayed in the Figure 6 (1-10):

(1) Primary model input data are derived from field observations or monitoring. Constant catchment properties are transferred within the model building blocks. Meanwhile, time variable properties enter the model as boundary conditions in the form of a time series.

(2) Other primary model input data are the hydraulic variables entering the hydrodynamic or flow balance model in the form of model parameters according to the schematization. Those properties can vary with the flow magnitude (Jiřinec, P., 2014; personal communication).

(3) Runoff response resulting from the hydrological simulation in the form of a time series enters the hydrodynamic model at the upstream boundary condition.

(4) Flow parameters resulting from the hydrodynamic simulation enter to the bank erosion and sediment transport model as parameters of the sediment conservation equations.

(5) The volume of bank material released by bank failure as calculated within the bank erosion model enters the sediment transport model as a non-consolidated sediment source.

(6), (7) Bed level change resulting from the morphological changes calculated by the bank erosion and sediment transport model in each time step is transferred to the hydrodynamic model in the form of updated bathymetry – the main building block of the model.

(8) Potential sources of pollution and their volume, estimated by the catchment balance model, are integrated with the flow balance model.

(9) Substances are routed according the average flow parameters estimated by the flow balance model and decayed by first-order degradation, specified within the water quality model. The individual river reaches provide information about characteristic concentrations, flow regime, total mass transport, point vs non-point sources, and structure of individual groups.

(10) After verification of the model results, the scenario can be proposed as variation of the primary model inputs after running the entire modeling scheme and the results can be compared with the model of the current state to obtain the efficiency estimate.

4.3 PROCESS SCHEMATIZATION AND DISCRETIZATION

After the design of the study and processing, the most important task is defining the individual parts of the hydrological and morphological cycle description within the language and logic of the modeling system. The main difficulties are connected with the translation of the natural process: chiefly, the time and spatial discretization of an unlimited environment. Even the most complex and detailed model requires a significant simplification or generalization within the key factors, processes, and breaking points of the topographical area. Various descriptions of the physical environment can lead to different results. Nevertheless, the inaccuracies can be mitigated by cross-checking the results obtained by more schematization routines, even though such process is time-consuming. An example of the analysis of such results is given in Fig 7. The calibration and verification process should eliminate these inaccuracies, but the data on event-driven mass transport is scarce or does not exist.

Once the process is well-described in a functional and verified model, the scenario modeling can be processed as the main aim of the study. The scenario design is based on the replacing of current datasets with a proposed variant or expected state. Both the model input boundary conditions data and the model structure building blocks, such as topography, can be replaced in order to estimate the effect of variations.

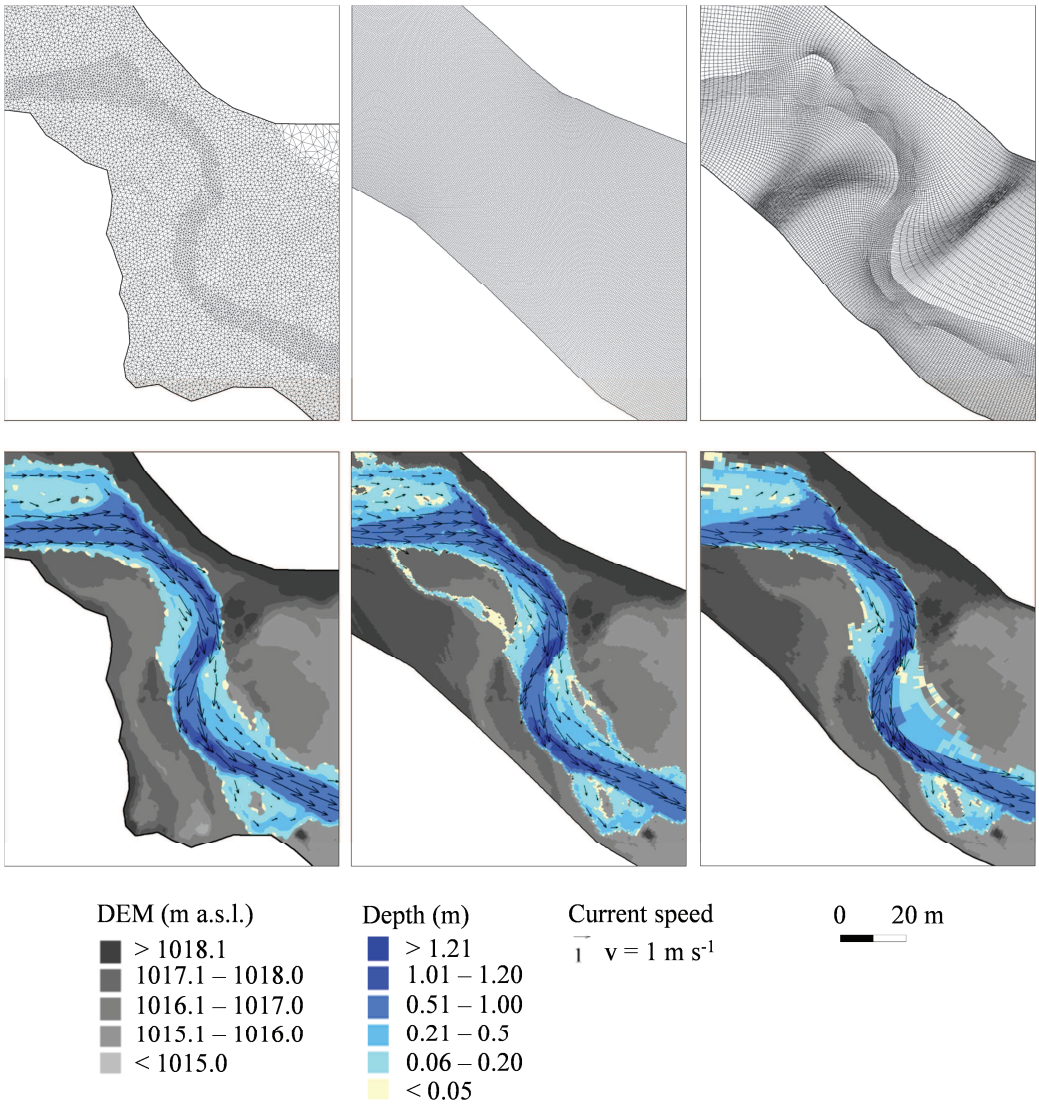

Figure 7: Results of the simulation based on different 2D horizontal plan schematizations. On the right and in the middle, there are curvilinear grids, with high and low levels of grid curvature, respectively. On the left, there is the flexible mesh based on the channel and floodplain triangulation. The significant source of inaccuracies is the spatial distribution of the point information. The individual results are placed below each grid. Note that only a limited number of the current speed vectors is displayed.

4.4 HYDROLOGY AS THE MOST IMPORTANT BOUNDARY CONDITION

If the implications of the consequences of the hydrological events (e.g. the morphological changes of channel bed and banks, destruction of artificial structures, changes in chemical properties of water) are to be studied, the driving forces and factors that affect changes in rainfall-runoff process in different temporal and spatial scales must be defined. This is essential for understanding the dynamics of fluvial processes and for identifying the thresholds for the initialization of the processes. Furthermore, an important point of view is the probability of the occurrence of such changes. From engineering studies, the movement of sediment with a specific grain size within the artificial channel is known to start when the bed shear stress exceeds a critical point. But can this information be transferred to a real case study? Once the proper hydrodynamic parameters and flow conditions of triggering runoff events are found, how should the importance of such consequences be evaluated? The probability of these occurrences (return period) of such flood consequences can be a key factor necessary for answering such questions. Knowing such probabilities, channels under different physical-geographical conditions are able to be compared.

Discussing the invalidity of the concept of hydrological stationarity (Matalas 1998), the aim was to quantify and qualify the impact of climate change-induced hydrological variations on the mass transport problem. The natural catchment of the Upper Vydra was tested together with Grosse Ohe (Schönberg gauge) and the Upper nested catchment (Taferlruck gauge) in order to detect any changes regarding the runoff conditions visible from long-term observations. The main question was, “How do the distributions of runoff conditions change during the year and what implication do these changes have on the frequency and magnitude of high-flow events?” The non-parametric Mann - Kendall test (Hirsch et al. 1982) was applied to all meteorological and hydrological data sets to detect monotonic trends. SEN’s nonparametric method (Gilbert 1987) was used to calculate the slope of linear trends.

4.5 UNCERTAINTIES

Motto: *"All models are in fact wrong, but some can be useful." (Box 1976)*

According to Van De Wiel et al. (2011) uncertainty is a degree to which we are unable to calculate the error of the model. The issue is discussed mostly regarding hydrological models (Beven 1989; Beven 2000; Montanari 2007). Accuracy in this sense means the capability of the model to simulate the real process. The level of accuracy of models used in hydrology is highly dependent on the sufficiency of the physical environment description, or in other words, the real process schematization. From the general point of view, we commit significant inaccuracies during the discretization and generalization process, even if the input data scale is very high. The inaccuracies are mostly based on the insufficient physical description of the real process caused by spatial and temporal discretization and conceptualization (Beven 1989). However, main uncertainties are caused by natural stochasticity (Schmelter et al. 2011) and therefore also have a probabilistic nature (Montanari 2007). It is not possible to include all parts of the environment, especially focusing on micro scales in any kind of model. Nevertheless, a "correct model" should include a description of all the key drivers and crucial parts of the physical process.

According to Schmelter et al. (2011, 2012), an important source of uncertainty in the deterministic sediment transport model is derived from the parameter $\tau_{c,}$ because the value cannot be measured directly, but must be estimated. He proposes to replace the pure deterministic approach by Bayesian probabilistic parameter estimation, while Buffington & Montgomery (1997) propose that it is more appropriate to replace the single value of τ_c by its frequency distribution. Other significant sources of uncertainties come from the upscaling of regional results and from the utilization of the suggested parameterization setup found in literature (León, 2000).

Uncertainties come from numerical simulation instabilities as well. Any inaccuracy in the model can cause a perturbation that, even if they are small, can propagate in the form of unsteady pulses throughout the whole model (Vested 2014).

It is difficult to calculate the uncertainty of the dynamic mass transport model because of the computational time. The necessary time for the Monte Carlo approach requiring many runs would be enormous (Van De Wiel et al. 2011). Therefore, the list of possible uncertainties was processed (Tab 6) and the means of inaccuracies mitigation were implemented.

Table 6: Main sources of uncertainties and the measures implemented. Note: τ_c is critical shear stress, ω_s is settling velocity, and SWE means snow water equivalent.

Model	Process	Source of uncertainty	Measure
WQ Balance	Non-point pollution	Non-point sources are calculated in addition to known point sources	Calibration on various years' datasets
WQ Balance	Degradation	First-order degradation is determined by a yearly constant empirical decay coefficient	Calibration on various years' datasets.
2D HD	Flow distribution	Turbulence model underestimates the losses in higher Froude numbers	Verification by comparing the resulting water levels with observed datasets of various flood events
1D HD	Velocity distribution	Distributed velocity is calculated based on the conveyance distribution according the conveyance-depth relation along the cross section	Verification by comparing 1D HD results with results obtained by detailed 2D model in the same experimental site
ST	Particle remobilization	Determining of τ_c, ω_s, erosion power, and erosion coefficient	Sensitivity analysis, verification on various events
SHE model	Runoff response	Insufficient description of soil, geological, and vegetation properties	Detailed calibration on SWE, groundwater depth, and discharge, sensitivity analysis, comparison with different models

5 SYNTHESIS AND DISCUSSION

The issue of the qualitative/quantitative consequences of mass transport from the catchment has been a scope of interest of many researchers and decision-makers.

The qualitative aspect of the mass transport problem can be regarded from two general perspectives: (1) Wash load caused by non-point source pollution and remobilized by high-flow activity, as regarded in the work of Lair et al (2009), or the approach described by (2) Nilsson & Malm-Renöfält (2008), stressing the problems caused by less dilution and self-purification during low-flow acitivity. The catchment-scale water-mass transport model is capable of solving both of the aspects by including the whole year's hydrological regime, and therefore was selected for the Case Study I processing. The importance of the linking of flow conditions with the WQ model is presented in Nilsson & Malm-Renöfält (2008). The WQ balance model as the result of mass transport processes governing the catchment was tested in the rural basin of the Olšava River. Several scenarios for WQ improvement were designed according the EU legislative requirements and tested by comparison with the model of the current state. The model tested the efficiency of these measures considering water pollution from both point and non-point pollution sources and the combination of the two. This region of the Olšava River Basin is typical for the heterogeneous mixture of pollution sources, variable topography and land use, limited data on pollution sources, and a relatively sparse network of regularly-available WQ-monitoring data. The scenarios of the pollution reduction measures were based on the implementation of wastewater treatment at small, untreated municipal sources, application of tertiary treatment at large, communal point sources, and grassing of arable land that was at high risk of soil erosion.

The secondary output from the WQ model is the quantification of non-point sources in the form of annual total yields and the seasonal regime. The Case Study I thus represents a *balance* model of non-point pollution. Nevertheless, the studies of Aksoy & Kavvas (2005), Buzek (2000), and Schwarz (2006) state that non-point pollution originates from the catchment drainage during the occasional *high-flow events*. According to Förstner et al. (2004), not only current stream sediments, but also particles that could potentially enter the sediment cycle should be included in the mass transport evaluation. Alatorre et al. (2012) has successfully used numerical modeling to study the sources of sediment in the catchment under various land use scenarios. Thus, the mass transport during high-flow events was considered as the main focus of Case Study II.

The primary aim of Case Study II was to identify threshold values for potential remobilization of polluted riparian sediment in different environments associated with a similar problem.

According to Lair et al. (2009), floodplain pollution represents a severe impact on the integrity of freshwater ecosystems. It is due to the unpredictability of the form of non-point pollution, timing, and magnitude. Water managers have to consider all the threats regarding mass transport by being aware of all the key sources of mass in the catchment. It can be direct pollution leaked in the river network by high-flow activity or indirect ("secondary") pollution, caused by desorption of pollutants stored in the particle-pollutant complexes in old fluvial deposits. Such deposits tend to be remobilized mostly by main recipient high-flow activity, and thus, the problem requires a hydrodynamic solution approach. The problem of mass transport derived from the industrial, highly-anthropogenically-modified river courses and riparian zones in the Elbe Basin is an example (Case Study II).

Similar goals, as Case Study II presents, can be partially found in the EU-funded project AquaTerra "Integrated modelling of the river-sediment-soil-groundwater system" (Lair et al. 2009) focused on the Western Black sea basin; in the work of Jacoub & Westrich (2006) on fine-grained sediment transport modeling in the Upper Rhine floodplains; or in the study of Büttner et al. (2006) focused on the modeling of the tendencies of the deposition of polluted sediments in the Middle Elbe floodplain. However, being the first numerical modeling study on the fine-grained sediment remobilization issue in the Czech Republic, having such a spatial extent, and due to the scarce or non-existing similar solutions in foreign literature, there was an additional partial aim of the methodological approach design and verification. The main prerequisites were the limited data availability and the need of an appropriate method design for the objective evaluation and comparison of the remote sites with different hydrological and hydrodynamic flow conditions. The remobilization of fine-grained sediments was estimated by using various types of horizontal flow discretization (1D, 1D CS-distributed, 1D+ and 2D) based on shallow water equations using depth-averaged modeling approaches. The applicability of each method tested is discussed in the table 7.

After comparing the results obtained from each run, the simple excess shear stress (1D CS distributed) evaluation was regarded to be sufficient in the case of the nearly-prismatic long and narrow channel of Bílina, thus, the computational time for the entire reach assessment could be reduced by several magnitudes. A similar approach of the evaluation of the shear stress maps was used in (Aggett & Wilson 2009), even though the scope of the study was different, dealing with channel avulsion risk evaluation. The 1D+ method was used in the study of Lindenschmidt et al. (2008), where the 1D-model oversimplification of the flow through the polder structure was unacceptable. The experience gained from the Bílina River experimental site B8-B9 allows a comparison between the computational time of different horizontal plan schematizations. The 1D model simulates 4 days real-time in 1.5 minutes, while the 2D simulation needs 480 minutes. In

the case of the Elbe riparian zones, there was the obvious need of the more complex hydrodynamic description that was well-provided by the 2D curvilinear hydrodynamic model, even though the computational speed in the large mesh was one-to-one with the real time of the simulation. Cook & Merwade (2009) discuss the effect of channel schematization on flood-extent prediction advantaging detailed 1D (dense cross sections) or 2D models, though they have the largest limitation from computational and user time. Horritt & Bates (2002) advantage simple 1D models, even on meandering sites. The schematization selection is strongly dependent on the purpose of the case study and the input data extent.

The main contribution of Case Study II is the resulting data of the tendencies of fine-grained sediment and its remobilization at 31 polluted sites. The dataset resulting from the numerical modeling studies gains international importance in representing the first classification of the secondary pollution threats caused by old ecological burdens of the Northern Czech Republic. According to the evaluation, the remobilization of fine-grained sediments occurs as expected when site is connected with the transient flow. The RP of the causal hydrological conditions ranged from <1 year at less stable sites up to >100 years at sites where remobilization occurred after a high dividing structure experienced overflow. The statistical evaluation points out areas of special interest, most of which are situated up to 35 km upstream from the German border. Causal discharges are reached during 150 days within an average year. Flow parameters at remobilization were observed within the range 0.12–0.89 $m \cdot s^{-1}$ in the case of depth-averaged velocities and within 0.12–7.8 $N \cdot m^{-2}$ in the case of bed shear stresses. As seen in the qualitative survey of sediment deposits, numerous toxic pollutants were found to occur in alarming concentrations at all sites. The results' environmental aspects were therefore discussed with a view to the threat of downstream aquatic ecosystems' possible secondary pollution.

Table 7: Methods tested for fine-grained sediment remobilization assessment (Case Study II.) with channel topography described by cross-sections. The comparison is based on the data requirements, problems faced, and the applicability for the evaluation of the entirety of Case Study II. Note that "Excess bed shear stress" is referring to the method of analyzing the shear stress maps (based on the conveyance distribution, described in detail in Kaiglová et al. 2015).

	2D MT	1D AD	1D+ AD	1D ST	Excess bed shear stress
Method description	Two-dimensional HD model with Mud-Transport module	One-dimensional HD model with Advection-Dispersion module	One-dimensional HD model where the channel is divided into 2-3 sections described as individual branches linked by length-less channels	One-dimensional HD model with Sediment-Transport module	Calculation of shear stress distribution based on 1D HD results distribution in the axial and radial dimension
Channel description	DTM of river channel, interpolated from cross sections	Characteristic cross-sections	Characteristic cross-sections divided into functional zones	Characteristic cross-sections	Characteristic cross-sections
ST description	Advection - Dispersion equation	Advection - Dispersion equation	Advection - Dispersion equation	Engelund-Hansen equation	Excess bed shear stress (over a defined threshold e.g. τ_c)
ST Data requirements	• Exact definition of sediment layer extent • Density of the sediment • Grain diameter • Critical shear stress for erosion • Critical shear stress for deposition • Settling velocity of the suspended particles • Parameters of erosion as part of A-D equation: - Erosion coefficient and power • Dispersion of the suspended sediments in *x* and *y* direction • Inflow of suspended sediments from the upstream reach			• Exact definition of sediment layer extend • Grain diameter • Density of the sediment • Critical shear stress for erosion	• Grain diameter • Critical shear stress for erosion • Definition of sediment layer extend
Problems	• No sufficient data available • Very long computational time of the dynamic calculation • The accuracy of the bathymetry is highly dependent on the distance from the cross-section	Fine-grained sediment is not the characteristic material of the channel, the mean cross-sectional velocity is not an adequate flow description	• The more difficult the schematization, the more problems with stability criteria • The purpose-built schematization tends to be difficult to calibrate. Even after calibration, there is a risk of deviation from reality. • Can be applied only in some reaches where channel is divided into a part with current and a dry part, during normal conditions.	Fine-grained sediment is not the characteristic material of the channel, the mean cross sectional velocity is not an adequate flow description	• Results difficult to verify • The definition of the sediment layer can lead to misinterpretation • The accuracy of the maps is highly dependent on the distance from measured cross-section • The conversion of 1D point results into a spatial distribution is only theoretical and can lead to misinterpretation
Applicability	Yes	No	In special localities where channel can be divided into 2-3 parts and fine-grained sediments are characteristic for such parts	No	Yes

Similar method as Case Study II, but focusing only on solid particle (sediment) transport was used in Case Study III. The study was focused on the evaluation of gravel remobilization competence in a fully-natural stream of the Javoří Brook in order to detect causal flow conditions of fluvial changes. The remobilization of bed material consisted of well-sorted gravel that was forced by local depth averaged velocities 1.8±0.1 $m \cdot s^{-1}$, resulting in excess shear stress ($\tau_e = \tau - \tau_c$) varying within 16.3±8.2 $N \cdot m^{-2}$. The RP of the short discharge time series (4 years) from the *in situ* water stage measurement is difficult to estimate. Nevertheless, the flood event recorded in June 2013 was used as the real-case boundary condition that affected the entire catchment at a larger scale (Upper Vydra, Modrava gauge), where the long-term monitoring and RP evaluation is available. Thus, the causal *in situ* discharges were related with official monitoring data and the resulting return period of the remobilization could be estimated as $Q_1 - Q_3$.

The distribution of particles and flow characteristics are necessary in order to describe the entrainment processes over the channel well (Bialik & Czernuszenko 2013). According to Jacoub & Westrich (2006), each granulometric fraction of the sediment sample has to be simulated individually, even though the approach eliminates particle interactions and lead to misinterpretation of the results. The grain size was varied in order to describe the movement of individual fractions separately. The remobilization of the middle and higher grain fractions ($D_{40} - D_{90}$) was evaluated using the arbitrary set remobilization criteria. Lower fractions were not examined due to grain hiding, a highly important and unpredictable effect. The method of site-specific grain entrainment relation to the causal flow conditions was proposed. The method called "*remobilization rating curves*" aggregates individual results into a general reach property. Thus, the method could serve for the sediment transport competence assessment in various reaches.

By comparing the channel morphology before and after the flood events, the magnitude of the eroded material can be established (e.g. Eaton & Lapointe 2001; Pizzuto et al. 2010). However, flood events are largely unpredictable; thus, the data about channel morphology before a flood event is often missing. Remote sensing technologies can solve this absence of a detailed topography description, as the data resulting from a remote survey can cover much larger regions than geodetic surveys. Case Study III benefits from the presence of highly spatially distributed datasets on channel morphology surveyed by UAV Photogrammetry (Miřejovický 2012-2014, unpublished results) pre- and post- flood event. The advantage of highly-distributed topographical data on hydrodynamic modeling was discussed in detail in Aggett & Wilson (2009) and Anders et al. (2009). The important source of uncertainty lies in the lack of precise knowledge about channel boundary variability that plays with the flow conditions' key role in mountainous channel modulation (Brown & Pasternack 2014). Nevertheless, the qualitative

evaluation by comparing the results obtained by numerical model and UAV photogrammetric survey showed a convincing agreement.

Due to the statistical evaluation (RP) of the causal flow conditions, the results from remote sites of different geographical conditions are comparable, bringing the overview of reach stability and the screening of the mass transport initialization issue. The flow conditions represented by flow velocities or excess shear stress are comparable across geographical scales as well. Case Study I brought information about the average transport conditions that are indirectly derived from the in-stream concentrations. Case Studies II and III refer in more detail to the specific flow conditions necessary for mass transport initialization.

Even in disregarding the conclusion statement of Papalexiou et al. (2013) that the frequency of extremes values (RP) evaluated using Gamma distribution is underestimated, thus the occasional high-flow events are not as rare as according to the RP evaluation, there is another problem with the predictive ability of RP. All the results of this study (joined by the RP characteristics) are based on the assumption of the hydrological stationary that, according to Matalas (1998), cannot be achieved in hydrology, being that they are the "*manifestation of climate*" (the hydrological boundary conditions). Therefore, the importance or reliability of our results that are based on the probabilistic evaluation of RP obtained in various regions should be discussed by focusing on the question of the hydrological stationarity. The key drivers of the oscillations or trend behavior are different in each of the studied environments. They can be divided into natural causes (climate change) and anthropogenic causes (channel modification, land use change, etc.). It is necessary to focus on the "*natural*" oscillations, present all over Central Europe. Those can be sufficiently described in the numerical models and can be most directly understood by analyzing the long-term runoff time series. According to Lu et al. (2013), who has studied sediment load response to climate change, a 1% change in precipitation can cause a 2% change in the sediment load. Thus, the precipitation records were studied together with temperature and land cover time-series in order to detect any dynamic progress in each component of the runoff response.

Focusing then on the nearly-natural catchment (Case Study III) located in the core of the Bohemian Forest (National Parks Šumava and Bayerischer Wald), the current most-discussed topic is the influence of climate change (regional factor) and forest disturbance (local factor) of the natural environment caused by the wind storm-induced bark beetle outbreaks. Although there are several studies focused on the effects of the bark beetle outbreak on biodiversity (Jonášová & Prach 2004; Müller et al. 2010), WQ (Beudert et al. 2015), or surface reflectance (Hais 2003; Hais et al. 2009), the effect of those drivers on the hydrological regime still remain unclear or uncertain.

The first expectation could be that the highly-notable influence of the bark beetle infestation on the whole hydrological regime of the mountain range would have a strong influence on the fluvial processes observed in the experimental reach of Javoří Brook. Nevertheless, the hydrological analysis of three Bohemian Forest catchments revealed only small changes in annual runoff yields of all studied runoff time series (Upper Vydra, Große Ohe, and Upper Große Ohe). This was in accordance with the insignificant changes in precipitation yields. Analyzing of trend behavior in intra-annual variability and high-flow measures was later done in order to detect any effect on magnitude or frequency of high-flow events consequently affecting the fluvial processes in the experimental reach of Javoří Brook. In the main findings of Case Study III, the low flow measures significantly increased in the late summer/early autumn period, while total runoff yields did not change. This underpins the importance of diminished evapotranspiration losses from severely disturbed stands, which enable more groundwater recharge during summer and likely describes the effect of a bark beetle infestation. The indirect evidence of the forest disturbance effect is the 9% increment of the runoff coefficient observed in the nested catchment of the Upper Große Ohe River corresponding with 30% of the area covered by dead forest. In contrast, the overall warming in February (+1.8°C) and April (+4°C) accelerated snow melt and significantly increased runoff and high flows in March in all catchments, irrespective of size, land cover, or land cover changes, while precipitation yields and intensities did not change. The increasing trend in April temperatures was reported even from a longer time-series evaluation by Bässler (2008), who places the first beginning of the trend existence in the year 1961. The most pronounced trend in air temperature took place in the period from 1980, and according to Bässler, could support the bark beetle infestation. Similar air temperature trend patterns were detected in other Czech headwater catchments as well (Kliment et al. 2011).

The frequency of high flow events is slightly increasing in Case Study III, though the magnitude remains unchanged. That could mean that the return period is overestimated, which could be caused by the hydrological stationarity assumption, and an overall underestimation of the risk processes connected with the mass transport initialization topic. Clever water management, connected with flood-risk mitigation, the magnitude of the remobilization caused by individual flood events should not increase from natural causes. As seen in Case Study I, the magnitude of wash load-induced mass transport could be decreased by implementing strategies required by the EU legislatives. Numerous measures to mitigate secondary pollution of aquatic ecosystems caused by the old ecological burdens must be implemented. The results of Case Study II can serve as a basis for the detection of most problematic sites and prioritizing measure design.

6 CONCLUSIONS

The thesis is focused on the issue of the mass transport initialization. The topic was solved by numerical modeling methods, selected from a broad scale of evaluation tools. The complex modeling system was designed and used at different spatial and temporal scales (Case Studies I, II, III). Several modeling approaches were compared and discussed regarding the data and computational time requirements within the 3 case studies (I-III). Case Studies were designed to deal with different environmental risks caused by the mass transport initialization expected in Central Europe. The *mass balance model* (Case Study I) was set up in the peripheral area of the Czech Republic, represented by Olšava catchment, while mass transport *process based models* simulating the non-stationary high-flow episodes were set up first in the *polluted* Elbe River environment (Case Study II) and in a *natural* environment in the core of the Šumava mountains (Case Study III).

The results of the Case Study I are the differentiation of the WQ pollution sources, the non-point pollution quantification, and the measures for WQ improvement application and evaluation. The results of the Case Study II and III bring information about the site-specific causal flow conditions necessary for the entrainment of solid particles, widely-dispersed shear stresses about 0.12–7.8 $N \cdot m^{-2}$ and 16.3±8.2 $N \cdot m^{-2}$, for fine-grained sediment of Case Study II and coarser particles of Case Study III, respectively. Those particles were heavily polluted in Case Study II, but untainted in Case Study III.

The non-stationarity of the natural (Case Study III) rainfall-runoff process, namely climate change and forest disturbance (bark beetle outbreak or windbreak) was discussed. No significant role of those drivers was proven regarding the magnitude of the high-flow events, but the increment in the frequency of those events can be expected as a consequence.

REFERENCES

Aggett, G.R. & Wilson, J.P., 2009. Creating and coupling a high-resolution DTM with a 1-D hydraulic model in a GIS for scenario-based assessment of avulsion hazard in a gravel-bed river. *Geomorphology*, 113(1-2), pp.21–34.

Aksoy, H. & Kavvas, M.L., 2005. A review of hillslope and watershed scale erosion and sediment transport models. *Catena*, 64(2-3), pp.247–271.

Alatorre, L.C. et al., 2012. Soil erosion and sediment delivery in a mountain catchment under scenarios of land use change using a spatially distributed numerical model. *Hydrology and Earth System Sciences*, 16(5), pp.1321–1334.

Alila, Y. et al., 2009. Forests and floods: A new paradigm sheds light on age-old controversies. *Water Resources Research*, 45.

Allen, J.R.L., 1964. A review of the origin and characteristics of recent alluvial sediments. *Sedimentology*, 5(1 965), pp.89–191.

Anders, N.S., Seijmonsbergen, A.C. & Bouten, W., 2009. Modelling channel incision and alpine hillslope development using laser altimetry data. *Geomorphology*, 113(1-2), pp.35–46.

Armaş, I. et al., 2013. Morpho-dynamic evolution patterns of Subcarpathian Prahova River (Romania). *Catena*, 100, pp.83–99.

Basile, P. a. et al., 2010. Simulation of erosion-deposition processes at basin scale by a physically-based mathematical model. *International Journal of Sediment Research*, 25(2), pp.91–109.

Bässler, C., 2008. Klimawandel – Trend der Lufttemperatur im Inneren Bayerischen Wald (Böhmerwald) Climate change – trend of air temperature in the Innerer. *Silva Gabreta*, 14(1), pp.1–18.

Beudert, B. et al., 2015. Bark Beetles Increase Biodiversity While Maintaining Drinking Water Quality. *Conservation Letters*, p.n/a–n/a.

Beven, K., 1989. Changing ideas in hydrology — The case of physically-based models. *Journal of Hydrology*, 105(1-2), pp.157–172.

Beven, K., 2000. On model uncertainty, risk and decision making. *Hydrological Processes*, 14(14), pp.2605–2606.

Bialik, R.J. & Czernuszenko, W., 2013. On the numerical analysis of bed-load transport of saltating grains. *International Journal of Sediment Research*, 28(3), pp.413–420.

Bogaart, P.W. & van Balen, R.T., 2000. Numerical modeling of the response of alluvial rivers to Quaternary climate change. *Global and Planetary Change*, 27(1-4), pp.147–163.

Box, G.E.P., 1976. Science and Statistics. *Journal of the American Statistical Association*, 71(356), pp.791–799.

Brown, R. a. & Pasternack, G.B., 2014. Hydrologic and topographic variability modulate channel change in mountain rivers. *Journal of Hydrology*, 510, pp.551–564.

Bryan, R.B., 2000. Soil erodibility and processes of water erosion on hillslope. *Geomorphology*, 32(August 1999), pp.385–415.

Buffington, J.M. & Montgomery, D.R., 1997. A systematic analysis of eight decades of incipient motion studies, with special reference to gravel-bedded rivers. *Water Resources Research*, 33(8), pp.1993–2029.

Büttner, O. et al., 2006. Numerical modelling of floodplain hydraulics and suspended sediment transport and deposition at the event scale in the middle river Elbe, Germany. *Acta hydrochimica et hydrobiologica*, 34(3), pp.265–278.

Buzek, L., 2000. Eroze lesní půdy při vyšších vodních srážkách a tání sněhové pokrývky (na příkladu střední části Moravskoslezských Beskyd). *Geografie – Sborník ČGS*, 105(4), pp.317–332.

Colby, B., 1963. *Fluvial sediments: a summary of source, transportation, deposition, and measurement of sediment discharge* Geological., Washington: US government printing office.
Cook, A. & Merwade, V., 2009. Effect of topographic data, geometric configuration and modeling approach on flood inundation mapping. *Journal of Hydrology*, 377(1-2), pp.131–142.
Dettinger, M.D. & Cayan, D.R., 1995. Large-scale atmospheric forcing of recent trends towards early snowmelt runoff in California. *Journal of Climate*, 8, pp.606–623.
DHI, 2014. *MIKE 11, MIKE 21 & MIKE 3 flow model - Scientific documentations*, Horstholm.
Droppo, I.G. et al., 2009. Dynamic existence of waterborne pathogens within river sediment compartments. Implications for water quality regulatory affairs. *Environmental science & technology*, 43(6), pp.1737–43.
Eaton, B.C. & Lapointe, M.F., 2001. Effects of large floods on sediment transport and reach morphology in the cobble-bed Sainte Marguerite River. *Geomorphology*, 40, pp.291–309.
Eder, a. et al., 2014. Re-suspension of bed sediment in a small stream – results from two flushing experiments. *Hydrology and Earth System Sciences*, 18(3), pp.1043–1052.
Engelund, F. & Fredsøe, J., 1976. A Sediment Transport Model for Straight Alluvial Channels. *Nordic Hydrology*, 7(5), pp.293–306.
Engelund, F. & Hansen, E., 1967. *A monograph on sediment transport in alluvial streams*, Copenhagen: Tekniks forlag.
EP, 2000. Water Framework Directive WFD 2000/60/EC.
Fang, H., Chen, M. & Chen, Q., 2008. One-dimensional numerical simulation of non-uniform sediment transport under unsteady flows. *International Journal of Sediment Research*, 23(4), pp.316–328.
Fang, H. wei et al., 2013. Effects of sediment particle morphology on adsorption of phosphorus elements. *International Journal of Sediment Research*, 28(2), pp.246–253.
Förstner, U. et al., 2004. Historical Contaminated Sediments and Soils at the River Basin Scale. *Journal of Soils and Sediments*, 4(4), pp.247–260.
Galapatti, R., 1983. *A depth-integrated model for suspended transport, Report No. 83-7*, Delft.
Ghoshal, K. et al., 2013. Turbulence, suspension and downstream fining over a sand-gravel mixture bed. *International Journal of Sediment Research*, 28(2), pp.194–209.
Gilbert, R.., 1987. *Statistical Methods for Environmental Pollution Monitoring*, New York: John Wiley & Sons.
Gourgue, O. et al., 2013. A depth-averaged two-dimensional sediment transport model for environmental studies in the Scheldt Estuary and tidal river network. *Journal of Marine Systems*, 128, pp.27–39.
Grabowski, R.C., Droppo, I.G. & Wharton, G., 2011. Erodibility of cohesive sediment: The importance of sediment properties. *Earth-Science Reviews*, 105(3-4), pp.101–120.
Haan, C.T., Barfield, B.J. & Hayes, J.C., 1994. *Design Hydrology and Sedimentology for Small Catchments*, San Diego: Academic Press Inc.
Haddadchi, A., Ryder, D.S., et al., 2013. Sediment fingerprinting in fluvial systems: review of tracers, sediment sources and mixing models. *International Journal of Sediment Research*, 28(4), pp.560–578.
Haddadchi, A., Omid, M.H. & Sdehghani, A. a., 2013. Total load transport in gravel bed and sand bed rivers case study: Chelichay watershed. *International Journal of Sediment Research*, 28(1), pp.46–57.
Hais, M. et al., 2009. Comparison of two types of forest disturbance using multitemporal Landsat TM/ETM+ imagery and field vegetation data. *Remote Sensing of Environment*, 113(4), pp.835–845.
Hais, M., 2003. Heis_2003.pdf. *Acta Universitas Carolinae*, 2, pp.97–107.
Hannaford, J. & Marsh, T., 2006. An assessment of trends in UK runoff and low flows using a network of undisturbed catchments. *International Journal of Climatology*, 26, pp.1237–1253.
Hardy, R.J., 2013. Treatise on Geomorphology. In J. Shroder & A. C. W. Baas, eds. *Treatise on Geomorphology*. San Diego, CA,: Academic Press, pp. 147–159.

Hein, T. et al., 2005. The importance of altered hydrologic retention in large regulated rivers: examples from the Austrian Danube. *Archiv für Hiyrobiologie, Large Rivers*, (15), pp.425–442.
Heitmuller, F.T., 2014. Channel adjustments to historical disturbances along the lower Brazos and Sabine Rivers, south-central USA. *Geomorphology*, 204, pp.382–398.
Le Hir, P. et al., 2014. Simulating tidal marshes evolution in estuarine systems under climate change , using a schematic process-based 3D model. In SHF, ed. *Conference Proceedings of SHF Conference : «Small scale morphological evolution of coastal, estuarine and river systems*. Nantes, pp. 6–7.
Le Hir, P., Cayocca, F. & Waeles, B., 2011. Dynamics of sand and mud mixtures: A multiprocess-based modelling strategy. *Continental Shelf Research*, 31.
Hirsch, R.M., Slack, J.R. & Smith, R.A., 1982. Techniques of trend analysis for monthly water quality data. *Water Resources Research*, 18, pp.107–121.
Hjulström, F., 1935. *Studies of the morphological activity of rivers as illustrated by the river Fyris*, Upsala: Bull. Of Geol. Inst.
Horritt, M.S. & Bates, P.D., 2002. Evaluation of 1D and 2D numerical models for predicting river flood inundation. *Journal of Hydrology*, 268(1-4), pp.87–99.
Hrissanthou, V., 2005. Estimate of sediment yield in a basin without sediment data. *Catena*, 64(2-3), pp.333–347.
Huybrechts, N., Zhang, Y.. & Verbanck, M. a., 2011. A new closure methodology for 1D fully coupled models of mobile-bed alluvial hydraulics: application to silt transport in the Lower Yellow River. *International Journal of Sediment Research*, 26(1), pp.36–49.
Jacoub, G. & Westrich, B., 2006. Modelling transport dynamics of contaminated sediments in the headwater of a hydropower plant at the Upper Rhine River. *Acta Hydrochimica et Hydrobiologica*, 34, pp.279–286.
Jonášová, M. & Prach, K., 2004. Central-European mountain spruce (Picea abies (L.) Karst.) forests: regeneration of tree species after a bark beetle outbreak. *Ecological Engineering*, 23(1), pp.15–27.
Jun, Q., Zhifeng, Y. & Zhenyao, S., 2012. Three-dimensional modeling of sediment transport in the Wuhan catchments of the Yangtze River. *Procedia Environmental Sciences*, 13(2011), pp.2437–2444.
Jurajda, P. et al., 2010. Longitudinal patterns in fish and macrozoobenthos assemblages reflect degradation of water quality and physical habitat in the Bílina river basin. , 2010(3), pp.123–136.
El Kadi Abderrezzak, K. et al., 2014. A physical, movable-bed model for non-uniform sediment transport, fluvial erosion and bank failure in rivers. *Journal of Hydro-Environment Research*, 8, pp.95–114.
Kaiglová, J. et al., 2015. Numerical simulations of heavily polluted fine-grained sediment remobilization using 1D, 1D+, and 2D channel schematization. *Environmental Monitoring and Assessment*, 187.
Kiat, C.C. et al., 2008. Sediment transport modeling for Kulim River – A case study. *Journal of Hydro-environment Research*, 2(1), pp.47–59.
Kliment, Z. et al., 2011. Trend analysis of rainfall-runoff regimes in selected headwater areas of the Czech Republic. *Journal of Hydrology and Hydromechanics*, 59(1), pp.36–50.
Knapen, a et al., 2007. Resistance of soils to concentrated flow erosion: A review. *Earth-Science Reviews*, 80(1-2), pp.75–109.
Kombiadou, K. & Krestenitis, Y.N., 2012. Fine sediment transport model for river influenced microtidal shelf seas with application to the Thermaikos Gulf (NW Aegean Sea). *Continental Shelf Research*, 36, pp.41–62.
Kondolf, G.M., Piégay, H. & Landon, N., 2002. Channel response to increased and decreased bedload supply from land use change: Contrasts between two catchments. *Geomorphology*, 45, pp.35–51.
Kouwen, N. et al., 1993. Grouped Response Units for Distributed Hydrologic Modeling. *Journal of Water Resources Planning and Management*, 119, pp.289–305.

Kroiss, H., Zessner, M. & Lampert, C., 2006. daNUbs: Lessons learned for nutrient management in the Danube Basin and its relation to Black Sea euthrophication. *Chemistry and Ecology*, 22(5), pp.347–357.

Krüger, F. et al., 2006. Methods to calculate sedimentation rates of floodplain soils in the middle region of the Elbe River. *Acta Hydrochimica et Hydrobiologica*, 34, pp.175–187.

Kuraś, P.K., Alila, Y. & Weiler, M., 2012. Forest harvesting effects on the magnitude and frequency of peak flows can increase with return period. *Water Resources Research*, 48, p.W01544.

Lair, G.J. et al., 2009. How do long-term development and periodical changes of river-floodplain systems affect the fate of contaminants? Results from European rivers. *Environmental pollution (Barking, Essex : 1987)*, 157(12), pp.3336–46.

Lane, S.N., 1998. Hydraulic modelling in hydrology and geomorphology: a review of high resolution approaches. *Hydrological Processes*, 12(8), pp.1131–1150.

Langhammer, J., 2005. Classification of the dynamics of water quality changes in the Elbe River basin. *Journal of Hydrology and Hydromechanics*, 53(4), pp.205–218.

Langhammer, J., 2010. Water quality changes in the Elbe River basin, Czech Republic, in the context of the post-socialist economic transition. *GeoJournal*, 75, pp.185–198.

Leon, L.F. et al., 2000. Integration of a nonpoint source pollution model with a decision support system. *Environmental Software Systems*, 15(2-3), pp.249–255.

Li, S. & Duffy, C.J., 2011. Fully coupled approach to modeling shallow water flow, sediment transport, and bed evolution in rivers. *Water Resources Research*, 47(3), p.n/a–n/a.

Li, S.S., Millar, R.G. & Islam, S., 2008. Modelling gravel transport and morphology for the Fraser River Gravel Reach, British Columbia. *Geomorphology*, 95(3-4), pp.206–222.

Lindenschmidt, K.-E., Huang, S. & Baborowski, M., 2008. A quasi-2D flood modeling approach to simulate substance transport in polder systems for environment flood risk assessment. *The Science of the total environment*, 397(1-3), pp.86–102.

Liu, W.-C., Hsu, M.-H. & Kuo, A.Y., 2002. Modelling of hydrodynamics and cohesive sediment transport in Tanshui River estuarine system, Taiwan. *Marine pollution bulletin*, 44(10), pp.1076–88.

Lu, X.X. et al., 2013. Sediment loads response to climate change: A preliminary study of eight large Chinese rivers. *International Journal of Sediment Research*, 28(1), pp.1–14.

Matalas, N.C., 1998. Note on the Assumption of Hydrologic Stationarity. *Journal of Contemporary Water Research and Education*, 112(1), pp.64–72.

Merritt, W.S., Letcher, R. a. & Jakeman, A.J., 2003. A review of erosion and sediment transport models. *Environmental Modelling & Software*, 18(8-9), pp.761–799.

Meselhe, E. a. et al., 2012. Numerical modeling of hydrodynamics and sediment transport in lower Mississippi at a proposed delta building diversion. *Journal of Hydrology*, 472-473, pp.340–354.

Meyer-Peter, E. & Müller, R., 1948. Formulas for bed load transport. In *Proc. 2nd Congr. IAHR. Vol. 2, paper 2.* Stockholm: IAHR.

Montanari, A., 2007. What do we mean by " uncertainty "? The need for a consistent wording about uncertainty assessment in hydrology. , 845(October 2006), pp.841–845.

Müller, J. et al., 2010. Learning from a " benign neglect strategy" in a national park: Response of saproxylic beetles to dead wood accumulation. *Biological Conservation*, 143, pp.2559–2569.

Naik, M.G., Rao, E.P. & Eldho, T.I., 2009. A kinematic wave based watershed model for soil erosion and sediment yield. *Catena*, 77(3), pp.256–265.

Nesměrák, I., 2009. *K problematice náhrad hodnot pod mezí stanovitelnosti při chemických analýzách a monitorování stavu vod: vliv náhrady hodnot pod mezí stanovitelnosti polovinou meze stanovitelnosti na statistické charakteristiky souborů hodnot.*, Praha: Výzkumný ústav vodohospodářský T.G. Masaryka.

Nilsson, C. & Malm-Renöfält, B., 2008. Linking flow regime and water quality in rivers: a challenge to adaptive catchment management. *Ecology & Society*, 13.

Paiva, R.C.D., Collischonn, W. & Tucci, C.E.M., 2011. Large scale hydrologic and hydrodynamic modeling using limited data and a GIS based approach. *Journal of Hydrology*, 406(3-4), pp.170–181.

Papalexiou, S.M., Koutsoyiannis, D. & Makropoulos, C., 2013. How extreme is extreme? An assessment of daily rainfall distribution tails. *Hydrology and Earth System Sciences*, 17(2), pp.851–862.
Papanicolaou, A.N. et al., 2008. Sediment Transport Modeling Review—Current and Future Developments. *Journal of Hydraulic Engineering*, 134(January), pp.1–14.
Pizzuto, J., O'Neal, M. & Stotts, S., 2010. On the retreat of forested, cohesive riverbanks. *Geomorphology*, 116(3-4), pp.341–352.
Pores, S., 2009. Meiobenthology. In Berlin: Springer-Verlag.
Recking, A. et al., 2012. A field investigation of the influence of sediment supply on step-pool morphology and stability. *Geomorphology*, 139-140, pp.53–66.
Rijn, L. Van, 1993. *Principles of sediment transport in rivers, estuaries and coastal seas*,
Ritter, W.F. & Shirmohammadi, A., 2001. *Agricultural Nonpoint Source Pollution: Watershed Management and Hydrology*, Fla: Lewis publishers.
Rose, C.W., 1993. Erosion and sedimentation. In *Hydrology and Water Manage- ment in the Humid Tropics: Hydrological Research Issues and Stra- tegies for Water Management*. Cambridge: University press, pp. 301–343.
Rosendorf, P. & Prchalová, H., 1998. *Elimination of nonpoint pollution of surface and subsurface waters. (Omezování plošnéhoznecištení povrchových a podzemních vod v CR: etapová zpráva za rok*, Výzkumný ústav vodohospodářský T.G. Masaryka.
Shields, A., 1936. *Anwendung der Ahnlichkeitsmechanik und der Turbulenzforschung auf die Geschiebebewegung*, Berlin: Mitteilung der preussischen Versuchsanstalt fur Wasserbau und Schiffbau.
Schmelter, M.L., Erwin, S.O. & Wilcock, P.R., 2012. Accounting for uncertainty in cumulative sediment transport using Bayesian statistics. *Geomorphology*, 175-176, pp.1–13.
Schmelter, M.L., Hooten, M.B. & Stevens, D.K., 2011. Bayesian sediment transport model for unisize bed load. *Water Resources Research*, 47(11), p.n/a–n/a.
Schwartz, R., 2006. Geochemical characterization and erosion stability of fine-graineg gryone field sediments of the Middle Elbe River. *Acta hydrochim. Hydrobiol.*, 34, pp.223–233.
Silva, A.R., Falorca, I. & Fael, C., 2014. Stability of sandy slopes under hydrodynamic forces. In *Conference Proceedings of SHF Conference : «Small scale morphological evolution of coastal, estuarine and river systems*. Nantes: SHF, p. 2.
Simpson, G. & Castelltort, S., 2006. Coupled model of surface water flow, sediment transport and morphological evolution. *Computers & Geosciences*, 32(10), pp.1600–1614.
Smart, G.M. & Jaeggi, M.N.R., 1983. *Sediment Transport on Steep Slopes. Mitteilung nr. 64 of the Laboratory for Hydraulics, Hydrology and Glaciology*, Zurich: the Federal Technical University.
Solari, L., 2001. *Topics in fluvial and lagoon morphodynamics*, Firenze: Firenze University Press.
Stone, P.M. & Walling, D.E., 1997. Particle Size Selectivity Considerations in Suspended Sediment Budget Investigations. In Amsterdam, ed. *Proceedings of the 7th International Symposium, Baveno, Italy 22–25 September 1996 - The Interactions Between Sediments and Water*. Baveni: Springer Netherlands, pp. 63–70.
Tassi, P., 2007. *Numerical modelling of river processes: flow and river bed deformation*. Disertation thesis. University of Twente.
Tayfur, G. & Singh, V.P., 2012. Transport capacity models for unsteady and non-equilibrium sediment transport in alluvial channels. *Computers and Electronics in Agriculture*, 86, pp.26–33.
Tucker, G.E. & Hancock, G.R., 2010. Modelling landscape evolution. *Earth Surface Processes and Landforms*, 35(1), pp.28–50.
Vanoni, V.A., 1984. Fifty Years of Sedimentation. *Journal of Hydraulic Engineering*, 110, pp.1021–1057.
Van der Veen, A. et al., 2006. Spatial distribution and bonding forms of heavy metals in sediments along the middle course of the River Elbe (km 287...390). *Acta Hydrochimica et Hydrobiologica*, 34, pp.214–222.

De Vente, J. et al., 2013. Predicting soil erosion and sediment yield at regional scales: Where do we stand? *Earth-Science Reviews*, 127, pp.16–29.
Vested, H.J. et al., 2013. Numerical modelling of morphodynamics—Vilaine Estuary. *Ocean Dynamics*, 63, pp.423–446.
Vested, H.J. et al., 2014. Numerical simulation of estuarine and river morphology. In *Conference Proceedings of SHF Conference : «Small scale morphological evolution of coastal, estuarine and river systems*. Nantes: SHF.
Walling, D.E. et al., 2000. The particle size characteristics of fluvial suspended sediment in the Humber and Tweed catchments, UK. *Science of the Total Environment*, 251-252, pp.205–222.
White, D.A. et al., 1992. A spatial model to aggregate point-source and nonpoint-source water-quality data for large areas. *Computers & Geosciences*, 18, pp.1055–1073.
Van De Wiel, M.J. et al., 2011. Modelling the response of river systems to environmental change: Progress, problems and prospects for palaeo-environmental reconstructions. *Earth-Science Reviews*, 104(1-3), pp.167–185.
Wilby, R.L., O'Hare, G. & Barnsley, N., 1997. The North Atlantic Oscillation and British Isles climate variability, 1865-1996. *Weather*, 52, pp.266–276.
Wilcock, P., 1993. Critical shear stress of natural sediments. *Journal of Hydraulic Engineering*, 119(4), pp.491–505.
Wilcock, P.R., 2004. *Lecture notes – Sediment transport – The sediment problem*, Retrieved from: http://calm.geo.berkeley. edu/geomorph/wilcock/WilcockSTLecture3.pdf.
Wilcock, P.R. & Crowe, J.C., 2003. Surface-based Transport Model for Mixed-Size Sediment. *Journal of Hydraulic Engineering*, 129(2), pp.120–128.
Wu, B., Maren, D. Van & Li, L., 2008. Predictability of sediment transport in the Yellow River using selected transport formulas. *International Journal of Sediment Research*, 23, pp.283–298.
Yang, C.., 1973. Incipient motion and sediment transport. *Journal of the Hydraulics Division1*, 99(10), pp.1679–1704.
Yang, C.T., Huang, J. & Greimann, B.P., 2004. *User's manual fbr GSTAR-ID (Generalized Sediment Transport model for Alluvial Rivers - One Dimension), version 1.0*, Denver: Denver: U.S. Bureau of Reclamation, Technical Service Center.
Yu, G. et al., 2009. Effect of incoming sediment on the transport rate of bed load in mountain streams. *International Journal of Sediment Research*, 24, pp.260–273.
Zampieri, M. et al., 2015. Observed shift towards earlier spring discharge in the main Alpine rivers. *Science of The Total Environment*, 503-504, pp.222–232.
Zeng, S., Xia, J. & Du, H., 2013. Separating the effects of climate change and human activities on runoff over different time scales in the Zhang River basin. *Stochastic Environmental Research and Risk Assessment*, 28(2), pp.401–413.

7 ORIGINAL SCIENTIFIC PAPERS ON THE MODELING OF MASS TRANSPORT CAUSAL CONDITIONS

Scientific papers (Tab 8) based on the original findings are organized in three subchapters. First, the WQ balance model is presented as a simple method of mass transport identification and pollution tracking. The second group of papers develops the concept of mass remobilization during the high-flow events in detailed form. Three papers describe the development of an integrated modeling tool for the morphological cycle analysis based on the remobilization of sediments caused by local flow conditions examined by 1D, 1D+ (pseudo 2D), and 2D-hydrodynamic models. The third group examines the non-stationarity of the hydrological system. The study analyzes the observed long-termed changes of the flow in a nearly-natural catchment in order to provide an overview of the predictive nature of the results obtained.

Table 8: Classified list of scientific papers contained by the thesis

Category	Full reference
Papers printed in the WoS journal	Kaiglová, J., Langhammer, J., 2014. Analysis of efficiency of pollution reduction measures in rural basin using MIKE Basin model. Case study: Olšava river basin. Journal of Hydrology and Hydromechanics, 62 (1), pp. 43-54. Kaiglová, J., Langhammer, J., Jiřinec, P., Janský, B., Chalupová, D., 2015. Numerical simulation of heavily polluted fine-grained sediments remobilization using 1D, 1D+ and 2D channel schematization. Environmental Monitoring and Assessment, 187 (3). In press, avaliable online
Paper under review in the WoS journal	Bernsteinová, J., Bässler, C., Zimmermann, L., Langhammer, J., Beudert, B., 2015. Changes in runoff of two neighbored catchments in the Bohemian Forest related to climate and land cover changes. Journal of Hydrology and Hydromechanics. In Review. Langhammer, J., Ye, S., Bernsteinová, J., 2015. Runoff response to climate warming and forest disturbance in a mid-mountain basin, Water. In Review.
Papers printed in the scientific journal indexed in the Scopus database	Kaiglová, J., Langhammer, J., Jiřinec, P., Janský, B., Chalupová, D., Ferenčík, M., 2015. Numerical modelling of the heavily polluted fine-grained sediments remobilization in the northern Czech Republic. Ecohydrology & Hydrobiology. In press, avaliable online.
Scientific paper in peer-reviewed proceedings	Kaiglová, J., Langhammer, J., 2014. Numerical modelling of gravel remobilization competence in mountain stream. In: Hudec, M., Csáky, A., 2014. Sciencia Iuvenis, UKF, Nitra, pp. 208-216.

7.1 MASS TRANSPORT BALANCE MODEL AT THE CATCHMENT SCALE (CASE STUDY I)

Kaiglová, J., Langhammer, J., 2014. Analysis of efficiency of pollution reduction measures in rural basin using MIKE Basin model. Case study: Olšava river basin. *Journal of Hydrology and Hydromechanics*, 62 (1), pp. 43-54.

J. Hydrol. Hydromech., 62, 2014, 1, 43–54
DOI: 10.2478/johh-2014-0007

Analysis of efficiency of pollution reduction measures in rural basin using MIKE Basin model. Case study: Olšava River Basin

Jana Kaiglová, Jakub Langhammer*

Charles University in Prague, Faculty of Science, Albertov 6, 128 43, Prague, Czech Republic.
* Corresponding author. E-mail: jakub.langhammer@natur.cuni.cz

Abstract: This paper presents the results of testing the applicability of the MIKE Basin model for simulating the efficiency of scenarios for reducing water pollution. The model has been tested on the Olšava River Basin (520 km^2) which is a typical rural region with a heterogeneous mix of pollution sources with variable topography and land use. The study proved that the model can be calibrated successfully using even the limited amount of data typically available in rural basins. The scenarios of pollution reduction were based on implementation and intensification of municipal wastewater treatment and conversion of arable land on fields under the risk of soil erosion to permanent grassland. The application of simulation results of these scenarios with proposed measures proved decreasing concentrations in downstream monitoring stations. Due to the practical applicability of proposed measures, these could lead to fulfilment of the water pollution limits required by the Czech and EU legislation. However, there are factors of uncertainty that are discussed that may delay or limit the effect of adopted measures in small rural basins.

Keywords: Water quality; Modelling; Rural basins; MIKE Basin; Non-point pollution; Land use.

INTRODUCTION

The rural basins represent specific and frequent problems for water management and planning due to the difficulties in identification and calculation of pollution coming from dispersed and non-point sources, a long-term perspective of change, and the frequent lack of systematic monitoring and relevant data. To evaluate information on the changes in water quality and to simulate the effect of potential measures for water pollution reduction, a number of mathematical models are available for use as versatile and easy-to-use tools for research and water management. The standard water quality models applied for the assessment of water quality in streams, e.g. QUAL2E/2K (Brown and Barnwell, 1987; Chapra et al., 2006), MIKE 11 (Havn et al., 1995) and HSPF (EPA, 2000), are usually based on a one-dimensional (1-D) conceptualization of stream hydraulics and steady-state runoff (Borah and Bera, 2003; Højberg et al., 2007; Wang et al., 2006).

The rapid development of GIS technology and the availability of detailed spatial data allowed the construction of comprehensive modelling tools for simulation of hydrological processes and contamination of the water environment, including the U.S. EPA Basins (EPA, 2001), MIKE Basin (DHI, 2008), WMS (Nelson et al., 2002) and SWAT (Arnold and Fohrer, 2005). The comprehensive models present techniques available to assess and complete the information on the pollution in space and time, and to assess the impact and efficiency of the proposed measures for abatement of the pollution (Borah and Bera, 2003).

The modelling tools require data at the level of detail that is often unavailable in typical rural catchments of small and medium size, although the solution of problems with water pollution in these basins is essential for fulfilment of objectives of water management legislation; namely the Water Framework Directive 2000/60/EC (hereinafter referred to as WfD, EC, 2000) and Nitrate Directive (EEC, 1991).

This article presents the results of research that aims at identifying the potential and limits of the MIKE Basin model for analysis and dealing with tasks related to the application of the requirements of the EU WfD (EC, 2000) in water management. The article points to the following objectives:

1. Analysis of the efficiency of point pollution reduction measures required by the current legislation in a rural basin by means of a complex model,
2. Calculation of the potential effect of measures for elimination of non-point pollution, designed with respect to their practical applicability,
3. Testing of the suitability of the MIKE Basin model for application in a small basin with limited sources of input data.

The MIKE Basin model was used for simulating the impact of measures for water quality improvement in the Olšava River Basin. This model was chosen because of its potential for solving complex issues on different basin scales (Jha and Gupta, 2003) and because of the acceptable qualitative and quantitative input data requirements. The MIKE Basin model is also being used by Czech water management authorities for modelling the impact of measures implemented in river basin management plans (RBMPs) prepared by water board authorities.

The model was applied to a case study of the Olšava River Basin, at the border between the Czech Republic and Slovakia, representing a typical rural basin with a complex structure of pollution sources and burdened with long term problems with water pollution (Langhammer and Kliment, 2009). The study evaluated the potential and limits for the application of this modelling tool in finding strategies to improve the state of water quality in the Olšava River Basin. The indicators BOD_5, COD, $N\text{-}NH_4$, $N\text{-}NO_3$ and P_{total} represent the basic parameters for water quality assessment and for environmental planning purposes. The simulation period is based on the same time horizon as is required in current water management legislation for setting up water management plans compliant with the EU WfD (EC, 2000).

MATERIALS AND METHODS

Study area

The Olšava River Basin is situated on the fringe of the Carpathian Range in Central Europe, at the border between the Czech Republic and Slovakia. With a size of 520 km^2, the basin is typical of the rural country in a peripheral region with a diverse mixture of pollution sources and long-lasting problems with high levels of water pollution (Langhammer, 2010).

This basin is a part of the drainage basin of the Black Sea. The fan-shaped river network is made up of three main streams – Olšava, Šťávnice (Luhačovický Creek), and Nivnička (Fig. 1). The headwaters of the Olšava River are at an altitude of 622 meters above sea level, the mouth at Kunovice, where the Olšava runs in the Morava River, is at 178 m a.s.l.

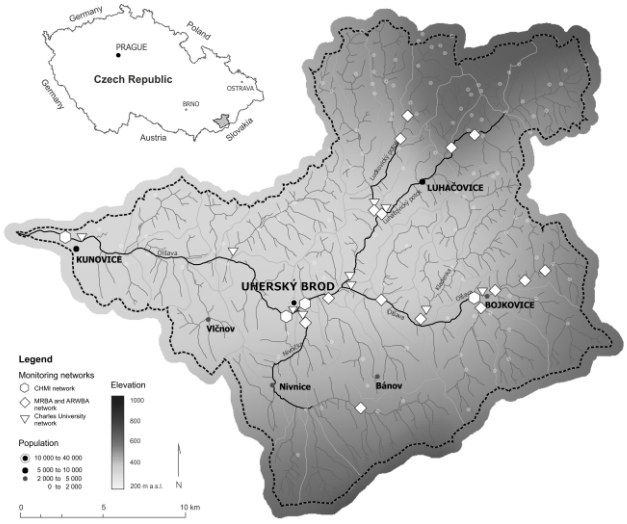

Fig. 1. Study area – Olšava River Basin, Czech Republic.

The average temperature reaches 9,1°C and the average precipitation rate varies from 625 mm in western lowlands up to 925 mm in highlands on the east side of the catchment. The yearly mean runoff at the catchment mouth profile is 2.5 m^3.s^{-1}. The value of Q_{100} is 270 m^3.s^{-1} and during low flow period the runoff can drop below 0.5 m^3.s^{-1}.

The land use of the basin displays a mixture of categories where forests and intense agriculture are predominant (Fig. 2). The forested areas (39.4%) cover the headwater regions and are protected as MAB UNESCO Biosphere Reserve White Carpathians. The share of permanent grassland (4%) has considerably increased since 1990, particularly because of the foundation of the biosphere reserve. The population of 50,300 inhabitants is concentrated in the lowland part of the river basin in the vicinity of Uherský Brod (17,500 inhabitants) and the Luhačovice Spa Resort (5,600 inhabitants). The arable land is spread over 43.3%, and together with the other agricultural categories of land use, represents 54% of the basin area.

Due to the Flysh bedrock, variable topography and unsuitable location of arable land, the agricultural land in the Olšava River Basin is at a high level of erosion risk (Damaška and Jurča, 1995; Langhammer and Kliment, 2009). More than 50% of the arable land is located on slopes with a gradient above 5°, and more than 20% of the arable land is located on slopes with a gradient above 8°. The erosion risk is evenly spread over the basin, even in the headwater regions where the precipitation totals and intensity are highest (Kliment et al., 2007).

More than 65% of the municipalities have a population lower than 1000 inhabitants. Only 37.6% of the population is connected to the integrated system of wastewater treatment (Table 1).

Table 1. Population integrated into a system of water treatment in the catchment of Olšava River. Data: IPR, 2010

Category of municipalities	Count	Average population	Proportional rate of the category on total population of the catchment (%)	Share of population connected to sewerage system (%)	Share of population connected to wastewater treatment plant (%)
< 1,000 inh.	41	583	20.4	64.9	18.9
1,000 – 1,999 inh.	11	1 233	11.6	65.1	65.5
2,000 – 4,999 inh.	7	3 613	21.6	85.0	85.8
5000 > inh.	4	13 590	12.0	86.0	77.0
Total	63	117 098	100.0	69.0	37.6

In the Olšava River Basin, 49 direct-point sources of pollution are recorded in the Integrated Pollution Register (IPR, 2010). These point sources consist mostly of the municipal source, but there are also several significant local industrial sources, producing emissions of high concentration of organic pollution. The direct pollution sources from agriculture are comprised of livestock, pork, and poultry breeding.

Because of its peripheral geographical position, the region remains underdeveloped, regardless of the economic development of the Czech Republic after the fall of the Communist regime in 1989 and accession to the EU in 2004. This lack of development results in limited coverage of wastewater treatment and a lack of modern sewage treatment technologies.

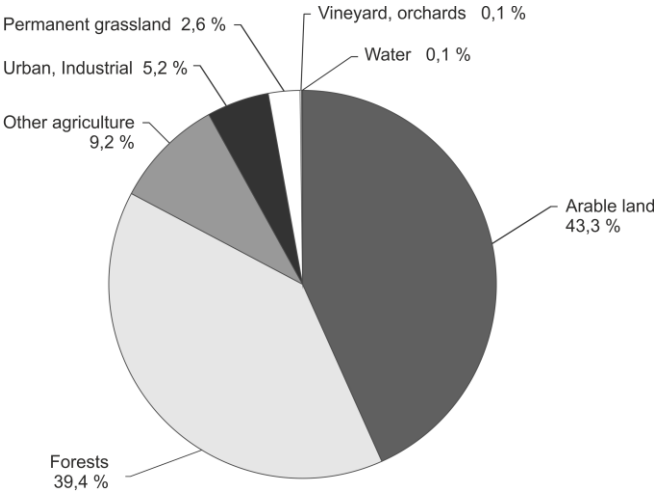

Fig. 2. Share of key land use categories in the Olšava River Basin. Data: CORINE land cover, 2000.

MIKE Basin model

The MIKE Basin (DHI, 2008) is a conceptual model that is fully integrated into the ArcGIS environment. The simulation runs on a whole catchment scale to include all the important pollution sources and pathways of contamination transport, such as surface and subsurface water uses, land use, and water structures.

The model is built up as a conceptual river network with water user connection nodes. The catchment is divided into sub-catchments belonging to the specific river reaches that are the subjects of water quality modelling. Pollution sources enter the model as a function of water users or in the form of a specific load runoff at the sub-catchment outflow. The specific load runoff can be calculated manually or with a Load Calculator tool.

The water quality module of the model simulates reactive steady-state transport of the most frequent water quality indicators – dissolved oxygen, BOD_5, COD, $N\text{-}NH_4$, $N\text{-}NO_3$, P_{total}, E. coli, and one user-specified conservative substance.

The degradation processes for all substances, expressed using reactive transformations (e.g. ammonia/nitrate, DO/BOD_5), are described by first-order decay rates. The steady-state qualitative and quantitative balance is calculated in time steps specified by the user, according to the project properties and task specifications.

The MIKE Basin model uses the ArGIS environment to provide pre-processing for data inputs and post-processing visualization and spatial analysis of model results.

Model setup and parameterization

For the purpose of modelling in the MIKE Basin model, the Olšava River Basin has been conceptualized into 38 sub-catchments, drained into individual nodes, corresponding to individual river reaches (Fig. 3).

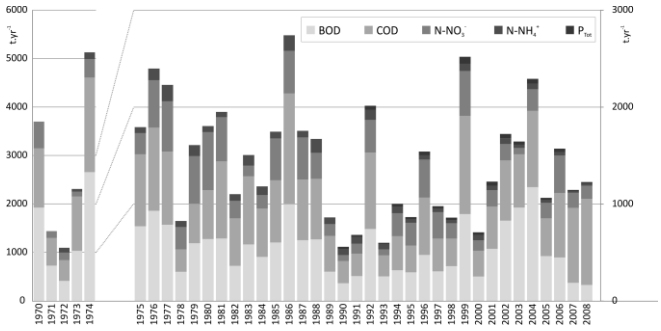

Fig. 3. Change of water pollution in selected water quality indicators in the closing profile of the basin - Olšava at Kunovice, since 1970. The missing values are caused by the later initiation of monitoring. Data: CHMI.

While the model requires quite a wide set of input parameters for the correct run of the model, the input parameters were derived from various data sources. The information on river network morphometry and basic hydraulic properties of streams was derived from the DIBAVOD geodatabase (WRI, 2010) and digital elevation model with 10-meter grid resolution, using the ArcGIS pre-processing tools.

The direct pollution sources, which were represented in the model as water users, consisted of a set of 46 entities. For each water user, there was a complete set of information on discharge and concentrations of selected pollution indicators – DO, BOD_5, COD, $N\text{-}NH_4$, $N\text{-}NO_3$ and P_{total} in the yearly average concentration. Additionally, some water users provided more information. The most important water users in the basin are the municipal wastewater treatment facilities, treating the wastewater both from municipalities and local industry, where the required data are available (IPR 2010).

In available data sources, there are almost no records on pollution discharges and concentrations from small and dispersed-point sources such as individual farms or individual houses. These small direct sources were added to the group of non-point sources. As basic input data, the MIKE Basin set-up further requires monthly values of concentrations, decay coefficients, and the retention time for each stream segment.

The parameters and coefficients for simulation of non-point sources were based on values of specific load balance for sub-catchments that had been calculated. The values from the observed catchments were extrapolated to the unobserved sub-catchments based on the assumption that the processes driving the material transport are homogeneous in the basin. Degradation rates of non-point pollution sources were iteratively optimized during the calibration process and are based on the concept of distance-dependent decay of pollutants. Values of loads per capita were based on assumption of Ritter and Shirmohammadi, 2000; and Synáčková, 1996.

The general time step for simulation was set to one month. All data available on different time scales were processed accordingly. The balanced model aims to represent values that are characteristic for each month of a year. In order to eliminate random extreme values, the characteristic values were calculated according to the methodology of Nesměrák 2009; Tachecí, 2009. To eliminate extreme or outlier values, the concentrations are considered as a function of discharge. Based on observed data, the logarithmic function is applied for low-flow conditions and the linear function for normal flow conditions. For every monitoring profile, each set of functions was calculated based on the whole time period of evaluated measurements (2000–2007). The observed concentration values thus were replaced according to the logarithmic regression curve for low flows and a linear regression curve for discharges [Q∈<QMmin, QMmax>], where QM represents the average monthly discharge during the observed period (2000–2007). The regression was calculated as a relative seasonal distribution of discharges during the whole observed period for every monitoring profile. The monthly characteristic value of discharge was calculated as an average of all daily values in individual months during the whole period 2000–2007. Values of concentration were extracted from the individual logarithmic or linear functions.

The temperature correction for all parameters was performed as a part of the MIKE Basin simulation using the empirical coefficient RateCorr.

$$R(T) = R_{20} \cdot RateCorr^{(T-20C)} \,, \tag{1}$$

where *R(T)* represents the factor for actual temperature T (°C), R_{20} is the degradation coefficient at the temperature 20°C and *RateCorr* is a constant set by the user.

This coefficient was set at the default as 1.07 and considered as a calibration parameter.

The self-purification process is described by a degradation coefficient (k_x), length of a river reach (L), and a residence time (T_d). Parameters L and T_d were easily estimated from the GIS and the field survey. The coefficient of mass degradation (k_x) had to be calculated for every substance and every group of reaches included in an upper catchment of individual water quality profiles. For the issues of water resources management planning, the calculation of degradation rate is represented by the simple first-order decay equation (DHI, 2008) (2):

$$\frac{dX}{d_{T_d}} = -k_x \cdot X \,, \tag{2}$$

where X represents a mass concentration and T_d represents the residence time. This simplification includes the assumption that

individual substances are not reciprocally involved. In the case of parameter N-NO_3, there is a need to apply an enhanced degradation rule (DHI, 2008) (3) to describe the nitrification process as:

$$\frac{dNO_3}{dt} = K_{NH_4} \cdot NH_4 - K_{NO_3} \cdot NO_3 \,, \qquad (3)$$

where K_{NH_4}represents the nitrification coefficient at 20°C [1/day], $K_{NO_3}$is the denitrification coefficient at 20°C [1/day] and NO_3 and NH_4 refer to the amount of nitrogenous substances. Although N-NO_3 concentration may be predominantly produced by the nitrification of N-NH_4, other sources of N-NO_3, such as the agricultural sources of non-point pollution, are also significant.

The calculation of a degradation coefficient was based on empirical studies done for the Czech environment (Behrendt et al., 1995).

The MIKE Basin Water Quality module is unable to reflect the yearly variability in the degradation coefficients because the coefficients remain constant for the whole model run. The decay coefficients were thus applied as average values derived from the supplementary data sources (Table 2). Values were calculated according Nesměrák, 2009 (4).

$$\mathrm{K_x} = \log\left(\frac{1}{\mathrm{PRA_{PS}}}\right), \qquad \text{where } \mathrm{PZS_{BZ}} = 10^{\mathrm{a/Q}} \qquad (4)$$

where K_x is a degradation coefficient, PRA_{PS} represents a procentual residue of point sources after the self-purification process during the low flow period, a is a nonlinear coefficient of the logarithmic function found for each monitoring site, and Q represents the discharge of a characteristic month. From the resulting monthly characteristic coefficients, the average value was calculated and used for the water quality model set-up.

The Load Calculator tool was used to calculate the input data for modeling the impact of non-point sources on water quality in the basin. The calculation is based on a principle of typical concentrations, related to the respective number of inhabitants, livestock, and arable land, and is spatially expressed as shape file. The result is calculated in the form of a time series of specific loads that are used as further input to the model. The applied coefficients were derived from observed and reported values from the basin and calculated values of specific loads (Ritter and Shirmohammadi, 2010, Synáčková 1996). The input data is publically available from municipal and state statistical sources (CSO, 2012). The hydraulic retention time was derived for each river reach from a combination of GIS data and field observation (5).

$$\mathrm{Tr} = \frac{\mathrm{v_a}}{\mathrm{L}}\,, \qquad (5)$$

where Tr represents the hydraulic retention time, v_a is the flow velocity in the given reach, and L is the river reach length.

The value of the river reach length L was calculated from the DIBAVOD geodatabase (WRI, 2010). The mean flow velocity v_a was derived from the results of repeated hydrometric measurements at 10 monitoring stations in the monitoring network maintained by Charles University in Prague (Langhammer and Kliment, 2009), and periodically repeated since 2001. The measured velocity values were related to the respective discharge values, and the derived function was used for characteristic monthly velocities based on calculated characteristic monthly discharge values.

Model calibration and validation

The model was calibrated to obtain the highest possible agreement between the simulated and observed values using the Nash-Sutcliff model efficiency coefficient (6).

$$E_f = 1 - \frac{\sum_i^n (Y_{oi} - Y_{mi})^2}{\sum_i^n (Y_{mi} - \overline{Y}_m)^2}\,, \qquad (6)$$

where Y_{oi} represents observed values and Y_{mi} are modeled values (Nash and Sutcliff ,1970).

The water quality model calibration was based on comparing the average monthly values of concentrations of water quality indicators and discharge values for monitoring profiles in the basin with simulated values. Main calibration parameters were decay constants k_t and the temperature coefficient RateCorr.

For the calibration of the coefficient of change of concentration of non-point pollution in the Load Calculator module, the sub-catchments of Nivnička were selected, as they intersect with the village of Nivnice. Nivnice produces livestock which graze on the land. The validation of calibrated parameters was performed on the sub-catchment ZPPOv009, where the cooperative of Nezdenice is located.

The decay coefficients were compared to keep the homogeneity in the areas with similar physiographic features. For stream segments with reservoirs, the retention times were prolonged up to 100 hrs. to correctly describe the effect of the reservoir on the stream water quality.

After the calibration, the model was validated with the dataset from 2006. The continuous simulation revealed varying effects of point and non-point pollution sources and distribution of pollution levels across the basin in the year.

The best conditions in terms of water quality are detected in the winter because of the lower average precipitation and runoff values as well as limited discharge at most of the point pollution sources.

During the spring, elevated values of load from non-point sources are evident. The high load from non-point pollution sources and from inter-basins is recorded in the upper parts of all major tributaries of the basin.

Summer represents the most critical period of the year in terms of water pollution. The low discharge, high water temperature and high levels of wastewater discharges from point sources are the reasons for the critical concentrations of organic pollutants, especially in the municipal sources. Since September, the levels of water pollution both at headwaters and lower parts of the basin decrease because of the higher average runoff, lower temperatures and lower volumes of wastewater discharges.

Although the basin is located in a typical rural area, the presence of relatively important municipal and industrial (food industry, machinery) point sources makes its water quality regime more complex. The resulting variability of pollution is thus driven by a mixture of factors, including physiography, agricultural activity, and municipal and industrial wastewater discharges.

The critical stream segments in terms of water pollution can be identified, especially in the central part of the basin, as consequence of emissions from important point pollution sources, either from municipal wastewater or livestock production (Fig. 5). Fig. 5 shows the current state of water quality in individual reaches of the main streams of the Olšava River Basin. Concentrations of all evaluated substances were put into one figure as the resulting water quality class is, according to the Czech water quality classification standard CSN 75 7221 based on the worst-evaluated parameter.

Table 2. Parameters necessary for the MIKE Basin simulation and calibration and corresponding characteristic values.

Parameter	Units	Description	Data Source	Average	Min	Max
T_d	hour	Reach residence time	CUNI, MRBA, AWMA, CHMI	32.79	0.21	414.47
k_d	-	Coefficient of mass degradation	CHMI, MRBA, AWMA, IPR	0.11	0.01	0.30
L	Km	Reach length	WRI	1.86	0.11	13.22
F	km^2	Area of sub catchment	WRI, MIKE Basin	14.46	0.58	50.90
v_{st}	m/s	Mean flow velocity	CHMI, MRBA, AWMA, IPR	0.84	0.02	5.76
T	°C	Monthly characteristic water temperature	CHMI	10.53	0.38	21.74
$Q_{WaterUser}$	m^3/s	Discharge of extraction or emission of water by water user	IPR	0.04	0.00	250.00
$c_{WaterUser}$	mg/l	Characteristic concentration of emitted water (BOD_5, COD, $N\text{-}NH_4$, $N\text{-}NO_3$, P_{total})	IPR	49.52	0.08	500.00
Q	$l/s/km^2$	Specific runoff from sub catchment area	Calculation	0.21	0.03	1.16
LO_{NPS}	g/s	Specific mass transport from sub catchment area (BOD_5, COD, $N\text{-}NH_4$, $N\text{-}NO_3$, P_{total})	Calculation	0.04	0.00	0.22
c_{char} BOD_5	mg/l	Monthly characteristic concentrations according to the biological oxygen demand in 5 days	CHMI, MRBA, AWMA	1.45	0.16	5.26
c_{char} COD	mg/l	Monthly characteristic concentrations according to the chemical oxygen demand	CHMI, MRBA, AWMA	7.41	0.68	17.84
c_{char} $N\text{-}NO_3$	mg/l	Monthly characteristic concentrations of nitrate	CHMI, MRBA, AWMA	1.05	0.02	3.15
c_{char} $N\text{-}NH_4$	mg/l	Monthly characteristic concentrations of ammonia	CHMI, MRBA, AWMA	0.11	0.01	0.65
c_{char} P_{total}	mg/l	Monthly characteristic concentrations of total phosphorus	CHMI, MRBA, AWMA	0.11	0.01	0.48
Q	m^3/s	Monthly characteristic Discharge	CHMI	0.86	0.02	7.27

Abbreviations: CUNI (Charles University in Prague, Faculty of Science); MRBA (Morava River Basin Authority); AWMA (Agricultural Water Management Authority); CHMI (Czech Hydro-Meteorological institute); IPR (Integrated Pollution Register); WRI (Water Research Institute Prague).

Model scenarios

To decrease the level of water pollution in the Olšava River Basin, proposed scenarios were based on different types of measures. The measures were designed to fulfil the following criteria:

- compliance with the Czech and EU water management legislation,
- compliance with the Water Management plans issued by the River Basin Authorities and
- practical applicability.

Two groups of measures that focused on point and non-point sources were considered.

The measures proposed for decrease of load from direct pollution sources have been focused on improvement of efficiency of wastewater treatment, mainly at the municipal sources that primarily contribute to the overall pollution balance. These measures are required by the EU WfD (EC, 2000), and are implemented in the long-term plans of River Basin Authorities.

First, wastewater treatment facilities were proposed for communities currently not equipped with a wastewater treatment facility, according to the WfD requirements applied to communities with 2,000 inhabitants or more. In the second step, tertiary wastewater treatment technology was applied, as required by the WfD, for cities with 10,000 inhabitants or more. The WfD also requires the tertiary treatment in communities with 5,000 inhabitants or more, when they are located in vulnerable areas.

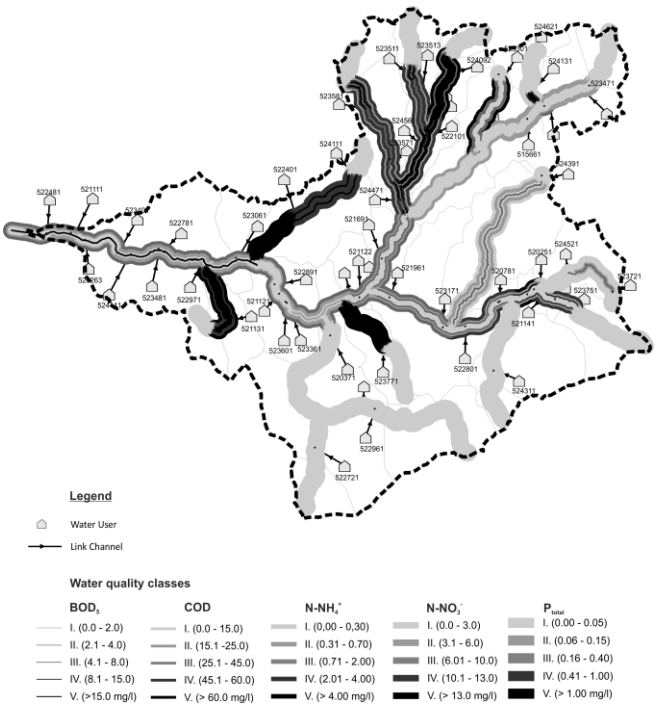

Fig. 5. Yearly average values of the model of the current state of the Olšava River Basin water quality.

The measures aimed to diminish the pollution loads from non-point sources were mainly focused on the changes in land use and land cover. The most critical land cover types were

identified as fields with arable land located on steep slopes with an inclination over 12° directly connected to a recipient. These areas were proposed for being transferred into the permanent grassland category. The experience of conversion of arable land into pastures in other regions proved that this form of activity can be economically beneficial (Withers, 2007), so the proposed change was considered as being potentially acceptable to the stakeholders.

In the MIKE Basin model, the scenarios for point pollution sources have been set up as a modification of the original time series and datasets. For the non-point pollution sources, the measurements were applied using the MIKE Basin Load Calculator. This tool is based on the spatial analysis of ArcGIS layers that contain information about the amount of fertilizer applied, count of livestock, and industrial and domestic sources. The value of concentration is added to the amount of pollution. The last step is to specify the value of decay within the drainage path towards the recipient. Those values were first estimated according the distance from the recipient and later calibrated and compared with values reported in relevant literature (Rosendorf and Prchalová, 1999).

Data Sources

The model is based on different sets of data supplied by various providers. The water quality data used for analysis of the current state and development of surface water pollution in the basin were supplied by the authorities providing monitoring in the region: the Czech Hydrometeorological Institute (CHMI), Morava River Basin Authority (MRBA), and Agricultural Water Board Authority (AWBA). These data were completed by the results from the network of monitoring secured by Charles University in Prague at 10 monitoring sites.

Water quality indicators were selected to be relevant to the parameters simulated by the MIKE Basin model and included DO, BOD_5, COD, $N\text{-}NH_4$, $N\text{-}NO_3$, and P_{total}. The assessment of long-term trends of water quality at the river mouth profile uses data from 1970–2010. The monitoring network covering the inner river network of the basin consists of 19 stations monitoring water quality and 8 stations for the monitoring of discharge. This interval was defined to prove the representativeness of individual datasets by including both dry (2003, $Q = 1.14\ m^3 \cdot s^{-1}$) and wet (2000, $Q_{year} = 4.3\ m^3 \cdot s^{-1}$) years.

The Integrated Pollution Register (IPR, 2010) database was used as a source of information on emissions of direct pollution. The DIBAVOD geodatabase (WRI, 2010) was used as a reference digital map resource, which was completed by the CORINE land cover (EEA, 2009) database and general topographic layers.

All acquired data were statistically processed to eliminate the gaps in time series. The missing values were filled by correlation with the most suitable and accurate time series.

RESULTS

Water quality changes in the Olšava River Basin

The Olšava River Basin has experienced intense water pollution over the last few decades with pollution occurring even in the small streams in the mountains.

The water quality is a long-term problem for water management of the basin. Extreme levels of pollution in key indicators, which were reached in the 1970s, decreased and there is an apparent positive shift in most indicators; however, the water quality in the basin since the late 1980s has improved only slightly and there are repeated peaks of pollution (Fig. 4). Pollution in BOD_5, ammonium nitrate or total phosphorus, displayed only limited change since the 1990s with repeated peaks of pollution. The decrease of concentrations in indicators reflecting industrial pollution (COD, $N\text{-}NH_4^+$) is linked to the efficiency of treatment in the major wastewater treatment facilities and to the decline of economic activities.

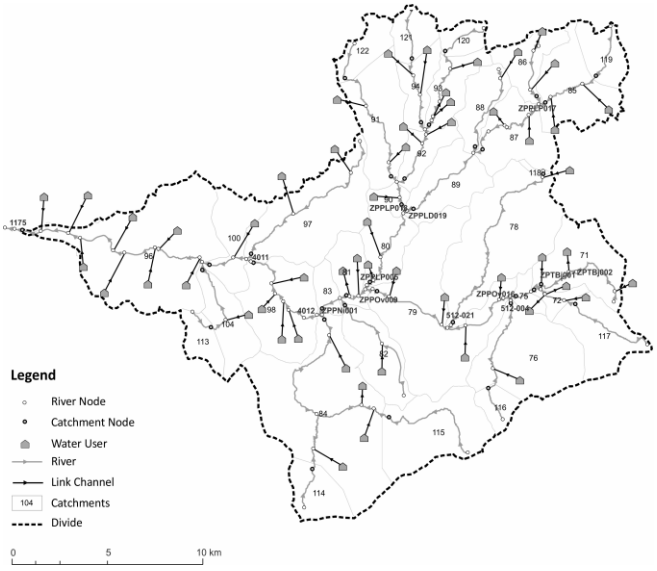

Fig. 4. Conceptualization of river network and sub-catchment structure in the MIKE Basin model for the Olšava River Basin.

The low average discharge of recipients is not adequate to the spatially-concentrated emissions from municipal and local industrial pollution and makes the ecosystem vulnerable. This vulnerability can be documented by the extreme peak of pollution caused by water treatment failures after the floods in 2006 which resulted in unprecedented concentrations of organic pollutants compared to the last 20 years.

The contamination of surface waters by toxic waste from local industry, mainly by heavy metals (Cd, Hg), was eliminated during the 1990s. However, the decrease of elevated concentrations of pollutants was not due to these systematic measures, but occurred as a result of the economic collapse of the former industrial activities during the transformation era of the Czech economy in the 1990s. The Olšava River Basin did not follow the trend of quick depollution that occurred in large streams in the Czech Republic since major political changes in 1990 when the decline of economic activities went in conjunction with investments in wastewater treatment, which led to substantial and lasting improvements in water quality in large rivers (Langhammer, 2010).

Regardless of the apparent slow decrease in pollution, the remaining levels of concentrations in most indicators can be regarded as high in respect to the basin characteristics. The actual pollution levels are comparable to the concentrations observed for large rivers in industrial and urbanized areas. This montane basin, which is located in an underdeveloped region with scarce settlement and an extensive headwater area, is protected as a biosphere reserve. It has the potential for a much lower level of pollution, particularly in the upper and central parts of the basin.

SIMULATION OF SCENARIOS OF POLLUTION DECREASE

Effect of point pollution decrease

The scenario was based on the simple application of a basic level of wastewater treatment for communities with more than 1,000 inhabitants and the application of tertiary wastewater treatment for communities above 5,000 inhabitants in vulnerable zones, delimited according to the Nitrate Directive 91/676 EC. These measures were applied for the real numbers of inhabitants currently connected to wastewater treatment facilities. For the rest of the inhabitants in these communities, there was an applied wastewater treatment efficiency of 87% in BOD_5 and 81% in COD.

The results indicate a significant increase in water quality, especially in the ammonia nitrogen (7.9%) and BOD_5 (5.1%) parameters (Table 3). The highest effect of the measure is shown on lower reaches of the Olšava River under Uherský Brod (Fig. 6), where the application of a more strict wastewater treatment standard would shift the water pollution level from water quality class V to III, i.e., from the worst class to a mid-level class. The same improvement has been detected in small streams polluted by currently untreated municipal wastewater, including Ludkovický, Vlčnovský, and Bánovský Creek. The pollution levels of small tributaries in rural sub-catchments remain unchanged.

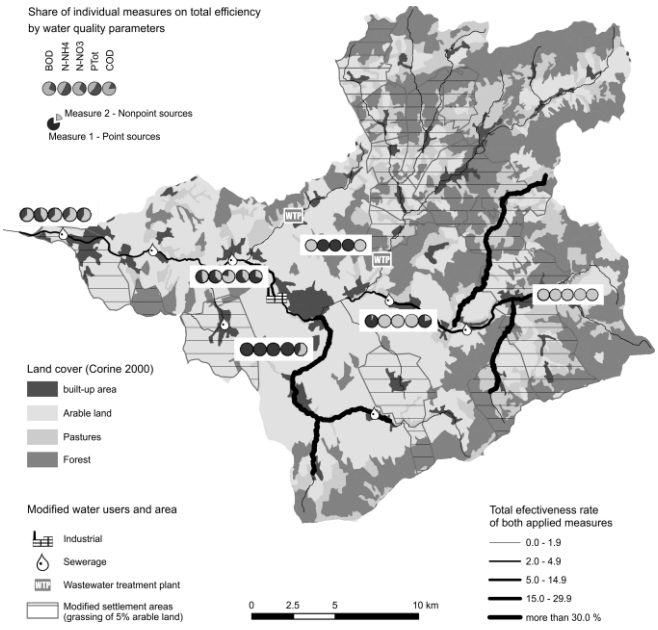

Fig. 6. Total effectiveness of two measures applied in the model of the current state of water quality in the Olšava River Basin in parameters BOD_5, $N\text{-}NH_4^+$, $N\text{-}NO_3$, P_{total} and COD.

Effect of non-point pollution reduction

In the sub-catchments with the most critical levels of pollution related to agriculture, this model scenario proposed converting 5% of the arable land to grassland. The share of arable land suggested for conversion was based on expert estimates of realistic scenarios applicable in the current socioeconomic conditions of the area. The main aim of land use development is to reduce erosion potential by considerate exploitation of the most exposed parts of arable land (Psotová, 2008).

Table 3. Efficiency of scenarios.

Parameter	Point pollution reduction %	Nonpoint pollution reduction %	Point + Nonpoint %
BOD_5	5.1	5.6	10.4
COD	3.9	3.1	6.6
NH_4^+	7.9	7.8	13.8
NO_3^-	2.7	7.2	8.3
P_{total}	3.8	5.1	7.5

The efficacy of this measure is highest for both forms of nitrogen: ammonia (7.8%) and nitrates (7.2%). The positive effect of this measure is apparent mainly in the small sub-basins in the flat central and lower parts of the basin, as well as in the upper parts of the basin where the arable land is often located in unsuitable conditions in terms of slope and erosion vulnerability.

Cumulative effect of both point and non-point pollution reduction

The scenario combining measures at point and non-point pollution sources showed the potential of the basin for reducing pollution under the current conditions. The highest efficiency was achieved in the ammonia nitrogen parameter where the reduction achieved was 13.8%. The decrease of pollutant concentrations was achieved in the central part of the basin, and was particularly apparent in the northern part of the basin at Luhačovický and Ludkovický Creek. The positive effect of implementation of tertiary treatment is apparent at all major wastewater treatment facilities and the respective river reaches, namely at the cities of Luhačovice, Uherský Brod, and Kunovice (Fig. 6).

The decrease in load by organic pollution in the BOD_5 indicator is apparent in the reaches under the small municipal sources without previous wastewater treatment. The decrease in load especially applies to the small effluents at the communities of Vlčnov, Bánov, or Petrůvka in the lower part of the basin. The changes in organic pollution in COD were marginal.

The proposed measures led to a decrease of concentrations of nitrates by 8.3%. The concentrations of nitrates at the monitoring stations show non-declining levels during the whole period of observation. The suggested measures, especially the changes in land use structure, seem to indicate that positive results are possible. The total phosphorus concentrations declined by 7.5%, again mainly due to the changes in land use. The major impact of the proposed measures is apparent in the headwater region and at small effluents in the central part of the Olšava River Basin.

Table 4. MIKE Basin simulation results of two most effective scenarios.

		Measure 1: Enhanced effeciency of wastewater tretment plants (%)					Measure 2: Grassing of selected agricultural lands (%)				
		BOD_5	$N\text{-}NH_4$	$N\text{-}NO_3$	P_{total}	COD	BOD_5	$N\text{-}NH_4$	$N\text{-}NO_3$	P_{total}	COD
Gauging profile Kunovice 1175	SPRING	4.7	9.5	2.9	3.5	4.4	7.5	5	4.6	6.1	3.6
	SUMMER	6.1	9.5	3.9	4.2	3.3	7.3	7	6.6	6.6	7
	AUTUMN	7.2	11.8	4.4	4.8	4.7	7.1	5.7	5.9	6.3	5.9
	WINTER	3.7	7.6	2.4	3	2.8	7.6	5	5.2	6.3	43
	Average	*5.4*	*9.6*	*3.4*	*3.9*	*3.8*	*7.4*	*5.7*	*5.6*	*6.3*	*5.2*
Middle reaches of Olšava river 4012	SPRING	1.6	0	0.1	0.2	1.3	10.2	9.7	2.6	7.6	7.7
	SUMMER	1.5	0.1	0.1	0.1	1.2	19.9	19.5	6	17.9	17.3
	AUTUMN	1.9	0.1	0.2	0.2	1.6	15	14.3	4.8	12.9	12.4
	WINTER	1.1	0	0.1	0.1	0.8	12.3	11.3	2.9	9.5	9.3
	Average	*1.5*	*0*	*0.1*	*0.2*	*1.2*	*14.3*	*13.7*	*4.1*	*12*	*11.7*
Right side tributary Luhačovický stream ZPPLP005	SPRING	0	0.1	0.6	0.5	0	13	6.5	5.1	5.5	3.7
	SUMMER	0	0.2	0.6	0.5	0	7.9	6.3	5.7	5.9	2.9
	AUTUMN	0	0.6	0.7	0.7	0	8.7	5.9	5.4	5.8	3
	WINTER	0	0.4	0.4	0.3	0	14.1	6	5.3	5.8	3.5
	Average	*0*	*0.3*	*0.6*	*0.5*	*0*	*10.9*	*6.2*	*5.4*	*5.8*	*3.3*
Upper reaches of Olšava river ZPPOv016	SPRING	31.9	0.3	49.3	18.1	3.9	2	0	30.4	9.5	4
	SUMMER	19.5	0.1	42.9	35.4	8.7	1.6	0	26.9	19.4	3.5
	AUTUMN	19.6	0.2	41.6	27.4	6.7	1.6	0	26.2	15	3.2
	WINTER	30	0.4	52.5	26.9	4.8	1.9	0	32.5	14.5	3.8
	Average	*25.2*	*0.2*	*46.6*	*27*	*6*	*1.8*	*0*	*29*	*14.6*	*3.6*

The most intense positive effect of the proposed measures is apparent in the following regions (Fig. 6):

1. The lower part of the Olšava River from Uherský Brod to the mouth profile,
2. The upper part of the Olšava River up to Bojkovice,
3. The northern part of the basin at the confluence of Ludkovický and Luhačovický Creek,
4. At the left-side effluents of the Olšava River in the lower part of the Basin – Nivnička, Vlčnovský, and Bánovský Creek.

The changes in pollution load slightly affect the seasonal distribution of concentrations in the basin (Table 4). The most significant changes were detected in the indicators dependent on emissions from point pollution sources, e.g. $N\text{-}NH_4$ and BOD_5. The highest decrease in concentrations is apparent during summer and fall, when the maximum values of pollution load are observed. The lowering of the level of maximum pollution concentrations is highly positive, especially in view of the low discharge values in the summer period (Fig. 7) and can be regarded as a step towards decreasing the vulnerability of the river ecosystem.

Pollution load structure

The portions of non-point pollution on the total pollution balance are related to the rural character of the basin. In the upper parts of the basin, the non-point pollution in nutrients reaches 61–74%. In the lower parts, the share of non-point pollution is between 41–63%. Shares were derived from the model of the current state of the Olšava River Basin. All pollution sources that were not considered as point sources were automatically evaluated as non-point sources. The resulting high percentages of non-point pollution in nutrients on the overall balance have been compared to other studies.

However, these percentages are affected by incomplete information on discharge from local municipal point sources, which are unlisted in the integrated pollution register. These results are in line with the findings reported by different authors (Beránková et al., 2010; Langhammer, 2004). The high shares of non-point pollution, especially in nutrients, are common in rural basins. However, the case studies from different environments (Maillard and Santos, 2008; Salvetti et al., 2008; Wang et al., 2006) show that regardless of the similarities in land use, the non-point pollution sources can vary significantly, mainly due to different physiography (geology, lithology, soil conditions, land cover and others), climate conditions, and variations in load from local point pollution sources.

DISCUSSION

The mathematical models of a river network, and especially the models of water quality, are burdened by high levels of simplification due to the complexity of processes described and their conceptualization in the model (Beven, 2000). The generalization affects all aspects and phases of the model construction and use. However, there are several common shortcomings. The conceptualization of streams as 1-D hydraulic structures results in an incorrect representation of the flow, mainly on larger riverbeds; in addition, this representation is considered as homogenous in the horizontal and vertical aspects (Shanahan et al., 1998). The organic pollution indicators BOD_5 and COD are treated as individual substances that degrade over time, even when they are aggregate parameters of the redox processes in the stream. The processes affecting the variability and seasonality of the load from the point and non-point sources are substantially different and should be treated separately (Marsili-Libelli and Giusti, 2008; Pekarova et al., 2004). The calibration process and application of autocalibration tools can result in the application of parameter values that are far from the real conditions, and thus even the well-calibrated model can lead to misinterpretation and unexpected results (Paliwal et al., 2007).

The appropriate modelling tool, thus, has to be able to generalize the processes of water pollution transport and degradation at a level that allows the use of limited data inputs with adequate accuracy in results and in the robustness of the model. The comprehensive models including SWAT, HSPF, or MIKE Basins have some known general shortcomings resulting from the conceptualization of physical processes. The inaccuracies are reported in the generation of runoff and related material transport (Buchanan et al., 2011; Easton et al., 2008). The prevailing approach, based on the SCS curve number equation,

distributes the runoff and related pollutant loads in larger areas that correspond to the critical contributing areas that are highly differentiated in space (Beven, 2000). The concept of variable source areas, applied, e.g. in the SWAT-VSA model (Easton et al., 2008), seems to be able to improve the accuracy of results, mainly for storm runoff. However, such approaches are demanding for data and parameter calibration.

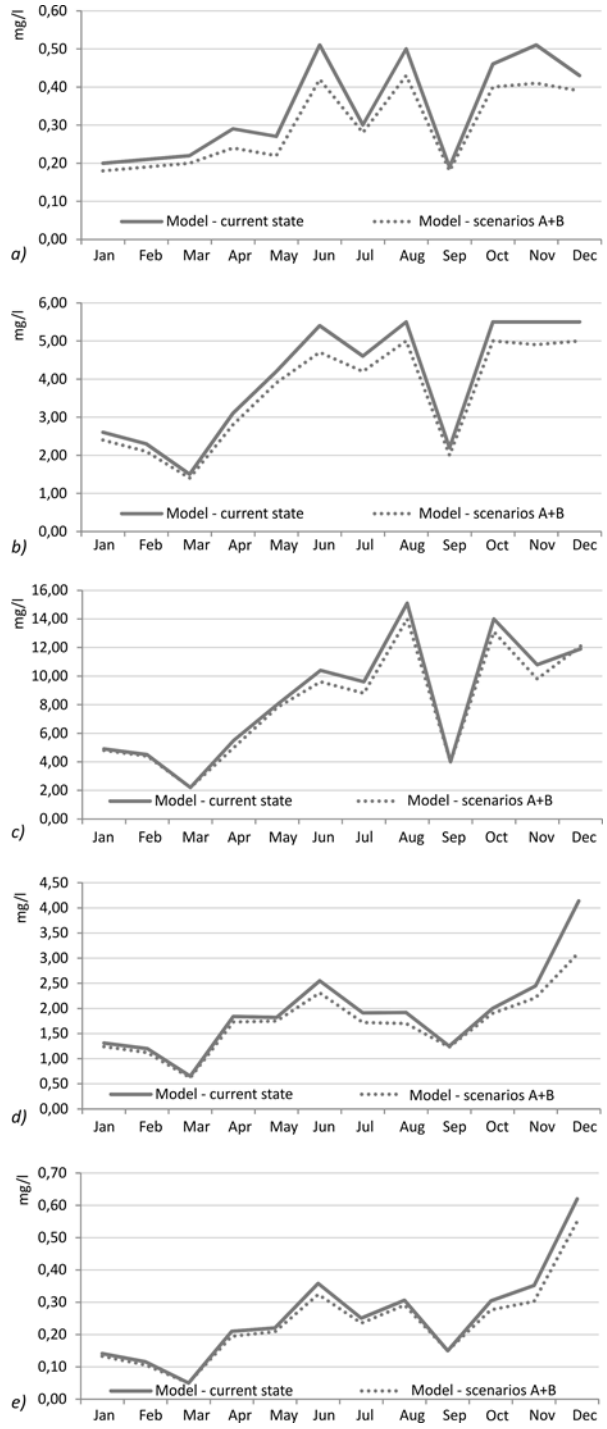

Fig. 7. Changes of seasonal variations of water quality after the application of simulated measures for selected indicators: a) N-NH_4^+, b) BOD_5, c) COD, d) N-NO_3 and e) P_{total}.

The balance between the required level of detail for input data and sufficient accuracy of the output is one of the key problems reported in a number of reports studying different water quality and non-point pollution models (Borah and Bera, 2003). The most common issue for complex models is the large sets of required input data and parameters that are not regularly observed and are difficult to be derived correctly. This problem was reported for the SWAT and HSPF models, applied either on small catchments (Engelmann et al., 2002; Saleh and Du, 2004) or in large basins (Santhi et al., 2001).

The MIKE Basin model seems to offer a reasonable balance between data requirements and accuracy of the results obtained. It can describe the most important key factors of water quality and screen the catchment for identifying the most important problems. Such approach is mostly beneficial in catchments of macro- and meso-scales where the lack of accurate data is often a limiting condition for a detailed assessment.

The conceptualization of the MIKE Basin model results in some simplifications that must be taken into consideration when analysing results in spatial detail. One simplification is the inability of the Water Quality module to describe the yearly variability of decay coefficients. The decay coefficient can be extremely variable in time and space (Behrendt et al., 1995). The model, however, uses only one average value of the decay coefficient per water quality model which cannot reflect the seasonal changes.

The correct analysis and interpretation of the model results are also affected by the way the model handles the combination of specific pollution loads within stream water quality. The specific pollution load is added only at the sub-basin nodes. The specific pollution loads affect the water quality continuously along the assessed stream segments; however, the model conceptualization makes these changes locally specific and abrupt.

The application of the model to the Olšava River Basin points to several typical problems related with water quality modelling and water management in rural catchments, which can affect the level of assessment uncertainty.

An imbalance between data availability and model requirements is one of the key issues for the correct setup of a water quality model, especially in the often-missing or incomplete data on water usage. The model requires the input of discharges and concentrations of pollution emissions in the form of a time series. This requirement is easily fulfilled at large municipal and industrial sources (Langhammer, 2004). However, the discharges and concentrations of pollutants from local point sources are usually not included in the common databases, are reported only by yearly average values, or in some cases, they are not monitored at all. The preparation of the input dataset is thus based partially on indirect calculations and averaging, and is burdened with uncertainty.

Another source of uncertainty is the sparse network of discharge and water quality monitoring on small streams, as they are necessary as data sources for boundary conditions and for model calibration. The monitoring networks in small basins are usually sparse, time series are short and the monitoring interval is infrequent (Beránková et al. 2010). The missing quantitative information must be taken from the most similar or the nearest profile. In rare cases, the quantitative values had to be balanced using the upper and lower profiles.

The low frequency of water quality monitoring in rural basins can also negatively affect the reliability of assessment in parameters reflecting the non-point pollution. The monthly sampling interval, which is standard for regular monitoring networks, covers mostly low and average discharges (e.g. Kulasova et al., 2012). When the nutrients are washed out with water erosion during high rainfall-runoff events (Kliment et al., 2007, pollution loads may be underestimated. Nevertheless, the

storm runoff from areas with extensive dairy or beef farming is burdened by intensive pollution from farmyard runoff, which has been proven to be a source of high levels of contamination, but usually is not included in any pollution estimates (Edwards et al., 2008). The underestimation of pollution loads at the level of basic monitoring as well as potential pollution sources can distort the whole picture of the actual pollution levels and result in incorrect calibration of models and misinterpretation of modelling results.

For practical applications of theoretical results of a modelling study, it is important to take into consideration the limited effect that the adopted water quality management measures have in rural basins, due to a variety of reasons. One of most critical problems is the large lag time between adoption of new management practices and water quality response. Experience from various environments indicates that the lag time between adoption of measures and the first measurable improvement in water quality in a small catchment can be higher than 10 years for nitrate pollution, and higher than 20 years for phosphorus (Meals et al., 2010).

The causes of such an elevated lag time are manifold, but they primarily depend on the intensity of previous agricultural practices and physiographic properties of the catchment. The key problems are the legacy sources of nutrients and the long residence time of pollution in groundwater systems (Sharpley et al., 2013). Analyses using isotope tracers in various model basins (e.g. Böhlke and Denver, 1995; Tomer and Burkart, 2003) proved the long residence time of nitrogen pollution in groundwater systems in environments previously exposed to intense fertilisation. This can result in stable elevated levels of pollution in rural catchments, despite changes in management (Langhammer, 2010). This principle can apply also to the Olšava Basin as it has been, as other rural basins in the Czech Republic, exposed to almost unrestricted fertilisation in the time of extensive agricultural production in 1970–80s (Langhammer and Kliment, 2009). In the Olšava Basin, the changes in agriculture were significant. Since 1990, 10.2% of arable land in headwater areas was converted into permanent grassland, which was followed by a sharp decrease of the use of fertilizers, due to economic reasons (Langhammer and Kliment, 2009). The minimal response in the change of nutrient loads in recipients may originate in persistent leaching of nutrients from the legacy loads and may hinder positive changes in the future.

Another aspect affecting the real efficiency of calculated pollution decline is the imbalance in measures focused on depollution in phosphorus and nitrogen from agricultural sources (Carpenter et al., 1998; Sharpley et al., 1994). The application of the EU Nitrate directive (EC, 1991) often leads to the preference of measures eliminating nitrate pollution, with a lack of adequate measures focused on the elimination of phosphorus in rivers. Systematic care on phosphorus pollution is essential for water quality improvements and reduction of extensive eutrophication processes (Deasy et al., 2010).

Other problems related to the pollution of small basins are the mismanagement of facilities, lack of systematic approach, and little enforcement of environmental legislation. The key sources of extensive pollution in small streams are local pollution sources that are not connected to the sewage network, and mismanaged wastewater treatment facilities at small municipalities (Langhammer and Rödlová, 2013). These sources have a significant effect on resulting water quality, but they are difficult to measure or estimate, as they are unlisted in official databases (Meals et al., 2010).

The lag time between change in management practices and water quality improvement should be considered as an important phenomenon in the evaluation of success of adopted measures in rural basins. In the case of the Olšava River Basin, the modelling study indicates that despite the abovementioned discussed factors that are slowing improvement of water quality, the basin has the potential to recover from intense past pollution and achieve the requirements of EU environmental legislation. However, the water management of the basin should pay attention to all potential factors that may potentially slow pollution recovery and properly set up a water quality monitoring system that is able to recognize the changes in reaction to adopted measures.

CONCLUSIONS

The MIKE Basin model used in this study was tested for practical applicability for the screening of rural catchments and for modelling the efficiency of proposed scenarios for the reduction of water pollution. The model tested the efficacy of measures designed to decrease water pollution by changes at point and non-point pollution sources.

The model was applied in the Olšava River Basin, Czech Republic, representing a typical rural region with a heterogeneous mixture of pollution sources, variable topography and land use, limited data on pollution sources, and a relatively sparse network of regular water quality monitoring data. The data from official sources were completed by the data from the author's long-term monitoring of water quality in the basin to check the model results and reliability.

The study indicated that this tool could be used successfully to build up and calibrate a functional complex water quality model, even with the limited amount of data typically available in rural basins. This limited availability of data is important for practical applicability of the model. The water managers usually build the models using standard data sources provided by the water management authorities. These standard data sources are limited in the peripheral regions.

The scenarios of the pollution reduction measures were based on the implementation of wastewater treatment at small untreated municipal sources, application of tertiary treatment at large point sources, and grassing of arable land at high risk of soil erosion. The simulation results proved that the measures proposed for reduction of water pollution with a view of their practical applicability can lead to fulfilment of the limits required by the Czech and EU legislation.

The positive effect of the proposed measures, indicated by simulations, can be less intense in practice due to several factors, typical for water quality management in rural basins. First, in small rural basins, there is a frequent lack of regular and systematic monitoring, and thus the design of simulations and proposed measures can be based on inappropriate values. Second, the depollution measures in rural basins are frequently focused on elimination of nitrogen and disregard phosphorus pollution. However, for efficiency of measures, both of the key nutrients should be appropriately treated. Last, but not least, the water management in small agricultural basins is often inefficient due to the poor state or mismanagement of wastewater treatment facilities and insufficient enforcement of the environmental legislation.

Acknowledgement. The research presented in this paper was supported by Charles University in Prague Research Center UNCE 204003/2012, and Research Program PRVOUK P43 with the support of grant project GAČR P209/12/0997.

REFERENCES

Arnold, J.G., Fohrer, N., 2005. SWAT2000: Current capabilities and research opportunities in applied watershed modelling. Hydrol. Process., 19, 563–572.

Beránková, T., Vogel, R.M., Fiala, D., Rosendorf, P., 2010. Estimation of phosphorus loads with sparse data for agricultural watersheds in the Czech Republic. Hydrological Sciences Journal, 55, 1417–1426.

Beven, K., 2000. On the future of distributed modelling in hydrology. Hydrol. Process., 14, 3183–3184.

Borah, D.K., Bera, M., 2003. Watershed-scale hydrologic and non-point-source pollution models: Review of mathematical bases. Transactions of the ASAE 46, 1553–1566.

Böhlke, J.K., Denver, J.M., 1995. Combined Use of Groundwater Dating, Chemical, and Isotopic Analyses to Resolve the History and Fate of Nitrate Contamination in Two Agricultural Watersheds, Atlantic Coastal Plain, Maryland. Water Resour. Res., 31, 2319–2339.

Brown, L.C., Barnwell, T.O., 1987. The enhanced stream water quality models QUAL2E and QUAL2E-UNCAS: documentation and user manual. US Environmental Protection Agency. Office of Research and Development. Environmental Research Laboratory, Athens.

Buchanan, B., Easton, Z.M., Schneider, R., Walter, M.T., 2011. Incorporating Variable Source Area Hydrology into a Spatially Distributed Direct Runoff Model1. JAWRA Journal of the American Water Resources Association.

Carpenter, S.R., Caraco, N.F., Correll, D.L., Howarth, R.W., Sharpley, A.N., & Smith, V.H., 1998. Non-point pollution of surface waters with phosphorus and nitrogen. Ecological applications, 8, 3, 559–568.

Chapra, S., Pelletier, G., Tao, H., 2006. QUAL2K: A modelling framework for simulating river and stream water quality, Version 2.04. Documentation and User's Manual. Civil and Environmental Engineering Department, Tufts University, Medford, MA, USA.

CSO, 2012. Czech Statistical Office - Public Database.

Damaška, J., Jurča, V., 1995. Extended sources of water contamination. Vodni Hospodarstvi, 45, 173–176.

Deasy, C., Quinton, J.N., Silgram, M., Bailey, A.P., Jackson, B., Stevens, C.J., 2010. Contributing understanding of mitigation options for phosphorus and sediment to a review of the efficacy of contemporary agricultural stewardship measures. Agr. Syst., 103, 2, 105–109.

DHI, 2008. MIKE Basin 2008. User´s Guide. DHI, Horsholm.

Easton, Z.M., Fuka, D.R., Walter, M.T., Cowan, D.M., Schneiderman, E.M., Steenhuis, T.S., 2008. Re-conceptualizing the soil and water assessment tool (SWAT) model to predict runoff from variable source areas. J. Hydrol., 348, 279–291.

EC, 1991. Council Directive 91/676/EEC of 12 December 1991 concerning the protection of waters against pollution caused by nitrates from agricultural sources. (OJL375, 31.12.91, pl) European Communities, Brussels.

EC, 2000. Directive 2000/60/EC of the European Parliament and of the Council of 23 October 2000 establishing a framework for Community action in the field of water policy. Official Journal of the European Communities L327, 1–73.

Edwards, A.C., Kay, D., McDonald, A.T., Francis, C., Watkins, J., Wilkinson, J.R., Wyer, M.D., 2008. Farmyards, an overlooked source for highly contaminated runoff. J. Envrion. Manage., 87, 4, 551–559.

EEA, 2009. CORINE Landcover database.

EEC, 1991. Council Directive 91/676/EEC of 12 December 1991 concerning the protection of waters against pollution caused by nitrates from agricultural sources. Official Journal of the European Communities, 1991, 1–8.

Engelmann, C.J.K., Ward, A.D., Christy, A.D., Bair, E.S., 2002. Application of the BASINS Database and NPSM Model on a Small Ohio Watershed. Journal of the Astronomical Society of Western Australia, 38, 289–300.

EPA, U.S., 2000. Hydrological Simulation Program - FORTRAN, User's Manual. Ver. 12. U.S. EPA, National Exposure Research Laboratory, Athens, GA.

EPA, U.S., 2001. Better Assessment Science Integrating Point and Non-point Sources User's Manual. Version 3.0. U.S. Environmental Protection Agency, Washington, D.C.

Havn, K., Madsen, M.N., Drge, J., Singh, V.P., 1995. MIKE 11-a generalized river modelling package. Computer models of watershed hydrology, 733–782.

Højberg, A.L., Refsgaard, J.C., Van Geer, F., Jørgensen, L.F., Zsuffa, I., 2007. Use of models to support the monitoring requirements in the water framework directive. Water Resour. Manag., 21, 1649–1672.

IPR, 2010. Integrated Pollution Register. Ministry of the Environment of the Czech Republic.

Jha, M.K., Gupta, A.D., 2003. Application of Mike Basin for water management strategies in a watershed. Water International, 28, 27–35.

Kliment, Z., Langhammer, J., Kadlec, J., Goudie, A., Kalvoda, J., 2007. The suspended load and soil erosion processes in mesoscale catchment areas. In: Goudie, A.S., Kalvoda, J. (Eds.): Geomorhoplogical Variations. P3K, Prague, 221–252.

Kulasova, A., Smith, P.J., Beven, K.J., Blazkova, S.D., Hlavacek, J., 2012. A method of computing uncertain nitrogen and phosphorus loads in a small stream from an agricultural catchment using continuous monitoring data. J. Hydrol., 458, 1–8.

Langhammer, J., 2004. Modelling the structural changes of water quality in the Elbe river basin. Ekologia Bratislava, 23, 157–169.

Langhammer, J., 2010. Water quality changes in the Elbe River basin, Czech Republic, in the context of the post-socialist economic transition. GeoJournal, 75, 185–198.

Langhammer, J., Kliment, Z., 2009. Water quality changes in selected rural catchments in the Czech Republic. Ekologia Bratislava, 28, 312–332.

Langhammer, J., Rödlová, S., 2013. Changes in water quality in agricultural catchments after deployment of wastewater treatment plant. Environmental monitoring and assessment, 1–17.

Maillard, P., Santos, N.A.P.A., 2008. A spatial-statistical approach for modeling the effect of non-point source pollution on different water quality parameters in the Velhas river watershed-Brazil. J. Environ. Manage., 86, 158–170.

Marsili-Libelli, S., Giusti, E., 2008. Water quality modelling for small river basins. Environmental Modelling & Software 23, 451–463.

Meals, D.W., Dressing, S.A., Davenport, T.E., 2010. Lag time in water quality response to best management practices: A review. J. Environ. Qual., 39, 1, 85–96.

Nash, J., Sutcliffe, J.V., 1970. River flow forecasting through conceptual models part I-A discussion of principles. J. Hydrol., 10, 3, 282–290.

Nelson, E.J., Dellman, P.N., Ruiz, C.E., Manwaring, C.T., 2002. Watershed Modeling System Hydrological Simulation

Program; Watershed Model User Documentation and Tutorial.

Nesměrák, I., 2009. On the compensation of values below the detection limit in chemical analysis and monitoring of water quality status: the effect of substitution of values below the detection limit by the half of the quantification limit to the statistical characteristics of sets of values. Výzkumný ústav vodohospodářský T.G. Masaryka, Prague. (In Czech.)

Paliwal, R., Sharma, P., Kansal, A., 2007. Water quality modelling of the river Yamuna (India) using QUAL2E-UNCAS. J. Envrion. Manage., 83, 131–144.

Pekarova, P., Miklanek, P., Roncak, P., Adamkova, J., Chriastel, R., Metelkova, M., Pekar, J., 2004. Identification and assessment of long-term trends of surface water quality determinands in Slovakia for implementation of the EU WfD. J. Hydrol. Hydromech., 52, 317–328.

Psotová, H., 2008. The concept and strategy for the nature protection in Zlin Region, except protected areas. (mimo CHKO). In: Ochrana Přírody a Krajiny Ve Zlínském Kraji. Veronica, Brno, 12–15. (In Czech.)

Ritter, W.F., Shirmohammadi, A., 2010. Agricultural Nonpoint Source Pollution. Watershed Management and Hydrology, CRC Press, US, p. 352.

Rosendorf, P., Prchalová, H., 1999. Elimination of non-point pollution of surface and subsurface waters. (Report for 1998) (in Czech.)

Saleh, A., Du, B., 2004. Evaluation of SWAT and HSPF within BASINS program for the Upper North Bosque River watershed in central Texas. Transactions of the ASAE 47, 1039–1049.

Salvetti, R., Acutis, M., Azzellino, A., Carpani, M., Giupponi, C., Parati, P., Vale, M., Vismara, R., 2008. Modelling the point and non-point nitrogen loads to the Venice Lagoon (Italy): the application of water quality models to the Dese-Zero basin. Desalination, 226, 81–88.

Santhi, C., Arnold, J.G., Williams, J.R., Dugas, W.A., Srinivasan, R., Hauck, L.M., 2001. Validation of the SWAT model on a large river basin with point and non-point sources. Journal of the American Water Resources Association, 37, 1169–1188.

Shanahan, P., Henze, M., Koncsos, L., Rauch, W., Reichert, P., Somlyody, L., Vanrolleghem, P., 1998. River water quality modelling: II. Problems of the art. Water Sci. Technol., 38, 245–252.

Sharpley, A.N., Chapra, S.C., Wedepohl, R., Sims, J.T., Daniel, T.C., Reddy, K.R., 1994. Managing agricultural phosphorus for protection of surface waters: Issues and options. J. Environ. Qual., 23, 3, 437–451.

Sharpley, A., Jarvie, H.P., Buda, A., May, L., Spears, B., Kleinman, P., 2013. Phosphorus legacy: Overcoming the effects of past management practices to mitigate future water quality impairment. J. Environ. Qual., 42, 5, 1308–1326.

Synáčková, M., 1996. Water quality. ČVUT Publishing House. Prague. p. 208. (In Czech.)

Tachecí, P., 2009. Methodology for assessment of the impact of considered water quality improvement measures using MIKE-BASIN model. DHI, Prague. p. 63. (In Czech.)

Tomer, M.D., Burkart, M.R., 2003. Long-term effects of nitrogen fertilizer use on ground water nitrate in two small watersheds. J. Environ. Qual., 32, 6, 2158–2171.

Wang, C., Wang, Y., Wang, P., 2006. Water quality modeling and pollution control for the Eastern route of South to North water transfer project in China. Journal of Hydrodynamics 18, 253–261.

Withers, P.J.A, et al., 2007. The impact of pasture improvement on phosphorus concentration in soils and streams in an upland catchment in Northern England. Agriculture, Ecosystems and Environment, 122, 220–232.

WRI, 2010. DIBAVOD. Water Management Geodatabase. VUV TGM, Prague.

Received 2 January 2013
Accepted 22 October 2013

7.2 NUMERICAL MODELS OF MASS TRANSPORT INITIALIZATION (CASE STUDY II, III)

Kaiglová, J., Langhammer, J., Jiřinec, P., Janský, B., Chalupová, D., 2015. Numerical simulation of heavily polluted fine-grained sediments remobilization using 1D, 1D+ and 2D channel schematization. *Environmental Monitoring and Assessment*, 187 (3).

Kaiglová, J., Langhammer, J., Jiřinec, P., Janský, B., Chalupová, D., Ferenčík, M., 2015. Numerical modelling of the heavily polluted fine-grained sediments remobilization in the northern Czech Republic. *Ecohydrology & Hydrobiology*. In Press.

Kaiglová, J., Langhammer, J., 2014. Numerical modelling of gravel remobilization competence in mountain stream. In: Hudec, M., Csáky, A., 2014. *Sciencia Iuvenis*, UKF, Nitra, pp. 208-216.

Ecohydrology & Hydrobiology xxx (2015) xxx–xxx

Contents lists available at ScienceDirect

Ecohydrology & Hydrobiology

journal homepage: www.elsevier.com/locate/ecohyd

Original Research Article

Numerical modeling of heavily polluted fine-grained sediments remobilization in northern Czech Republic

Jana Kaiglová [a,b,*], Petr Jiřinec [b], Jakub Langhammer [a], Eva Ingeduldová [b], Dagmar Chalupová [a], Martin Ferenčík [c,d], Bohumír Jánský [a]

[a] Charles University in Prague, Faculty of Science, Department of Physical Geography and Geoecology, Albertov 6, 128 43 Praha 2, Czech Republic
[b] DHI a.s., Na Vrších 1490/5, 100 00 Praha 10, Czech Republic
[c] Department of Water-management Laboratories, Povodí Labe, státní podnik, Víta Nejedlého 951, Hradec Králové 500 03, Czech Republic
[d] Institute of Environmental and Chemical Engineering, Faculty of Chemical Technology, University of Pardubice, Studentská 573, 532 10 Pardubice, Czech Republic

ARTICLE INFO

Article history:
Received 2 December 2014
Received in revised form 20 January 2015
Accepted 9 February 2015
Available online xxx

Keywords:
Remobilization
Fine sediment
Numerical modeling
Pollution
Riparian zone
Elbe River

ABSTRACT

The northern part of the Czech Republic is regarded as significantly polluted by antecedent or ongoing heavy industrial production mainly concentrated in the riparian zones of the Elbe River and its tributaries. Toxic pollutants tend to persist in the environment for a long time bound with fine-grained sediments. Nevertheless, a high-flow event can induce a remobilization of those deposits and lead to secondary pollution of downstream aquatic ecosystems. Numerical modeling was used as a tool for remobilization probability assessment under local hydrodynamic conditions within 113 km of Elbe and Bílina river beds and riparian zones. The assessment was based on statistical evaluation of causal discharge, the actual discharge observed at the evaluated cross section at the time of remobilization defined as significant erosion of observed sediment depositions. MIKE modeling software by DHI was used with different levels of horizontal plan schematization according to site-specific flow conditions and available data sources. MIKE 11 and MIKE 21 were used for Bílina River and MIKE 21 C was used for the Elbe River. Sediment transport was calculated simultaneously with hydrodynamic simulation of the unsteady synthetic boundary conditions based on observed flood properties (MIKE 21 C, MIKE 21 MT). Remobilization assessment of Bílina River sediment was based on the shear stress map evaluation verified with the results obtained by 2D model of the experimental site. The study contributes to risk-based assessment of polluted sediment management of the Elbe and extends the current scope of remobilization prediction within a reasonable timeframe using a numerical modeling method.

1. Introduction

Fine-grained particles (<0.063 mm) originating from rock denudation, biological processes, dust fallout, untreated sewage, and industrial waste play an important role in the Elbe's aquatic ecosystems (Borovec, 1995). While coarse sediment is derived mostly from channel erosion, fine-grained sediment can originate from arable

* Corresponding author at: Charles University in Prague, Faculty of Science, Department of Physical Geography and Geoecology, Albertov 6, 128 43 Praha 2, Czech Republic. Fax: +420 271 736 912; mobile: +420 739 345 206.
E-mail address: jana.kaiglova@gmail.com (J. Kaiglová).

http://dx.doi.org/10.1016/j.ecohyd.2015.02.001
1642-3593/

land wash or occasionally from industrial or mining activities (Jánský et al., 2013). Although according to Aksoy and Kavvas (2005) only a small portion of sediment ultimately reaches the stream and can be transported during short, occasional periods of high-flow events, Haddadchi et al. (2013) state that 70–85% of sediment transported as suspended load originates from surface erosion. Contaminated sediment layers resulting from long-lasting deposition (Förstner et al., 2004) trapped in abandoned channels (Büttner et al., 2006) or other calm, slack water zones are considered to be potential hot spots of pollution because of the risk of mobilization under erosive hydraulic conditions (Jacoub and Westrich, 2006). The majority of the material is transported during high-flow river activity. Sediments are mobilized and accumulated according to local flow conditions once these exceed threshold values (e.g., critical shear stress for erosion τ_c and deposition τ_{cd}). According to Buzek (2000), a Moravian high-flow event observed in 1997 with a 100-year return period (RP) transported 51% of total recorded material suspended within the monitored period of 23 years. Schwartz (2006) reported reduction by 60% of long-term deposition in one middle Elbe groyne field as a consequence of a flood event in 2002. Although trends in sediment transportation under the influence of climate and land-use changes have been studied by numerous authors (Janský et al., 2010; Kliment, 2005; Cai et al., 2012; Walling and Fang, 2003), particular flow conditions for local remobilization require long-term observation or model assessment as an enhanced prediction tool.

According to van der Veen et al. (2006), under socialism (1950–1990) the Elbe was one of the most polluted rivers in Europe. The pollution was caused by heavy metals and organic contaminants from industrial and communal untreated sewage. Although water quality has improved significantly, sediment pollution still represents an important threat to the Elbe's aquatic ecosystems. According to Förstner et al. (2004) and Langhammer (2007), even though the Bílina River contributes almost insignificantly to Elbe water discharge (on average 6.5 $m^3 s^{-1}$ at the Bílina's confluence with the Elbe versus the Elbe's total 312 $m^3 s^{-1}$ at the German border), it has a significant impact on downstream water quality. Toxic matter together with cohesively acting fine particles forms a unity that can long persist in a riparian ecosystem (Droppo et al., 2009; Pores, 2009; Grabowski et al., 2011). Among other pollutants, heavy metals are regarded as being of special interest when bound to particles with low probability of degradation (Zeng et al., 2013). Once remobilized, toxin-bound fine-grained particles can be transported long distances in the form of wash load when shear velocity u^* greatly exceeds particle settling velocity w_s (Komar, 1988). Wash load contaminated particles can cause secondary pollution by desorption of the pollutant in the water environment (Segura et al., 2006). According to Borovec (1995), the coarser silt fraction (0.02–0.063 mm) may be enriched by pollutants as well due to the black and brown coating generated after a particle's long resistance in a single location. The qualitative properties of Elbe sediment have been described in several studies (Heininger et al., 2003; Rudiš et al., 2008; Schwartz, 2006).

Developments in hydroinformatics enable rapid implementation of theoretical sediment transport concepts with fine spatial and time distribution within a numerical modeling approach. Nevertheless, the entrainment of cohesive sediments, which is the main subject of this study, remains poorly understood due to its great complexity. In addition to appropriately describing sediment transport, the problem of sufficiently accurate flow parameter calculation plays a crucial role as it is a prerequisite for determining values for hydrodynamic variables used as the basis for sediment transport modeling, such as flow velocity, water depth and shear stress (Guerrero and Lamberti, 2013). According to Kiat et al. (2008), Simpson and Castelltort (2006) and Yang et al. (2004), flow and sediment transport should be simulated simultaneously as they significantly affect one another. Hardy (2013) has reviewed the current state of the art of process-based sediment transport modeling on different levels of flow schematization. The complex modeling system is extremely sensitive to the appropriate setting of parameters which, due to a lack of monitoring data, often must be estimated according to experience and corrected within a calibration process (Büttner et al., 2006; Jacoub and Westrich, 2006).

The present study continues on the topic of Elbe sediment remobilization as discussed by, for example, Heise et al. (2008), Kerner (2007), Rudiš (2000) and Schwartz (2006). It provides new knowledge of the Elbe fluvial system by implementing complex numerical hydrodynamic and sediment transport modeling as a tool for assessing remobilization risk. The main aims of the study are to (i) evaluate the probability of fine-grained, heavily polluted sediment remobilization at selected sites on the Upper Elbe and its left tributary the Bílina regarded as the main pollution sources; and (ii) discuss environmental aspects of the results thus obtained. In comparison with previous studies, an advantage lies in the ability to explore all expected hydrologic conditions while using RP as the main comparative parameter. Knowledge can thus be extrapolated beyond experience.

2. Materials and methods

With its total catchment area of 144,055 km^2, the Elbe River is an important European watercourse. The source and upper-middle course are located within the Czech Republic, where it drains an area of 48,750 km^2 (equal to 68% of the country). Fragments of the basin are located in Austria and Poland, but the largest part of the basin lies within Germany's borders. Average discharge at Hřensko (chainage 726.6 km), where the Elbe leaves the Czech Republic is 308 $m^3 s^{-1}$, while at the North Sea estuary the Elbe's discharge is more than double that amount, at 716 $m^3 s^{-1}$ under average runoff conditions. This study was conducted on the Elbe River reach between upstream chainage 965 km and Hřensko as well as on the Bílina River, left tributary (in the interval from upstream chainage 55 km to its confluence with the Elbe). The latter is regarded as one of the most polluted rivers in the Czech Republic (Langhammer, 2010; Přibylová et al., 2006) and a significant contributor to the overall water quality of the

Please cite this article in press as: Kaiglová, J., et al., Numerical modeling of heavily polluted fine-grained sediments remobilization in northern Czech Republic. Ecohydrol. Hydrobiol. (2015), http://dx.doi.org/10.1016/j.ecohyd.2015.02.001

Elbe basin (Heininger et al., 2003). According to Förstner et al. (2004), the Bílina River is an area of special concern for Elbe basin sediment remediation, particularly due to pollution from production of insecticides (DDT, lindane) that were widely used across the entire Elbe basin after 1950 (Krüger et al., 2006). Both rivers (Fig. 1) drain several extensive municipalities and industrial areas dominated chiefly by open pit mining, chemical industry (including refineries), food processing, and paper mills. The water bodies have been greatly modified all along the studied reaches (e.g., Matoušková and Dvořák, 2011). The water courses are permanently polluted by various ongoing industrial and communal discharges, among which chemical production (the companies Spolana and Synthesia Pardubice) and refineries (PARAMO, Chempark Záluží) still play the key role. Although excessive industrial production has been restricted in many areas since the 1990s and highly effective water treatment plants were installed (bringing significant improvements in water quality), pollution still remains within the water ecosystems in the form of particle-bound toxic pollutants deposited in calm backwaters or in riparian oxbow lakes (Chalupová et al., 2012). Those layers of mostly unknown composition and extent tend to be remobilized during high-flow events (e.g., in 2002 and 2013) and may be transported further downstream in the form of wash load. The persistence of toxic matter downstream from the sites has been proven by the degradation of water ecosystems as reported by Jurajda et al. (2010), among other authors, who observed a dramatic decrease in macrozoobenthos in the middle of the Bílina.

The case study sites were selected because they are areas of calm, slack waters where contaminated sediments long have been deposited. Moreover, the sources of toxic matter are located upstream very close to those sites. All sites have been known for many years from the results of previous studies (e.g., Petrůjová and Rudiš, 1996; Rudiš et al., 2007, 2008) and have been specified by the Elbe River basin authority (Povodí Labe, s. p.) or Charles University in Prague.

The Elbe longitudinal gradient is 0.47‰ upstream the confluence with Vltava and 0.35‰ downstream the confluence toward the state border. The gradient of Bílina varies along the longitudinal profile from milder gradient at the upstream model boundary 0.8‰ (Chainage 55–48 km), 4.4‰ (48–44 km), 1.5‰ (44–16 km), to 2‰ near the confluence with Elbe (16–0 km). The size of the flood plain, the typical flood extent and the flood propagation rate, those are the main differences between the rivers regarding the flood dynamics predetermining the hydrodynamic model selection.

The Upper Elbe basin is a part of Czech Massif geological formation characterized by consolidated granitic or gneiss substrate covered by Cretaceous (Upper Elbe) and Permokarbon (Bílina) sediment layers. The Massif is fractured by numerous faults predetermining the water courses direction. The typical bed material grain size in the main channel of both rivers Elbe and Bílina differs dramatically between the study sites and ranges typically from sand to gravel. Even the channel modifications predetermine the fine-grained sediment to be hidden at the berms or banks (in the case of Bílina) and in abandoned channels and calm slack water structures as old harbors or weir reservoirs (in the case of Elbe) not exposed to the average flow conditions (Schwartz, 2006). The bed roughness represented by Stricler's coefficient K_{st} (or Manning's M) varies from 6.7 in the case of dense impermeable areas up to 33.3 for the paved areas. The channel roughness is typically 32.8 for the Elbe 2D model and 22 in the case of Bílina 1D model characterized by higher gradients.

All case study sites are parts of larger model areas with sufficient flood plain width (up to the flood with return period 500 years, later Q_{500}) and boundaries which are situated sufficiently distant not to affect flow parameters

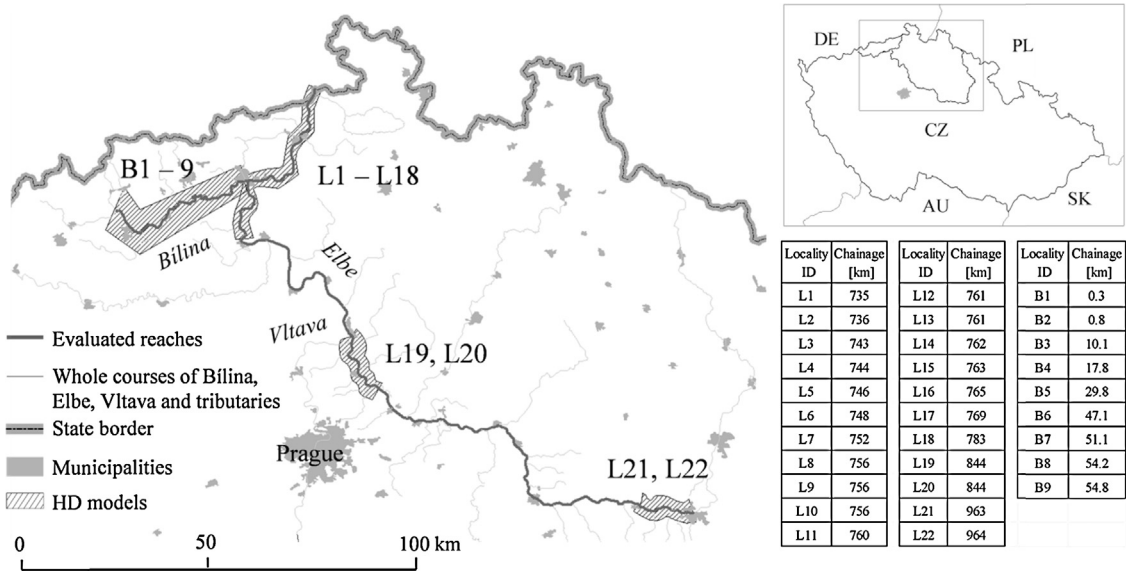

Locality ID	Chainage [km]
L1	735
L2	736
L3	743
L4	744
L5	746
L6	748
L7	752
L8	756
L9	756
L10	756
L11	760

Locality ID	Chainage [km]
L12	761
L13	761
L14	762
L15	763
L16	765
L17	769
L18	783
L19	844
L20	844
L21	963
L22	964

Locality ID	Chainage [km]
B1	0.3
B2	0.8
B3	10.1
B4	17.8
B5	29.8
B6	47.1
B7	51.1
B8	54.2
B9	54.8

Fig. 1. Localization of case studies. Individual studied sites and chainage are listed in the table (right column Bílina: B1–B9; middle and left columns Elbe: L1–L22). Hydrodynamic models are marked with hashed polygons.

Please cite this article in press as: Kaiglová, J., et al., Numerical modeling of heavily polluted fine-grained sediments remobilization in northern Czech Republic. Ecohydrol. Hydrobiol. (2015), http://dx.doi.org/10.1016/j.ecohyd.2015.02.001

at the study sites and to satisfy the requirement that velocity distribution be representative at the site. The models' lower boundaries are typically situated at gauging station cross sections with known rating curves (Q/H) and so the water stage for all discharge is known. Finally, four separate models (and model areas) have been used for flow schematization at case study sites: (i) the Elbe between Lovosice (km 786.3) and Hřensko gauging station, including a river length of ca 59 km; (ii) the Bílina between km 55.0 and the mouth of the Bílina into the Elbe (km 0.0); (iii) the Elbe between Kostelec nad Labem (km 856.9) and Mělník gauging station (km 836.7) at the confluence with the Vltava, with length of ca 20 km; and (iv) the Elbe between Pardubice (km 967.4) and Přelouč gauging station (km 951.0), ca 16 km long.

The comprehensive database used in the study was compiled first from data already available, chiefly topographic data provided by water management authorities (Povodí Labe, s. p. (later PLA) and Povodí Ohře, s. p. (later POH)), hydrological data on observed flood events for synthetic hydrograph compilation provided by the Czech Hydrometeorological Institute (CHMI), officially evaluated RPs for selected stations used for classification of results and measured daily values of total suspended loads for selected stations used for model results verification, CHMI. A second set of data was obtained by fieldwork, specifically sampling of fine-grained sediments. All together 66 samples characterizing 31 most polluted sediment spots along the studied reaches were collected and analyzed for granulometry and geochemistry (Medek et al., 2014). Granulometric curves were processed by the Department of Physical Geography and Geoecology at Charles University in Prague, and qualitative properties of toxin-bound sediment were determined in laboratories of POH and PLA. Modeling software was provided by DHI.

2.1. Hydrodynamic modeling as the basis for sediment transport evaluation

Hydrodynamic simulations were based on the fully dynamic solution of the shallow water (Saint-Venant) equations in x (1D) or x, y (2D) directions. The solution technique used was the method of finite differences on the implicit scheme of the ultimate number of computational points represented by so-called H and Q points (1D) or the mesh elements (2D).

The selection of an appropriate modeling approach (2D or 1D) for each of the 31 studied sites was conditioned upon four main prerequisites, as described here: (i) topographical data for schematization of hydrodynamic conditions were available in different qualities and formats. While Elbe bathymetry is measured in detail using the survey vessel Valentina II equipped with an echo sounder device, the topographical data for the Bílina channel's description consisted of a cross-sectional database with average longitudinal step of 70 m (POH 2010). (ii) The heavily modified and in many sites nearly prismatic channel of the Bílina is dominated by structures (102 bridges and weirs in the monitored reach) of varying capacities. Unlike the Elbe, where there are high-capacity bridges and weirs, mostly not operating during flood events, they can thus be schematized as the maximum elevation of the overflown edge. (iii) Based upon the expertise of local river administrators, expected conditions causing remobilization were estimated as up to the channel capacity ($<Q_{10}$) in the case of Bílina fine-grained sediment layers and varying significantly with the position of the Elbe site relative to the main flow. (iv) While Bílina sediments are deposited in bank zones and nearby structures, Elbe sediment layers are buried in oxbow lakes and riparian backwaters. Therefore, 2D curvilinear schematization (MIKE 21 C) of the Elbe and riparian zones was beneficial even though flow conditions are too complicated to be described by cross-sectional averaged parameters. In the case of the Bílina's narrow and nearly prismatic channel, 1D (MIKE 11) hydrodynamic schematization was used and computational time was dramatically reduced.

In order to illustrate and discuss possible misinterpretations due to simplification by the wash load concept (Section 4), the minimum residence time $Tr_{\min}$ (h) from the source to the German border was calculated based on the Chézy–Manning evaluation of the slope, reach length, velocity and cross-sectional variability (1).

$$Tr_{\min} = \frac{L}{M R^{2/3} \sqrt{S} 3600} \tag{1}$$

where L (km) is stream length between the study site and German border profile (Hřensko), M is the Manning roughness coefficient, R is the average hydraulic radius of the whole reach downstream study site, and S is the slope.

2.2. Sediment transport modeling

Different approaches were used in finding an appropriate set of flow parameters causing sediment remobilization. Sediment transport model schematization and parameterization reflected data and solution time requirements. The solution could thus be divided according to hydrodynamic schematization.

2.2.1. Sediment transport based on 2D models for middle and lower Czech Elbe water course

Fully interacting systems for sediment transport calculation were set up as a part of the MIKE 21 C designed for the river morphology calculations (Enggrob and Tjerry, 1998). The simulated, vertically averaged flow parameters directly affect the sediment transport calculation at time step t while the results of the sediment transport solution at t consequently influence hydrodynamics at $t+1$ by varying the bathymetry (accumulations or scours) and, optionally, roughness conditions. In the case of cohesive sediments, the general advection–dispersion formula (2) was used. Erosion and deposition are described by the source/sink term (DHI, 2012). Erosion follows the Partheniades formula, proposed by Ariathurai (1974) and deposition is described by Krone's (1962) deposition formulation.

$$\frac{\partial c}{\partial t} + u\frac{\partial c}{\partial x} + v\frac{\partial c}{\partial y} = \frac{1}{h}\frac{\partial}{\partial x}\left(hD_x\frac{\partial c}{\partial x}\right) + \frac{1}{h}\frac{\partial}{\partial y}\left(hD_y\frac{\partial c}{\partial y}\right) + Q_L C_L \frac{1}{h} - S \tag{2}$$

Please cite this article in press as: Kaiglová, J., et al., Numerical modeling of heavily polluted fine-grained sediments remobilization in northern Czech Republic. Ecohydrol. Hydrobiol. (2015), http://dx.doi.org/10.1016/j.ecohyd.2015.02.001

where c is depth-averaged mass concentration, u and v are depth-averaged flow velocities, D_x and D_y are dispersion coefficients, h is water depth, S is the deposition/erosion term, Q_L represents source discharge per unit horizontal area, and C_L is source discharge concentration.

Coarser sediments regarded as non-cohesive with D_{50} classified as fine sand (0.1–0.15 mm) were transported according to the Engelund–Hansen formula (1976) that was after comparison with Van Rijn theory for some areas on Elbe River regarded to be more suitable (3). The Engelund–Hansen approach does not take into account the value of critical shear stress (τ_c) due to the presumption that actual shear stress values are usually much higher than this laboratory experimental value.

$$\phi t = 0.1\frac{C^2}{2g}\theta^{2.5} \quad \text{Likewise} \quad \phi t = \frac{q_t}{\sqrt{(s-1)gd^3}} \tag{3}$$

where Φt [−] is total sediment transport rate, C is the Chézy roughness coefficient, θ is Shields Parameter, q_t is total sediment load, d is characteristic grain diameter, and g is gravity acceleration.

2.2.2. Sediment transport based on the 1D model for Bílina water course

The limitation of flow description on cross-sectional averaged values was regarded to be insufficient when dealing with non-uniformly located sediment bodies differing dramatically from cross-sectional average grain properties. Therefore, several variations on the Bílina model were tested in order to disaggregate flow parameters along the cross section. Chiefly, 1D+ (or pseudo 2D, separating cross section into several but usually 3 interlinked parts of the transient flow and berms) schematization dealing with the allocation of flow into 2–3 functional channel zones needed to be rejected due to its applicability only within selected reaches. For this reason, we had to retreat the actual sediment transport within the model and further explored the possibilities for evaluation based solely on the distribution of flow parameters. Such simplification was possible while dealing with the sole concept of sediment remobilization. Mean flow characteristics (velocity and depth) were distributed along the cross section based on the conveyance distribution with depth. With the linear interpolation routine, those results were distributed along the longitudinal direction in order to obtain 2D maps in the hourly time step and 1 m spatial resolution for the consequent shear stress calculation and evaluation. Resulting time varying maps of shear stress were explored in order to find areas with potential for sediment deposition (not exposed to the excess shear stress during average flow conditions) and further subjected to the remobilization criteria assessment.

2.3. Calibration and verification of hydrodynamic and sediment transport models

Calibration and verification of hydrodynamic models consisted of modifying bed roughness in order to obtain a good fit for simulated and observed water levels in the channel and inundation and overall hydrograph transformation during recent flood events (Table 1). The differences between the measured and simulated water level for the Elbe reach were in average -0.05 ± 0.08 m and -0.04 ± 0.07 m for flood events 2006 and 2011 respectively. In the case of Bílina River regarded to be affected mostly by the channel capacity discharges the calibration was processed by comparing the water levels subtracted from the official rating curves at the gauging stations with the simulated data. The tolerance of 0.05 m was regarded to be sufficient. Second calibration criterion was the flood wave propagation from between gauging stations. The fit was quantified with the Nash-Suttliff criteria above 0.95 and 0.90 in the case of Elbe and Bílina flood events respectively. The modification of bed roughness was done for the channel and the floodplain separately. By varying the Strickler's coefficient in the range of 5–10%.

Calibration and verification of the sediment transport model of was based on a comparison of total suspended loads originating from defined erodible layer describing the fine-grained sediment deposits and the measured values at the nearest downstream water quality monitoring profiles (CHMI) during the same high-flow events as those used for hydrodynamic model calibration (Table 1). Only one uniformed erodible layer was defined and characterized by the D_{50} grain diameter as the upper 5 cm of the sediment entered the simulation only, although the thickness of the erodible layer defined was much higher. Two sources of inaccuracies must be admitted: (i) total suspended load is measured on a daily instant basis and thus data are sparse and scarcely represent the overall situation during a flood event, and (ii) only the monitored sites were eroded while there was no data on the complex granulometric properties of the surrounding areas. The results were governed by the internal erosion from the isolated erodible layer definition only. Therefore, total suspended sediment concentrations loaded in the models represented only an estimated part of the total load

Table 1
Calibration and verification events. RP = return period, TSS = total suspended sediments. Data source: CHMI 2012, 2013.

Flood event [m/yyyy]	Magnitude/RP [m^3s^{-1}]/Q_y	Model site	Hydrological station	Max. TSS load [$mg\,l^{-1}$]/station
3/2006	2355/Q_5–Q_{10}	L1–L18	Ústí nad Labem (Elbe)	n.a.
	2403/Q_5–Q_{10}	L19, L20	Mělník (Elbe)	n.a.
1/2009	685/Q_{10}–Q_{20}	L21, L22	Přelouč (Elbe)	n.a.
	50.5/Q_{10}–Q_{20}	B1–9	Trmice (Bílina)	418/Trmice
8/2009	22.7/Q_2–Q_5	B1–9	Trmice (Bílina)	n.a.
1/2011	753/Q_2–Q_5	L1–L18	Ústí nad Labem (Elbe)	102/Prostřední Žleb
6/2013	1208/Q_1–Q_2	L19, L20	Mělník (Elbe)	176/Obříství
(second peak)	316/Q_1–Q_2	L21, L22	Přelouč (Elbe)	226/Valy

Please cite this article in press as: Kaiglová, J., et al., Numerical modeling of heavily polluted fine-grained sediments remobilization in northern Czech Republic. Ecohydrol. Hydrobiol. (2015), http://dx.doi.org/10.1016/j.ecohyd.2015.02.001

measured at the profiles (1/2 of the total concentrations at lower Elbe reach (L1–L18) where substantial part of the floodplain was eroded, only 10% of the concentrations at Upper Elbe reach (L19–L21) where only isolated localities were examined). The verification was therefore processed by comparing the tendency of the suspended sediment concentration resulted from the simulation with the measured concentration in the monitoring profile. Two objective criteria were observed, (i) the increment of the concentration per hour, (ii) the concentration wave culmination. The criteria (ii) were fulfilled in studied events 2011 and 2013 in the daily data comparison. The criteria (i) were during the flood event 2011 in Prostřední Žleb fulfilled in the first 2.5 days of the flood event where the steep increment of concentration ($1.7\ mg\ l^{-1}\ h^{-1}$ measured data vs. $1.8\ mg\ l^{-1}\ h^{-1}$ simulated data) was followed by slower increment ($0.3\ mg\ l^{-1}\ h^{-1}$ vs. $0.3\ mg\ l^{-1}\ h^{-1}$). Difference observed near the culmination ($0.6\ mg\ l^{-1}\ h^{-1}$ vs. $0.2\ mg\ l^{-1}\ h^{-1}$) can be explained by the sediment load from the upstream Elbe reaches. Sufficient results were obtained during the flood event 2013 ($1.3\ mg\ l^{-1}\ h^{-1}$ vs. $1.2\ mg\ l^{-1}\ h^{-1}$) but there was no comparable set for the flood event 2006 because of the lacking observed data due to the sampling difficulties (Halířová CHMI 2013, personal communication).

The parameter study of MIKE 21 MT model was processed at Bílina study sites for the most crucial parameters regarding the remobilization evaluation. The τ_c was varying within the interval of 0.6–0.8 N m^{-2} with an maximal expected error of 7.1% on the causal discharge evaluation; settling velocity ω_s varied within the interval 0.0001–0.0005 m s^{-1} and the maximal expected error was 8.5%.

2.4. Remobilization criteria

In order to eliminate movement of marginal importance and to assure objectivity in interpreting results, objective remobilization criteria were elaborated and used for all sites. Remobilization criteria were based on three conditions that needed to be fulfilled simultaneously:

(m) bed level change reaches −1 mm,
(n) bed level is eroded in consequent time with a rate of at least −1 mm h^{-1}, and
(o) suspended sediment current reaches the recipient.

Those remobilization criteria were arbitrary set based on the experiences from the verification runs. The criterion (m) should neglect the numerical oscillations of small magnitude. The criterion (n) should assure the eroding tendency of the flow conditions and criterion (o) should assure the environmental impact of the consequent process. Nevertheless the study does not exactly quantify the total load of the sediment and does not describe the erosion process of the lower compacted layers as it was not the primary aim.

Due to the unequal methodology for the Bílina evaluation, the remobilization criteria for evaluating results for the Bílina had to be adjusted accordingly. While simplifying the task for shear stress evaluation, remobilization criteria were only set for the selected sites as the exceedance of shear stress value over the proposed threshold of 1 N m^{-2}, which has been verified by the 2D hydrodynamic calculation with sediment transport included (MIKE 21 Mud Transport module) at experimental sites B8 and B9. The threshold value of shear stress $\tau \approx 1$ N m^{-2} was moreover supported by the similar τ_c proposed in the work of e.g. Grabowski et al. (2011), Houwing and van Rijn (1998), Van Rijn (1993), recommended in the reference manual of MIKE 21 C (DHI, 2012) and as well as by lessons from experience with those Elbe simulations that were most similar.

2.5. Hydrological approach and return period assessment

Hydrological data in the form of recent flood event hydrographs were transformed to synthetic hydrographs. The characteristic shape observed at individual reaches defined as speed and transformation was regarded as the slope of individual hydrograph limbs (Fig. 2). The hydrographs' rising limbs mostly consisted of three parts: (i) an initial concave slow rise, (ii) a sharp rise, and (iii) a convex slow rise reaching culmination. Data on observed magnitudes were considered in the form of duration of individual parts. The synthetic hydrographs were used in the form of hydrodynamic models' upper boundary conditions. The lower boundary was set accordingly based on the observation or iterative runs. The falling limb was used in one special case only where the emptying of the flood reservoir at the confluence of the Elbe and the Vltava had to be explored.

Causal discharges that fulfilled the remobilization criteria were evaluated in the form of RP (Table 2) in

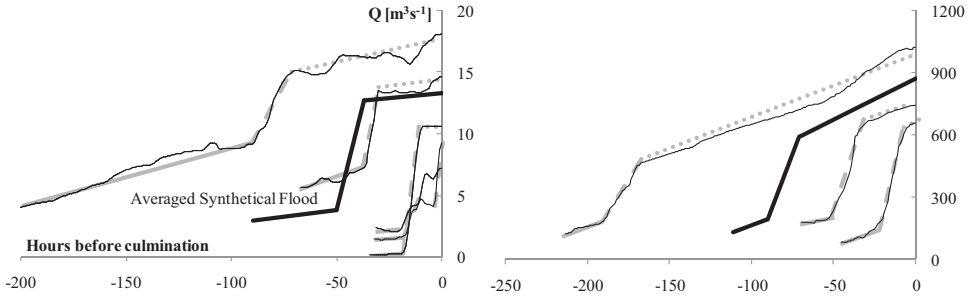

Fig. 2. Recently observed flood events at Bílina – Most (left) and Elbe – Kostelec nad Labem (right) gauging stations and resulting synthetic hydrograph. Note: phase (1) is delineated by straight grey line, phase (2) by dashed line, phase (3) by dotted line.

Please cite this article in press as: Kaiglová, J., et al., Numerical modeling of heavily polluted fine-grained sediments remobilization in northern Czech Republic. Ecohydrol. Hydrobiol. (2015), http://dx.doi.org/10.1016/j.ecohyd.2015.02.001

Table 2
Final results classification. The left column is classification based on wash discharge return period (RP). M-daily discharges (not exceeded in M days per year) are marked in italics and bold ($\mathbf{Q_M}$), *N*-year discharges (with return period of *n* years) are in regular font (Q_n).

Class	RP
1	$\leq \mathbf{Q_{80}}$
2	($\mathbf{Q_{80}}$; $\mathbf{Q_{15}}$>
3	($\mathbf{Q_{15}}$; Q_1>
4	(Q_1; Q_3>
5	(Q_3; Q_{10}>
6	(Q_{10}; Q_{50}>
7	$\geq Q_{50}$

order to obtain a parameter that would link results obtained within various geographic conditions. Using the probability of remobilization occurrence, the potential of secondary pollution was estimated and compared across the whole studied area. In order to classify the results obtained, 7 intervals based on RP were designed to represent most efficiently the individual results' variability. The class with the lowest number represented the highest remobilization tendency (lowest RP). Nevertheless, these classes reflect neither sediment pollution nor environmental risk after remobilization occurrence.

3. Results

The results are divided into 3 groups. First, the original results of old load samples were aggregated within the study sites to form the basis for remobilization tendency assessment. Second, the main contribution of the paper is presented as the results from numerical modeling of remobilization studies at the Northern Elbe basin study sites. Last, the environmental impact of remobilization is presented.

3.1. Old loads

The surveyed sediment database consisted of samples of varying granulometric properties. The parameter D_{50} further used for the sediment transport models (MIKE 11 AD CST, MIKE 21 MT, MIKE 21 C River Morphology) was in the range 0.003–0.1 mm in the case of Bílina sediments and 0.03–0.07 mm in the Elbe subaquatic samples (Fig. 3).

Toxic pollutants were found bound to all sediment samples (Table 3). The upper threshold for Elbe sediment pollution was regarded as the exceedance limit (FGG Elbe 2013).

All sediment samples were heavily polluted with heavy metals, particularly Pb, Hg, and Ni. At the Bílina sites and at Elbe sites downstream from the confluence with the Bílina, Cd greatly exceeded the limits in more than 80% of samples. Exceeded concentrations of Cu and As were found downstream of the Záluží petrochemical plant. High concentrations of PCBs were found in the majority of samples all along the surveyed course of the Elbe, but along the Bílina the parameter was exceeded in fewer than 30% of samples. The parameter HCB was significantly exceeded at Bílina sites and at Elbe sites downstream from the confluence with Bílina, while high concentrations of γ-HCH (lindane) were found at Bílina sites downstream from the Záluží petrochemical plant. The integrated parameter DDT (DDE, DDD, DDT) was highly exceeded in more than 80% of all surveyed samples except those from Elbe sites upstream from the confluence with the Vltava (70%) where the parameter TBT was exceeded in most samples. Highly exceeded concentrations of fluoranthene were found downstream of the Pardubice and Záluží petrochemical plants. For municipalities downstream from Pardubice and downstream from Ústí nad Labem, the concentrations of anthracene and b(a)pyrene exceeded the upper limits in all and in the majority of surveyed samples, respectively, but they were observed only in isolated samples from Bílina and middle Elbe sites.

3.2. Remobilization conditions

The results obtained by numerical modeling were evaluated in two ways. (i) The hydrodynamic parameters of causal flow were observed from simulation results at remobilization criteria time steps in order to understand

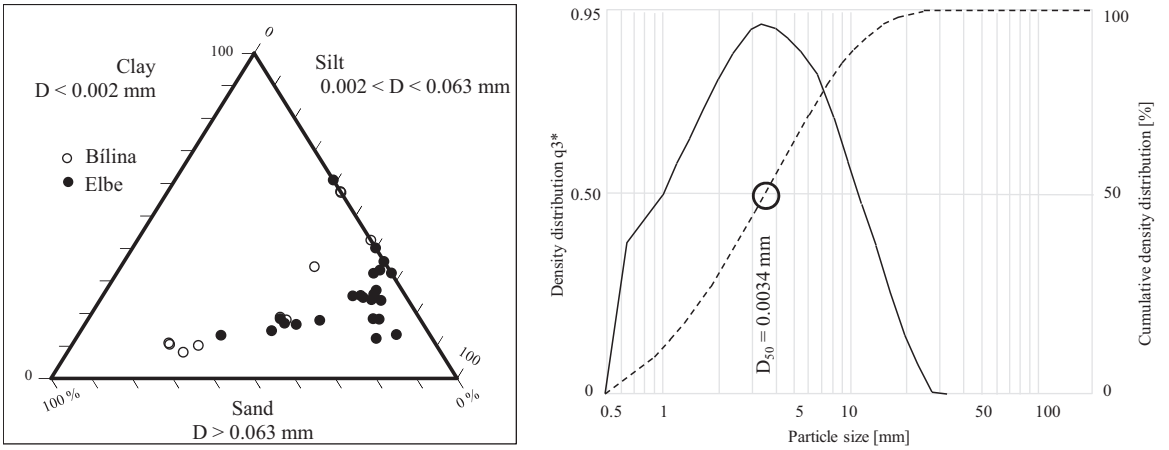

Fig. 3. Sediment data properties. Left is the triplot of all sediment samples' granulometric properties for each site. Right is a typical granulometric curve of a cohesive sample (in this case, site B9).

Please cite this article in press as: Kaiglová, J., et al., Numerical modeling of heavily polluted fine-grained sediments remobilization in northern Czech Republic. Ecohydrol. Hydrobiol. (2015), http://dx.doi.org/10.1016/j.ecohyd.2015.02.001

Table 3
Exceeded substances analyzed from sampled sediments (PLA, POH, FGG Elbe, 2013). The parameter is exceeded in *x*% of the samples while *x* is classified as follows: $x \leq 30$; $31 < x \leq 50$; $\mathbf{51 < x \leq 80}$; $\underline{\mathbf{x}} \geq \underline{\mathbf{80}}$.

Site	Exceeded substances
L1–L18	*Zn*, **Pb**, **Hg**, **Cd**, **Ni**, Cu, As, **PCBs**, **HCB**, **DDE**, **DDD**, **DDT**, *TBT*, **anthracene**, **fluoranthene**, **b(a)pyrene**
L19–20	Zn, **Pb**, **Hg**, *Cd*, **Ni**, Cu, As, **PCBs**, *α-HCH*, γ-HCH, **DDE**, **DDD**, *DDT*, **TBT**, anthracene, **fluoranthene**, *b(a)pyrene*
L21–22	*Zn*, **Pb**, **Hg**, *Cd*, **Ni**, *Cu*, **PCBs**, *HCB*, **DDE**, **DDD**, *DDT*, *TBT*, **anthracene**, **fluoranthene**, **b(a)pyrene**
B1–9	Zn, **Pb**, **Hg**, **Cd**, **Ni**, **Cu**, **As**, PCBs, HCB, **α-HCH**, **γ-HCH**,**DDE**, *DDT*, **fluoranthene**, anthracene, b(a)pyrene

the flow dynamics and conditions necessary for fine-grained sediment remobilization. (ii) The results were coupled by introducing RP evaluation for remobilization probability assessment. Because we are dealing with two streams having greatly differing flow characteristics that result in a distinction between the methods used, the results are first envisaged separately and later combined in an overview of all case study sites together.

Remobilization criteria were analyzed for all 22 Elbe sites (Table 4). The sites are distinguished primarily by flow conditions during high-flow events and can be divided into three morphological or functional groups: (i) artificial riparian structures such as navigation channels or harbor calm backwaters (L2–L5, L7–L13, L15–L18, L22), (ii) natural or semi-natural oxbow lakes with limited and regulated connections to the main channel under normal flow conditions (L21), and (iii) natural oxbow lakes connected with the main channel only during high-flow activity via overflowing an embankment or artificial spillway structure (L1, L6, L14, L19, L20). Therefore, water levels are equalized in the cases of (i) and (ii) and differ in the case of (iii).

Remobilization in the middle Elbe reaches (L1–L18) occurred mostly after the hydrodynamic connection of the site with the Elbe's main course, while in the uppermost sites (L19–L22), remobilization conditions were more complicated.

In general, 5 situations were observed: (a) sites with deposits were connected directly to the transient flow even under normal flow conditions. Erosion caused by backwater outwash primarily affected the inflow area and remobilization criteria were fulfilled with relatively small discharges and with RP even less than 1 year and variable flow conditions (RP < 1 year; $\nu = 0.4 \pm 0.3\ \mathrm{m\ s^{-1}}$; $\tau = 1.3 \pm 1\ \mathrm{N\ m^{-2}}$). (b) Despite being connected with the main flow, remote backwaters in harbors and other riparian structures were affected only by extraordinary high-flow activity (RP > 100 years; $\nu \approx 0.5\ \mathrm{m\ s^{-1}}$; $\tau \approx 1.5\ \mathrm{N\ m^{-2}}$). (c) A site was connected with transient flow only after the bank structure or dike overflowed. Thus, the water level in the main course differed from the riparian water body under average flow conditions. In those cases, remobilization greatly depended on the dividing structure's properties (RP ≈ 1–5 years; $\nu = 0.6 \pm 0.2\ \mathrm{m\ s^{-1}}$; $\tau = 2.2 \pm 2\ \mathrm{N\ m^{-2}}$). (d) A site was partly connected with the river through a functional pipe and so the water level in the body was equalized with the main course (Fig. 4). In such cases, remobilization criteria (m) and (n) were fulfilled under much lower flow conditions (RP ≈ Q_5 years; $\nu = 0.3\ \mathrm{m\ s^{-1}}$; $\tau = 0.7\ \mathrm{N\ m^{-2}}$) but sediment was only drifted in remote parts of the water body.

Table 4
Flow conditions at the remobilization criteria at Elbe sites. M-daily discharges (not exceeded in M days per year) are marked in italics and bold ($\mathbf{Q_M}$), *N*-year discharges (with return period of *n* years) are in regular font (Q_n).

Site ID	Chainage	Local discharge at Elbe/Vltava	RP	Local mean vertical velocity	Local shear stress
Units	km	$\mathrm{m^3\ s^{-1}}$	$\mathbf{Q_M}$ **days**/Q_n years	$\mathrm{m\ s^{-1}}$	$\mathrm{N\ m^{-2}}$
L1	735	946	$\mathbf{Q_5}$	0.50	1.62
L2	736	1783	$\mathbf{Q_2}$	0.16	0.23
L3	743	–	$>Q_{100}$	–	–
L4	744	1478	$\{Q_1; Q_2\}$	0.18	0.14
L5	746	404	$\mathbf{Q_{80}}$	0.89	7.84
L6	748	350	$\mathbf{Q_{120}}$	0.60	2.85
L7	752	588	$\mathbf{Q_{40}}$	0.42	1.80
L8	756	417	$\mathbf{Q_{80}}$	0.48	2.06
L9	756	324	$\mathbf{Q_{150}}$	0.23	0.47
L10	756	482	$\mathbf{Q_{50}}$	0.72	5.46
L11	760	1867	$\approx Q_2$	0.31	0.79
L12	761	412	$\mathbf{Q_{80}}$	0.12	0.12
L13	761	592	$\mathbf{Q_{40}}$	0.50	2.99
L14	762	474	$\mathbf{Q_{60}}$	0.18	0.27
L15	763	2372	$\approx Q_5$	0.29	0.72
L16	765	2563	$\approx Q_{10}$	0.71	3.32
L17	769	669	$\mathbf{Q_{30}}$	0.17	0.17
L18	783	393	$\mathbf{Q_{80}}$	0.60	2.37
L19	844	1406/1066	$>Q_{100}$	0.25	0.3
		128/1748	$\approx Q_5$	0.27	0.35
L20	844	1210/196	$\approx Q_{50}$	0.30	0.40
L21	963	912	$\{Q_{50}; Q_{100}\}$	0.55	1.40
L22	964	994	$>Q_{100}$	0.58	1.51

Please cite this article in press as: Kaiglová, J., et al., Numerical modeling of heavily polluted fine-grained sediments remobilization in northern Czech Republic. Ecohydrol. Hydrobiol. (2015), http://dx.doi.org/10.1016/j.ecohyd.2015.02.001

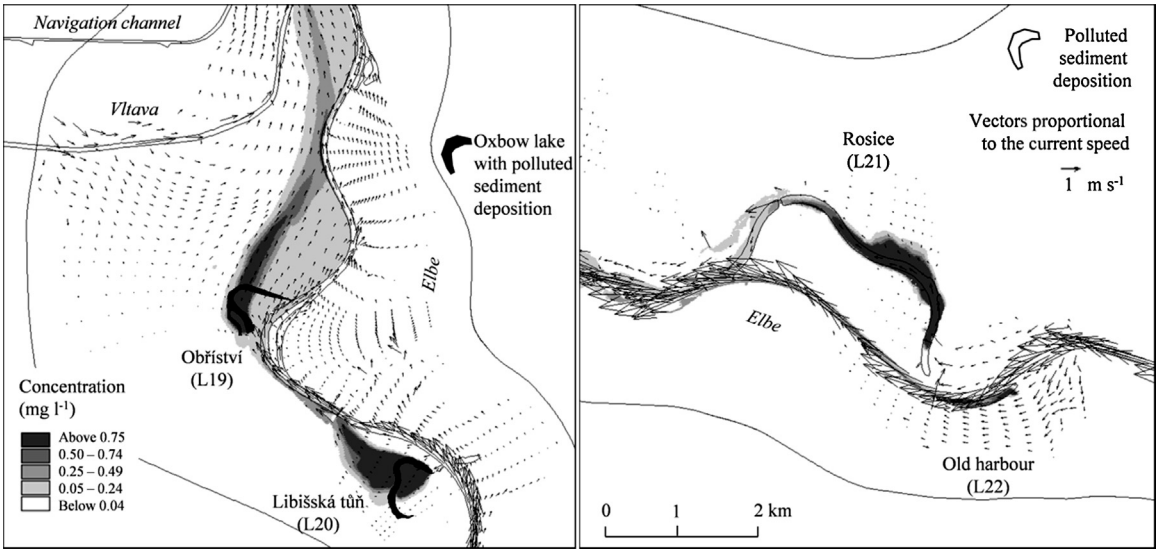

Fig. 4. Remobilization of fine-grained sediment layers at two selected sites. The left picture depicts L19 and L20 between the Spolana chemical plant and the Vltava confluence. Sediments are already progressively eroded after 1.5 days at the L19 site (Obříství) and after 10 h at the L20 site (Libišská tůň). Inundation is generated from the Elbe flood with RP corresponding to 50 years (Elbe discharge is 1480 $m^3 s^{-1}$, while Vltava discharge reached 1500 $m^3 s^{-1}$). The right picture depicts L21 and L22 downstream from the Paramo refineries. Sediments are eroded after flooding from upstream inundation (Elbe discharge is 912 $m^3 s^{-1}$).

Remobilization assessment was therefore based on criterion (o), considering the significant concentration contribution to the Elbe transient flow. Such situation occurred after an entire oxbow lake site was overflowed by the upstream inundation flow under much higher flow conditions (RP ≈ 50–100 years; $v = 0.6\ m\ s^{-1}$; $\tau = 1.4\ N\ m^{-2}$). (e) Sites L19 and L20 were also significantly affected by the Vltava tributary, which is the most significant runoff contributor to the Elbe. The remobilization assessment depended on the remoteness from the Vltava's main flow and on local current properties, and it was based on two scenarios: (i) During flooding from the Elbe (Fig. 3), both sites were connected to the transient flow and the local flow directions were nearly perpendicular to the Elbe's main course. Due to the depth and remoteness of the oxbow lakes, the flow parameters were smaller than at shallow sites ($v = 0.28 \pm 0.03\ m\ s^{-1}$; $\tau = 0.35 \pm 0.05\ N\ m^{-2}$) and the remobilization RPs were estimated as >100 and >50 years for L19 and L20, respectively. (ii) During flooding from the Vltava, the flow through site L19 was in the NW–SE direction, which diminished the erosive power due to its crossing a flat, cropland area. The flow conditions at remobilization were similar to the flood event generated from the Elbe even though remobilization occurred during flow with a smaller RP (RP ≈ 5 years; $v = 0.25\ m\ s^{-1}$; $\tau = 0.35\ N\ m^{-2}$). Due to its remoteness from the Vltava's main course, site L20 was only filled with a calm water column 5–6 m in depth and velocities were less than 0.01 $m\ s^{-1}$. Thus, the resulting τ of less than 0.001 $N\ m^{-2}$ was insufficient for erosion and remobilization was not observed even during the flood wave's regression.

The Bílina sites differ generally by the position of sediment layers within the channel. Deposits were primarily found burdened in bank structures or backwater areas. The remobilization criteria as defined for the Bílina were generally fulfilled after exposing those sediment deposits to transient flow conditions. Causal discharges (Table 5) greatly depended on site properties and varied from Q_{210} days near the confluence with the Elbe to Q_{10} years for the most stable site at the confluence with the left-tributary Bouřlivec stream. Local current speed after cross-sectional distribution dropped below 0.5 $m\ s^{-1}$, mostly 0.1–0.2 $m\ s^{-1}$ while average speed was generally three or four times higher at up to 0.8 $m\ s^{-1}$ at the time of remobilization. Such variation was multiplied by the different considerations of water depth properties and the ratio between shear stress distributed and averaged reaches up to 0.8/12 in the nearly prismatic channel at site B3. The causal flow remained within channel capacity that was sufficient for Q_{10} flow conditions throughout the entire reach.

The schematic plan (Fig. 5) depicts an overview of all sites sequentially listed in order to estimate the importance of each site as given by remobilization probability and remoteness from the German border. While the most remote sites (L19–L22, B5–B9) were evaluated as less vulnerable, as remobilization causal discharges had RPs of around Q_{50} or higher in the case of the Elbe and around Q_5 in the case of the Bílina, the nearest sites tended to be exposed to remobilization causal flow conditions at yearly or even sub-yearly frequency. The most exposed sites on the Elbe were found downstream from the confluence with the Ohře, chiefly downstream from the Lovosice industrial zone (downstream 790 km) and upstream from the border city Děčín (730 km).

3.3. Ecological aspects of the results

Water management authorities primarily operate on the basis of RP in addressing strategic measured design (e.g., flood protection). Situation maps (Fig. 6) thus serve as the summarizing output as they offer a comparison with flood extent maps (Floods Directive, 2007/60/EC).

Please cite this article in press as: Kaiglová, J., et al., Numerical modeling of heavily polluted fine-grained sediments remobilization in northern Czech Republic. Ecohydrol. Hydrobiol. (2015), http://dx.doi.org/10.1016/j.ecohyd.2015.02.001

Table 5
Flow conditions at remobilization criteria at the Bílina sites. M-daily discharges (not exceeded in M days per year) are marked in italics and bold ($\mathbf{Q_M}$), *N*-year discharges (with return period of n years) are in regular font (Q_n). Local flow conditions are distributed based on the conveyance distribution along the cross section (used) and cross section averaged.

Site ID	Chainage	Local discharge	RP	Local current speed distributed/cross section averaged	Local shear stress distributed/cross section averaged
Units	km	$m^3 s^{-1}$	$\mathbf{Q_M}$ **days**/Q_n years	$m s^{-1}$	$N m^{-2}$
B1	0.3	16	Q_1	0.2/0.3	0.8/2
B2	0.8	5	$\mathbf{Q_{210}}$	0.1/0.4	0.8/3
B3	10.1	24	$\approx Q_5$	0.2/0.8	0.8/12
B4	17.8	15.5	$\approx Q_1$	0.1/0.4	0.8/2.5
B5	29.8	20	$\approx Q_{10}$	0.1/0.5	0.8/5
B6	47.1	5	$\approx Q_5$	0.2/0.6	0.8/11
B7	51.1	4.5	$\approx Q_5$	0.5/0.6	0.8/9
B8	54.2	7	$\approx Q_5$	0.1/0.4	0.8/3.6
B9	54.8	3.6	$< Q_5$	0.1/0.4	0.8/3.6

During yearly occurring high-flow events, remobilization is expected at half of the sites. The most-exposed sites are situated along the Czech lower Elbe reach within the first 35 km (L2–4, L11) and consist mostly of harbor backwaters, as well as within the first 10 km of the Bílina tributary with its nearly prismatic channel. The expected Tr_{min} to the border profile in the case of a Q_1 flood event is 20 h. The sediment of downstream sites is heavily polluted, and particularly with DDT. The upper limit for DDT concentrations in sediment layers was exceeded in 88% of the samples from downstream Elbe sites (L1–L18), 50% of the samples upstream from the confluence with the Vltava, and 22% of the Bílina sediment deposit samples. The highest DDT value was found at site L5 in Děčín, where it alarmingly reached 871 $\mu g l^{-1}$. Sediment deposit remobilization causal discharge was evaluated as not exceeded only for 80 days per year. Toxin-bound sediments are therefore expected to contribute to the downstream Elbe pollution with yearly frequency. The value of 410 $\mu g l^{-1}$ DDT was measured at site B2 in Ústí nad Labem 800 m from the confluence with the Elbe. Deposits at B2 were evaluated as the most exposed to remobilization within the Bílina reach while causal discharge conditions were Q_{210} days. Although according to van der Veen et al. (2006) tributaries originating in the Ore Mountains have a high geochemical background of heavy metals, Hg, Ni, As and Cu concentrations greatly exceeded upper limits by as much as 143× (in the case of Ni concentration at site B6). Although the highest Hg concentrations were found at sites B2 and B8, upper limits were exceeded by 1–8.5× at all sites. In Elbe sediments, the highest exceedance of heavy metals was found at L15 (21.3× for Hg, 28.3× for Ni, 3.3× for Cd). Site L15 tends to be exposed to the remobilization process during flow conditions of Q_5 or higher.

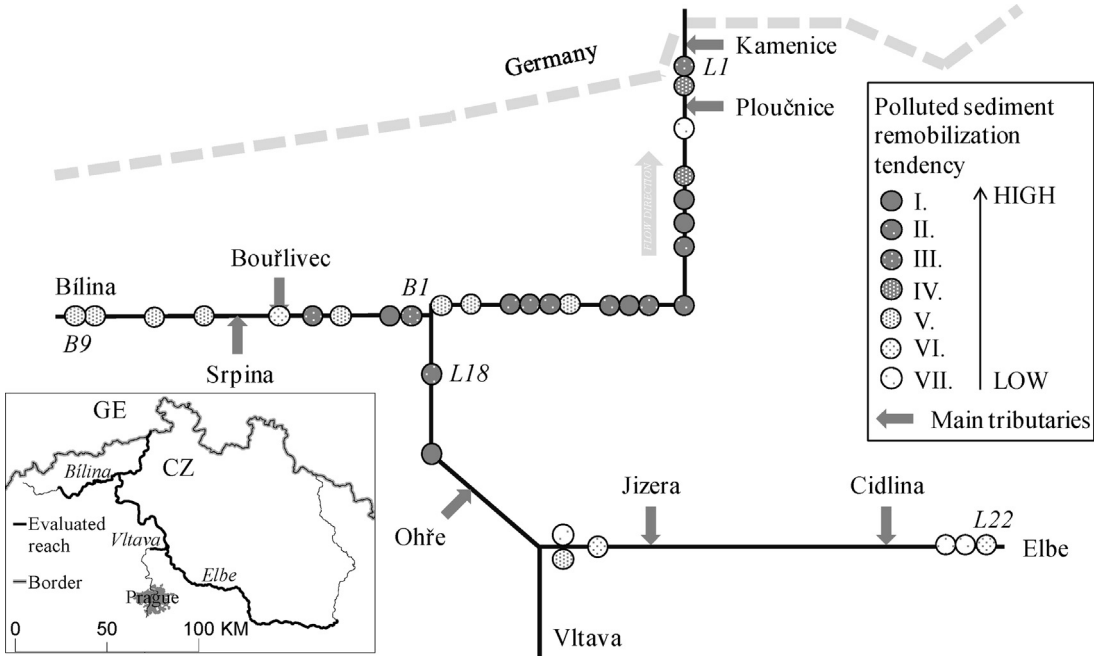

Fig. 5. Schematic plan of the evaluated river network with all sites classified based on causal flow conditions. Study sites are visualized from the border/confluence in ascending order.

Please cite this article in press as: Kaiglová, J., et al., Numerical modeling of heavily polluted fine-grained sediments remobilization in northern Czech Republic. Ecohydrol. Hydrobiol. (2015), http://dx.doi.org/10.1016/j.ecohyd.2015.02.001

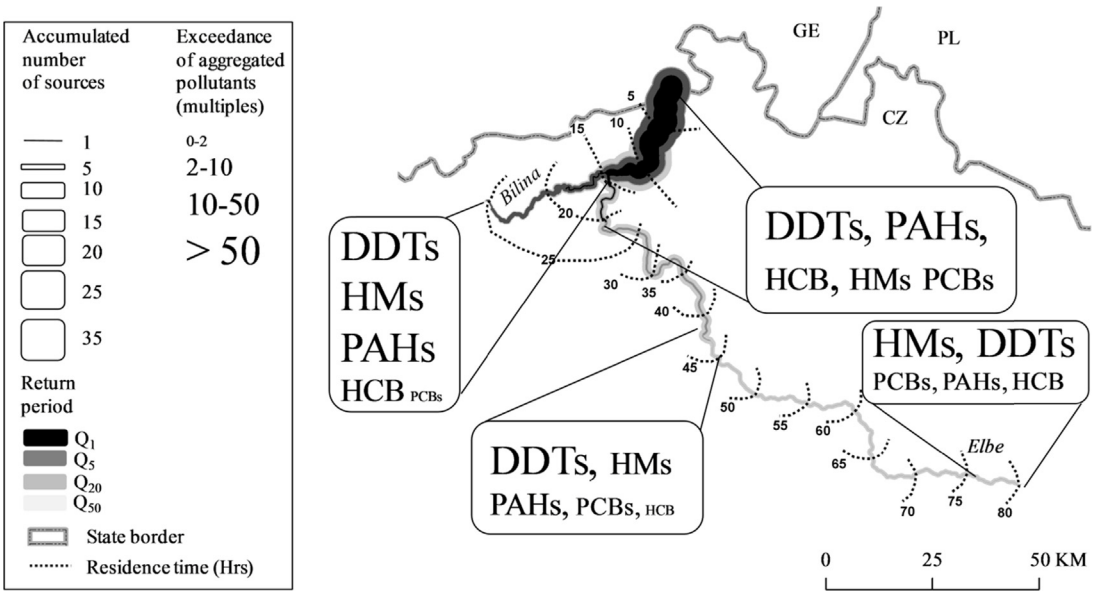

Fig. 6. Situation map of the entire area showing the overall situation at selected RP discharges (Q_1, Q_5, Q_{20}, Q_{50} and greater). Lines represent the number of secondary pollution sources propagating to the Elbe border profile at different RPs. The exceeded toxic substances are marked progressively according to the exceedance multiple of the upper limit concentration for Elbe sediments (FGG Elbe 2013). The accumulated number of upstream pollution sources at the profile Hřensko is 17 for Q_1, 29 for Q_5, 32 for Q_{20}, and 35 for Q_{50}.

4. Discussion

As reported by Förstner et al. (2004), the evaluation of experimental data shows there to be no simple correlation between cohesive sediment properties and critical shear stress. The results of principle component analysis show, however, that the most important properties include water content, bulk density, clay content and total organic carbon. Cohesive clay particles tend to aggregate into flocks of higher resistance and settling velocity (Houwing and van Rijn, 1998). The resistance to erosion is strengthened by the decreased permeability of the fine-particle bed, as described by such authors as Wu et al. (2008). The threshold conditions for fine-particle remobilization can further involve the sand–mud ratio (Van Rijn, 1993), organic material content (Grabowski et al., 2011), and pore water content (Winterwerp and van Kersteren, 2004). Moreover biotic factors can even significantly affect sediment resistance and settling velocity (Pores, 2009). The erosion rate generally stated declines with decreasing grain size and increasing sediment bulk density (Roberts et al., 1998).

The causal flow conditions at the remobilization of heavily polluted fine-grained deposits evaluated after fulfilling three objective criteria varied in the broad interval of velocities (0.12–0.89 m s^{-1}) and bed shear stresses (0.12–7.8 N m^{-2}). Nevertheless, by including the remobilization criterion (o), which considers the concentration's contribution to the main flow, flow parameters do not reflect threshold conditions for in situ scour development. We compared τ_c values obtained by studies on Central European water courses of a similar character. Schwartz (2006) proposed the interval 0.4–0.5 N m^{-2} for the uppermost sediment layer. The value resulted from τ_c in situ measurements, but it does not reflect local flow conditions during remobilization. Jacoub and Westrich (2006) estimated that τ_c in the Upper Rhine reached even 4 N m^{-2} by considering the highly cohesive properties of the studied sediment.

The study was focused on the remobilization tendency caused by the increasing flow activity at the flood wave rising limb. Carling et al. (2000) reported different tendency of the fine sand material on the Rhine secondary bed dunes accumulating during the rising limb and diminishing at the flow stagnation or decreasing tendency. Nevertheless, the fine-grained material is accumulated in calm slack water zones, thus this process is not expected. Witt and Westrich (2003) reported measuring τ_c with even greater variability (2–8 N m^{-2}). Although in our study a cohesive character was partly considered at all of the sites, deposits consisted of a mixture of clay, silt and finer sand particles with both unimodal and bimodal grain distribution. The limitation of the 2D hydrodynamic models used (MIKE 21 C) consists in their conceptualization of the vertical flow component. Although 3D schematization of sediment transport under shallow flow conditions would improve vertical velocity distribution (Jun et al., 2012), it is time- and data-demanding and often not suitable for reaches so large as those of the Elbe. In this study, the vertical component is conceptualized by the helical flow module.

The Bílina had to be schematized using a 1D horizontal plan description mainly due to its nearly prismatic long and narrow channel, which would otherwise require disproportionally extended computations consisting of small elements and thus result in extreme simulation times. Other reasons for this choice were that the only available source of bathymetric data was a database of cross sections at steps averaging 50–100 m, as well as the

Please cite this article in press as: Kaiglová, J., et al., Numerical modeling of heavily polluted fine-grained sediments remobilization in northern Czech Republic. Ecohydrol. Hydrobiol. (2015), http://dx.doi.org/10.1016/j.ecohyd.2015.02.001

Table 6
Comparison of results obtained by 1D shear stress map evaluation and 2D sediment transport calculation. Adopted according to Kaiglová et al. (2015).

Site chainage km from confluence	Site description	τ (N m^{-2})			Q (m^3 s^{-1})		
		1D	2D	Δ%	1D	2D	Δ%
55.040–54.770	Downstream from weir	0.8	1	20	5	5.8	13.8
54.680	Upstream from collapsed bridge	0.8	0.8	0	3.6	3.8	5.3
54.668	Downstream from collapsed bridge	1	1.1	9.1	4.5	7.9	43
54.285–54.005	Middle reach banks	1	1	0	7	8	12.5
53.780–53.605	Lower reach banks	0.9	0.8	12.5	7	6.8	2.9

existence of numerous structures where energy loss would need to be well described. The problem was therefore simplified and conceptualized as the exploration of shear stress map based on flow parameter distribution across and along the channel. The threshold shear stress value was based on experience gained from Elbe modeling and verified in the experimental study by applying the 2D model to reaches in B9–B8 (see Kaiglová et al., 2015) and comparing the causal discharge evaluation results of bed shear stress map analysis with causal discharge evaluation results obtained by detailed 2D modeling (Table 6). For instance the bed shear stress at the time of remobilization was compared for the two approaches as well. The comparison successfully proved the simplified concept's applicability at 80% of monitored sites.

The RP assessment served to link results of different geographic conditions and express the significance of individual results in terms of environmental risk assessment. The remobilization classes were therefore purpose-built and ranged from the highest tendency of sediment resuspension (I), meaning the highest probability of remobilization within contemporary hydrologic conditions, to the lowest tendency (VII). Nevertheless, our result classification does not reflect environmental impact after sediment entrainment.

The basic assumption was adopted that contaminated sediments can be transported for long distances, as in the study of Jacoub and Westrich (2006) from the Rhine basin. Nevertheless, sediment transport is predetermined by flow velocity. Thus, slack water zones (Schwartz, 2006), abandoned channels (Büttner et al., 2006), and inland harbors (Förstner et al., 2004) usually function as sediment sinks and owners must cover remediation expenses for emissions from the entire upper basin. While there is no information on the real effect of the resuspended sediment deposition in the Elbe cascade an analysis based on the Tr_{min} evaluation and weir cascade schematization was processed to bring an idea on the general question "What if the wash load concept is unrealistic?"

Tr_{min} (h) was calculated for all study sites and classified into 7 classes: (I) less than 11.5, (II) 11.5–23.0, (III) 23.1–34.5, (IV) 34.6–46.0, (V) 46.1–57.5, (VI) 57.6–69.0, and (VII) more than 69.0. The residence time parameter was considered by averaging two classification systems, the first obtained by RP classification, the second by Tr_{min} classification (Fig. 7). The new classification emphasizes

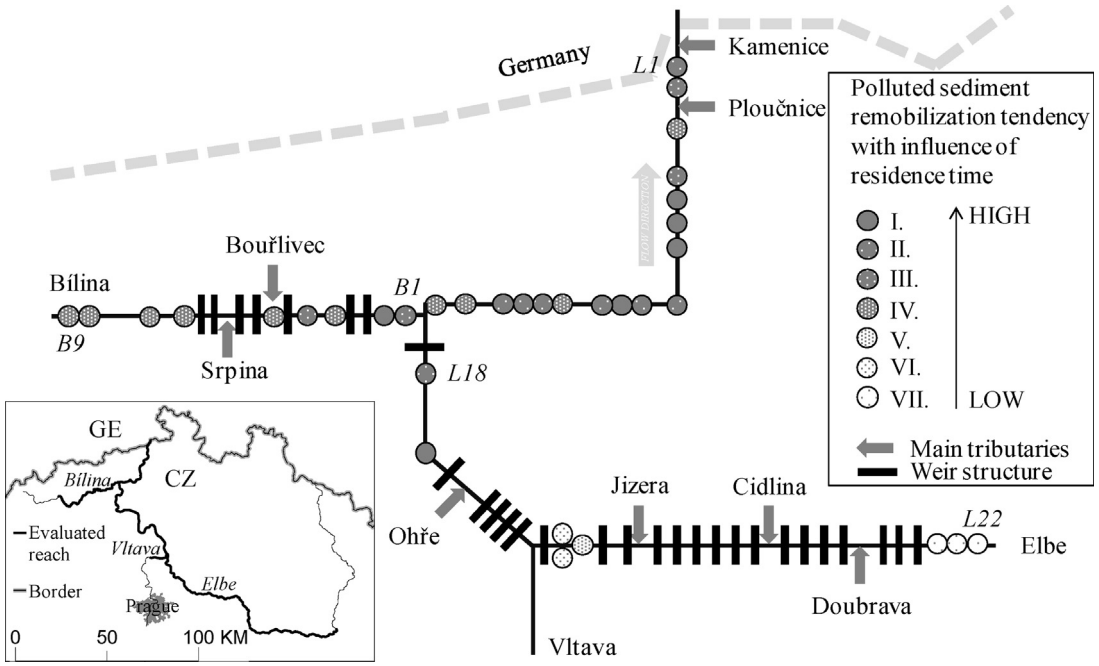

Fig. 7. Schematic plan of the evaluated river network with all sites classified according to causal flow conditions updated with the parameter of Tr_{min} (average class). Study sites are visualized from the border/confluence in ascending order. Weirs, as potential sinks of suspended sediments, are marked by black rectangles.

Please cite this article in press as: Kaiglová, J., et al., Numerical modeling of heavily polluted fine-grained sediments remobilization in northern Czech Republic. Ecohydrol. Hydrobiol. (2015), http://dx.doi.org/10.1016/j.ecohyd.2015.02.001

the importance of proximity to the border. Sites located near the border have greater importance for transport toward downstream reaches than do remote sites.

Furthermore, a visualization was employed of important flow obstacles which reduce the transport potential of the entire water course flow and may have a sediment trapping function. A significant number of structures are located upstream from the confluence with the Bílina on both examined courses. The real effect is nevertheless difficult to estimate once we are dealing with flood events during which the structures are not in operation and an unknown amount of water entering the dammed reach leaves immediately. Such condition was not therefore included into this study.

5. Conclusion

The tendency of sediment deposits to be remobilized during extraordinary flow conditions was tested at 31 sites on the Upper Elbe and one of its left tributaries, the Bílina, regarded as the important source of Elbe River pollution. A total of 113 km of river stretches were analyzed using 4 hydrodynamic models (schematized in MIKE by DHI, chiefly MIKE 21 C, MIKE 11 and MIKE 21) of different extents and horizontal plan schematizations coupled with sediment transport interactive simulation.

We have proposed causal site-specific discharges of significant polluted deposits remobilization with return periods ranging from <1 to >100 years depending on the site-specific hydrodynamic conditions during the flood event, mainly the connection with the main channel transient flow. Relativizing causal discharges using the return period assessment led to detection of the most crucial sites for future environmental risk mitigation.

The statistical evaluation highlighted areas of special interest, most of which are situated up to 35 km upstream of the German border and with competent discharges reached even during 150 days within an average year.

Flow parameters at remobilization were observed within the range 0.12–0.89 m s^{-1} in the case of depth-averaged velocities and within 0.12–7.8 N m^{-2} in the case of bed shear stresses.

As seen in the qualitative survey of sediment deposits, numerous toxic pollutants (DDTs, PCBs, TBT, heavy metals) were found to occur in alarming concentrations at all sites. The results' environmental aspects were therefore discussed with a view to the threat of secondary pollution of downstream aquatic ecosystems.

The study's primary contribution is to identify threshold values for potential remobilization of sediment burdened by old loads in different environments associated with a similar problem. These threshold values can serve as important information for identifying and mitigating risks related to old loads and hydrological extremes.

Conflict of interest

None declared.

Financial disclosure

This study was conducted as part of the project "SedBiLa", Bedeutung der Bílina als historische und aktuelle Schadstoffquelle für das Sedimentmanagement im Einzugsgebiet der Elbe and "SedLa" Bedeutung der Altsedimente der Elbe und ihrer Seitenstrukturen im Abschnitt von Pardubice bis Moldaumündung in the framework of the international initiative ELSA (Schadstoffsanierung Elbsedimente), provided by the Hamburg Department for Urban Development and the Environment (Freie und Hansenstadt Hamburg – Behörde für Stadtentwicklung und Umwelt) and agreed by the International Commission for the Protection of the Elbe River (ICPER). The research presented in this paper was supported by Czech Science Foundation project GAČR P209/12/0997 "The impact of landscape disturbance on the dynamics of fluvial processes".

Acknowledgements

The first author thanks to DHI a.s. for providing software support.

References

Aksoy, H., Kavvas, M.L., 2005. A review of hillslope and watershed scale erosion and sediment transport models. Catena 64 (2–3), 247–271.
Ariathurai, C.R., 1974. A Finite Element Model for Sediment Transport in Estuaries. (PhD thesis)University of Carolina, Berkley.
Borovec, Z., 1995. Zatížení sedimentů Labe a jeho přítoků toxickými prvky.(Toxic pollution load of the sediment of Elbe River and tributaries). Geografie – Sborník ČGS 100 (4), 268–274 (in Czech).
Büttner, O., Otte-Witte, K., Krüger, F., Meon, G., Rode, M., 2006. Numerical modelling of floodplain hydraulics and suspended sediment transport and deposition at the event scale in the middle river Elbe, Germany. Acta Hydrochim. Hydrobiol. 34, 265–278.
Buzek, L., 2000. Eroze lesní půdy při vyšších vodních srážkách a tání sněhové pokrývky (na příkladu střední části Moravskoslezských Beskyd).(Forested soils erosion during high precipitation snow melting events). Geografie – Sborník ČGS 105 (4), 317–332 (in Czech).
Cai, T., Li, Q., Yu, M., Lu, G., Cheng, L., Wei, X., 2012. Investigation into the impacts of land-use change on sediment yield characteristics in the upper Huaihe River basin, China. Phys. Chem. Earth 53–54, 1–9.
Carling, P.A., Gölz, E., Orr, H.G., Radecki-Pawlik, A., 2000. The morphodynamics of fluvial sand dunes in the River Rhine, near Mainz, Germany, I. Sedimentology and morphology. Sedimentology 47, 227–252.
Chalupová, D., Havlíková, P., Janský, B., 2012. Water quality of selected fluvial lakes in the context of the Elbe River pollution and anthropogenic activities in the floodplain. Environ. Monit. Assess. 184 (10), 6283–6295.
DHI, 2012. MIKE 11, MIKE 21 & MIKE 3 Flow Model – Scientific Documentations. Horstholm.
Droppo, I.G., Liss, S.N., Williams, D., Nelson, T., Jaskot, C., Trapp, B., 2009. Dynamic existence of waterborne pathogens within river sediment compartments. Implications for water quality regulatory affairs. Environ. Sci. Technol. 43 (6), 1737–1743.
Enggrob, H.G., Tjerry, S., 1998. Simulation of morphological characteristics of a Braided River. In: Proc. of the 1st IAHR Symposium on River, Coastal, and Estuarine Morphodynamics, Genova, pp. 585–594.
FGG, 2013. Sedimentmanagementkonzept der FGG Elbe. Vorschläge für eine gute Sedimentmanagementpraxis im Elbegebiet zur Erreichung überregionaler Handlungsziele. Flussgebietsgemeinschaft Elbe, Deutschland.
Floods Directive, 2007/60/EC.
Förstner, U., Heise, S., Schwartz, R., Westricht, R., Ahlf, W., 2004. Historical contaminated soils at the River Basin Scale. J. Soils Sediments 4 (4), 247–260.
Grabowski, R.C., Droppo, I.G., Wharton, G., 2011. Erodibility of cohesive sediment: the importance of sediment properties. Earth Sci. Rev. 105 (3–4), 101–120.

Please cite this article in press as: Kaiglová, J., et al., Numerical modeling of heavily polluted fine-grained sediments remobilization in northern Czech Republic. Ecohydrol. Hydrobiol. (2015), http://dx.doi.org/10.1016/j.ecohyd.2015.02.001

Guerrero, M., Lamberti, A., 2013. Bed-roughness investigation for a 2-D model calibration: the San Martín case study at Lower Parana. Int. J. Sediment Res. 28 (4), 458–469.

Haddadchi, A., Ryder, D.S., Evrard, O., Olley, J., 2013. Sediment fingerprinting in fluvial systems: review of tracers, sediment sources and mixing models. Int. J. Sediment Res. 28 (4), 560–578.

Hardy, R.J., 2013. Process-based sediment transport modeling. In: Shroder, J., Baas, F.A. (Eds.), Treatise on Geomorphology, vol. 2. Elsevier, pp. 147–159.

Heininger, P., Pelzer, J., Claus, E., Pfitzner, S., 2003. Results of long-term sediment quality studies on the River Elbe. Acta Hydrochim. Hydrobiol. 31, 356–367.

Heise, S., Krüger, F., Förstner, U., Baborowski, M., Götz, R., Stachel, B., 2008. Bewertung von Risiken durch Feststoffgebundene Schadstoffe im Elbeeinzugsgebiet. In: Zusammenfassungen der Studien. Hamburg Port Authority, Hamburg.

Houwing, E.J., van Rijn, L.C., 1998. In situ erosion flume (ISEF): determination of bed shear stress and erosion of a kaolinite bed. J. Sea Res. 39, 234–253.

Jacoub, G., Westrich, B., 2006. Modelling transport dynamics of contaminated sediments in the headwater of a hydropower plant at the Upper Rhine River. Acta Hydrochim. Hydrobiol. 34, 279–286.

Janský, B., Schulte, A., Česák, J., Rios Escobar, V., 2010. Mladotické jezero, západní Česko: jedinečná geneze a vývoj jezerní pánve. Geografie – Sborník ČGS 115 (3), 266–274.

Jánský, B., Langhammer, J., Calupová, D., Kliment, Z., Šobr, M., 2013. Project SebBiLa (Význam Bíliny jako historického a současného zdroje znečištění pro nakládání se sedimenty v povodí Labe). Vzorkovací plán, Praha.

Jun, Q., Zhifeng, Y., Zhenyao, S., 2012. Three-dimensional modeling of sediment transport in the Wuhan catchments of the Yangtze River. Procedia Environ. Sci. 13, 2437–2444.

Jurajda, P., Adámek, Z., Janáč, M., Valová, Z., 2010. Longitudinal patterns in fish and macrozoobenthos assemblages reflect degradation of water quality and physical habitat in the Bílina river basin. Czech J. Anim. Sci. 55 (3), 123–136.

Kaiglová, J., Langhammer, J., Jiřinec, P., Janský, B., Chalupová, D., 2015. Numerical simulations of heavily polluted fine-grained sediment remobilization using 1D, 1D+ and 2D channel schematization. Environ. Monit. Assess. 3 (115), 1–18.

Kerner, M., 2007. Effects of deepening the Elbe Estuary on sediment regime and water quality. Estuar. Coast. Shelf Sci. 75, 492–500.

Kiat, C., Ghani, C.A., Abdullah, A., Zakaria, R.N.A., 2008. Sediment transport modeling for Kulim River – a case study. J. Hydro-Environ. Res. 2 (1), 47–59.

Kliment, Z., 2005. Plaveniny jako produkt a indikátor vodní eroze půdy v geograficky rozdílných podmínkách České republiky. J. Hydrol. Hydromech. 53 (4), 231–244.

Komar, P.D., 1988. Sediment transport by floods. In: Baker, V.R., Kochel, R.C., Patton, P.C. (Eds.), Flood Geomorphology. Wiley, New York.

Krone, R.B., 1962. Flume Studies of the Transport of Sediment in Estuarial Shoaling Processes. Technical Report, Hydraulic Engineering Laboratory, University of California, Berkeley.

Krüger, F., Schwartz, R., Kunert, M., Friese, K., 2006. Methods to calculate sedimentation rates of floodplain soils in the middle region of the Elbe River. Acta Hydrochim. Hydrobiol. 34, 175–187.

Langhammer, J., 2007. Modelling the Elbe River water quality changes. In: Dostál, P., Langhammer, J. (Eds.), Model. Nat. Environ. Soc. PřF UK, Praha.

Langhammer, J., 2010. Water quality changes in the Elbe River basin, Czech Republic, in the context of the post-socialist economic transition. GeoJournal 75, 185–198.

Matoušková, M., Dvořák, M., 2011. Assessment of physical habitat modification in the Bílina River Basin. Limnetica 30 (2), 293–306.

Medek, J., Hájek, P., Král, S., Skořepa, J., Hönig, J., Kokšal, J., Neuhöfer, M., Bednárek, J., Janský, B., Langhammer, J., Chalupová, D., Jiřinec, P., Indeguldová, E., Kaiglová, J., 2014. SedBiLa – Bedeutung der Bilina als historische und aktuelle Schadstoffquelle für das Sedimentmanagement im Einzugsgebiet der Elbe. Project report. Povodi Labe, Hradec Kralove. 80 pp. Retrieved from: http://elsa-elbe.de/assets/pdf/Fachstudie_Sedbila_DE.pdf.

Petrůjová, T., Rudiš, M., 1996. Sledování plavenin a sedimentů v povodí Labe, Moravy a Odry. Návrh metod, metodik a ukazatelů pro odběry vzorků a jejich vyhodnocování (Monitoring of Sediment in the Elbe, Morava and Odra Basin. Methodological approach).Úvodní projekt. ČHMÚ, VÚV, Praha (in Czech).

Pores, S., 2009. Meiobenthology. Springer-Verlag, Berlin.

Povodi Labe, s.p., 2012. Project SebBiLa (Význam Bíliny jako historického a současného zdroje znečištění pro nakládání se sedimenty v povodí Labe), Vzorkovací plán. Hradec Králové (Importance of Bílina as the Historical and Current Source of Pollution of the Elbe River). (in Czech).

Povodí Ohře, s.p., 2010. Studie záplavového území toku Bílina Ústí nad Labem – Liběšice (km 0.000–40.250) Libešice – Ervěnický koridor (aktualizace) (km 40.000–61.200) (Flood Extend Assessment of Bílina River from Ústí nad Labem to Ervěnirký koridor).Povodí Ohře, státní podnik, Chomutov (in Czech).

Přibylová, P., Klánová, J., Holoubek, I., 2006. Screening of short- and medium-chain chlorinated paraffins in selected riverine sediments and sludge from the Czech Republic. Environ. Pollut. 144 (1), 248–254.

Roberts, J., Jepsen, R., Gotthard, D., Lick, W., 1998. Effects of particle size and bulk density on erosion of quartz particles. J. Hydraul. Eng. 124 (12), 1261–1267.

Rudiš, M., 2000. Assessment of polluted sediments in canalised section of the Czech Elbe River. J. Hydrol. Hydromech. 58 (1), 32–51.

Rudiš, M., Hájek, R., Hrubec, K., 2007. Determination of different types of sediments in a river reservoir and computation of their volumes. J. Hydrol. Hydromech. 55 (4), 213–222.

Rudiš, M., Valenta, P., Nol, O., 2008. Effects of Polluted Sediments in Flood Plains on Environment and Ground Water. VÚV T.G.M., Praha.

Schwartz, R., 2006. Geochemical characterization and erosion stability of fine-grained gryone field sediments of the Middle Elbe River. Acta Hydrochim. Hydrobiol. 34, 223–233.

Segura, R., Arancibia, V., Zúniga, M.C., Pastén, P., 2006. Distribution of copper, zinc, lead and cadmium concentrations in stream sediments from the Mapocho River in Santiago, Chile. J. Geochem. Explor. 91 (1–3), 71–80.

Simpson, G., Castelltort, S., 2006. Coupled model of surface water flow, sediment transport and morphological evolution. Comp. Geosci. 32, 1600–1614.

van der Veen, A., Ahlers, C., Zachman, D., Friese, W.K., 2006. Spatial distribution and bonding forms of heavy metals in sediments along the middle course of the River Elbe (km 287–390). Acta Hydrochim. Hydrobiol. 34, 214–222.

Van Rijn, L., 1993. Principles of Sediment Transport in Rivers, Estuaries and Coastal Seas. Aqua Publications, Amsterdam.

Walling, D., Fang, E.D., 2003. Recent trends in the suspended sediment loads of the world's rivers. Global Planet. Change 39, 111–126.

Winterwerp, C., van Kersteren, W.G., 2004. Introduction to the physics of cohesive sediment dynamics in the marine environment. In: van Loon, T. (Ed.), Developments in Sedimentology. Elsevier B.V., Amsterdam.

Witt, O., Westrich, B., 2003. Quantification of erosion rates for undisturbed cohesive sediment cores by image analysis. Hydrobiologia 494, 271–276.

Wu, B., van Maren, D., Li, S.L., 2008. Predictability of sediment transport in the Yellow River using selected transport formulas. Int. J. Sediment Res. 23 (4), 283–298.

Yang, C., Huang, T., Greimann, J.B.P., 2004. User's Manual for GSTAR-ID (Generalized Sediment Transport Model for Alluvial Rivers – One Dimension), version 1.0. U.S. Bureau of Reclamation, Technical Service Center, Denver.

Zeng, S., Dong, X., Chen, J., 2013. Toxicity assessment of metals in sediment from the lower reaches of the Haihe River Basin in China. Int. J. Sediment Res. 28 (2), 172–181.

Please cite this article in press as: Kaiglová, J., et al., Numerical modeling of heavily polluted fine-grained sediments remobilization in northern Czech Republic. Ecohydrol. Hydrobiol. (2015), http://dx.doi.org/10.1016/j.ecohyd.2015.02.001

NUMERICAL MODELLING OF GRAVEL REMOBILIZATION COMPETENCE IN MOUNTAIN STREAM

Jana Kaiglová, Jakub Langhammer

Department of Physical Geography and Geoecology, Charles University in Prague, Albertov 6, Czech Republic, jana.kaiglova@gmail.com, jakub.langhammer@natur.cuni.cz

Abstract

The montane streams represent highly dynamic water courses with fast runoff response on precipitation events. The consequences of rainfall-runoff processes are remaining within the channel in the form of changing morphology. The dramatic changes can be expected even with return period of one year. The study represents an application of the theoretical concepts of sediment transport initialization phase within an integrated numerical modelling system at the local scale. The causal flow parameters of gravel remobilization as results of the hydrodynamic simulations were explored within two fluvial-morphological simulation sets. First the conventional grain size parameter D_{50} was used within the event based reconstruction of the largest recorded flood in July 2013. Further the grain distribution frequency was discretized within the percentile classes that entered the model setup separately. Results of the discretization were analysed by the so called remobilization rating curves, designed and constructed as a tool for the remobilization competence evaluation.

Keywords

Gravels. Bed load. Modelling. Remobilization. Šumava.

INTRODUCTION

The connection between transport of sediments and hydraulic flow properties has been one of the general water resources management issues. Since the 19th century numerous works have aimed to establish the relation between sediment properties, flow velocity/power and the sediment transport mode and rate. For simplification purposes, the process can be divided into three parts, even though it is continuous certainly: Initialization (erosion, remobilization), Transport (load), and Sedimentation (accumulation). Fluvial morphology and its variability can be studied by several approaches: fieldwork (e.g. Yu et al., 2009), physical experimental models (e.g. Abderrezzak et al., 2013) or numerical modelling based on theoretical or conceptual description of real-case processes (e.g. Fang et al., 2008; Aggett and Wilson, 2009). The individual flow characteristics mostly predetermine the transport rate and consequently the type of sediments bedded (e.g. Allen, 1965), the channel morphology (Wyrick et al., 2013) and the horizontal plan evolution (e.g. Aggett and Wilson, 2009).

It is the grain size playing the key role in the understanding of the transport dynamics and sediment distribution within a catchment. It influences the erodibility, mean of transport, and settling velocity and according to Dade (2000) even the whole alluvial channel pattern of meandering vs. braided streams. Regarding the bed load of the gravel sediments according Meyer-Peter and Müller (1948) the settling velocity cannot exceed the excess shear stress and the particle is dragged on the bed. Dealing with the suspended load more complexity has to be accounted while according to Galapatti (1983) the suspended load is resulting from advection, diffusion and settling mechanisms. The sediment transport problem is often regarded in the form of sediment transport capacity, defined as the state of equilibrium established at the channel bottom (Vanoni, 1984).

As for initiation of particle movement, current studies are usually dealing with the relation of flow velocity and particle movement (e.g. Huang et al., 2006; Grabowski et al., 2011; Hardy, 2013). The frequently applied concept is relating disturbing forces τ_e (Excess shear stress [$N \cdot m^{-2}$]) inflicting the particle once the bed shear stress τ or shear velocity u [$m \cdot s^{-1}$] exceeds an threshold value of particle resistance due to gravity or cohesion τ_c (Critical shear stress) (e.g. Breusers, 1985). Beside the appropriate sediment transport description the

problem of sufficiently accurate flow parameter calculation plays a crucial role while pre-requesting the hydrodynamic variable values further used as a basis for sediment transport model as e.g. flow velocity, water depth or shear stress (Guerrero and Lamberti, 2013). According to Simpson and Castelltort (2006), Yang et al. (2004) and Kiat et al. (2008) flow and sediment transport should be simulated simultaneously while they are significantly affecting each other.

The study being processed on the 430 m long reach upstream the confluence with the recipient aimed to meet the following objectives. (1) To outline the reconstruction of the causal hydrodynamic conditions of the morphological changes during the high flow event in June 2013 with the return period of Q_2 – Q_5. (2) To propose and test the innovative assessment method of the sediment remobilization so called remobilization rating curve. The method is aiming to serve for the sediment remobilization competence of river reaches evaluation regardless the geographical conditions while including the runoff and grain size relativization.

MATERIAL AND METHODS

The case study is located at Javoří brook (Šumava Mts.; Czech Republic) that represents a small mountain stream with the catchment draining an area of 11 km^2. The location in the core of the Šumava National park allowed the natural dynamic evolution of numerous fluvial forms. Despite the high altitude (1172 ±139 m a. s. l.) and slope gradients (Ø catchment slope equals 11.2 %) of the upstream reaches the studied part near the confluence with the recipient Roklanský brook has quite mild longitudinal bed slope of 7‰ (Fig. 1) that according to Warburton et al. (2002) inhibits coarse bed load transport and encourages overbank sedimentation. The studied reach describes 430 m (while measured along the channel axis) of the river channel and riparian zonesand includes 6 active bank erosion structures and 4 extended accumulation bodies consisted of gravel material of various grain sizes. properties.

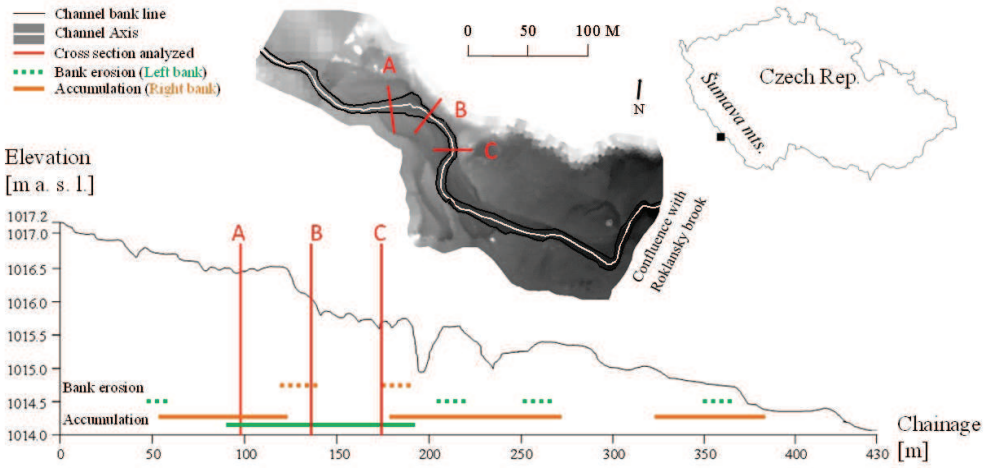

Fig. 1 Study location and characteristics - upper is the horizontal plan of Javoří brook represented by the model bathymetry, lower is the longitudinal bed slope of the studied reach with accumulations (solid line) and erosions (dotted line) localities and extends

The channel morphology as a consequence of former high flow stream power effects is changing dynamically with even yearly occurring (Q_1) flow conditions. The most recent extended morphological changes were observed during the summer flood event recorded in June 2013 (that corresponds to the magnitude of return period Q_2-Q_5). The June 2013 flood event was also the highest recorded within the 4 years long period of water stage data collection. The average runoff conditions (Q_a = 0.5 m^3·s^{-1}) were exceeded more than 20-

times.In the Upper Vydra basin mouth profile Modrava 5.3 km downstream from the locality the discharge reached 42.3 $m^3 \cdot s^{-1}$ (Q_a = 3.5 $m^3 \cdot s^{-1}$) during the fast flood wave culmination. The continuous monitoring of water depths is provided since the beginning of the 2010 hydrological year by two automatic gauges installed 1.2 km upstream the studied reach upper boundary. First is situated at Javoří brook (Ultrasonic based) upstream the confluence with Tmavý brook and second on the Tmavý brook (Pressure based). The proximity of the two devices allows the summing up the data and compounded hydrograph. The rating curve of the water level-discharge relationship results from (1) the field hydrometric measurements that are due to the remoteness of the studied locality and unpredictability of extreme flood events scarce regarding the high flow information. Thus the extrapolation towards the higher magnitude discharges had to be processed. The standard methods of the extrapolation by logarithmic, exponential and power curve equations using the R^2 objective criteria were tested with the large deviations and magnitudes in the higher water level area. (2) The best fit with measured data and the most realistic extrapolation was processed by fully dynamic numerical simulation of the 1D hydrodynamic model of the confluence with structures implemented (Fig. 2).

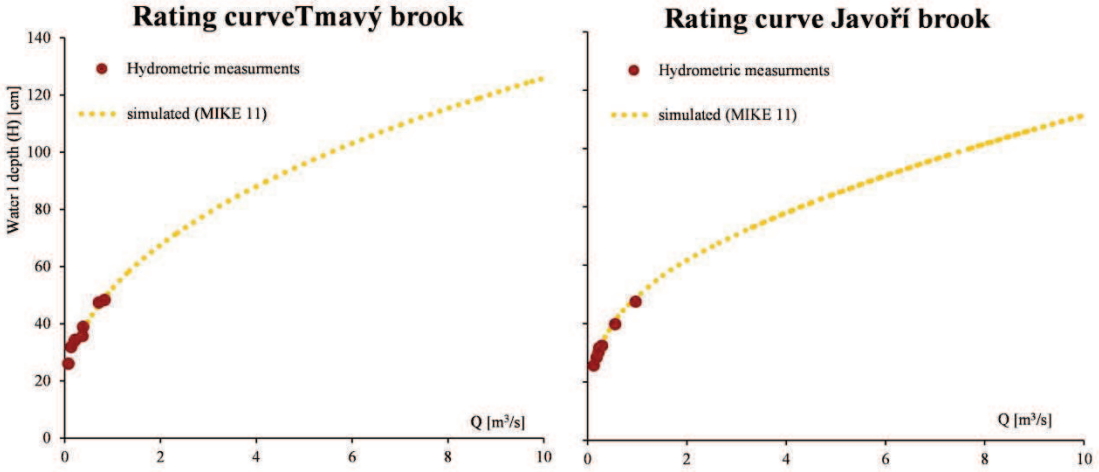

Fig. 2 Rating curve for the water level measurements of Javoří and Tmavý brooks resulting from the fully dynamic 1D hydrodynamic model (MIKE 11)

The DEM (Digital Elevation Model) for the model bathymetry construction was based on three data sources. (1) The submerged parts of the channel were measured with Geodetical GPS device with respect to the dominant break lines in the bed topography. (2) Not submerged zones were derived from the detailed UAV (Unmanned Aerial Vehicles) photogrammetry with vertical and horizontal resolution less than 1 cm (Langhammer et al., 2014). (3) The surrounding flood plains were filled with digital relief model of 4th generation DMR 4G (ČÚZK-Český úřad zeměměřický a katastrální).

The sediment survey was processed in the field in order to obtain the spatially distributed overview. The measurement techniques of the surface bed layer material were based on the concepts of manual and optical measurement in matrix (Bunte and Abt, 2001). The manual method was applied in the submerged parts of the channel (4 sampled sites) while the riparian fluvial accumulations (4 sampled accumulations based on the evaluation of 28 pictures) were analysed by Sedimetrics optic granulometry software (LUEL, 2005). The values of percentiles corresponding to the diameter of the 10 – 90 % of the sample (D_{10} – D_{90}) were calculated for the sediment characteristics relativization. The sediments of the river bed were of coarser character (D_{50} = 51.3±7.2 mm; D_{10} = 30.0±2.6 mm; D_{90} = 103.3±14.6 mm) than the not-submerged localities (D_{50} =36.4±5.3 mm; D_{10} = 10.8±2.5 mm; D_{90} = 100.1±16.4 mm). The remobilization assessment was done for grain sizes ranging from D_{40} – D_{90}.

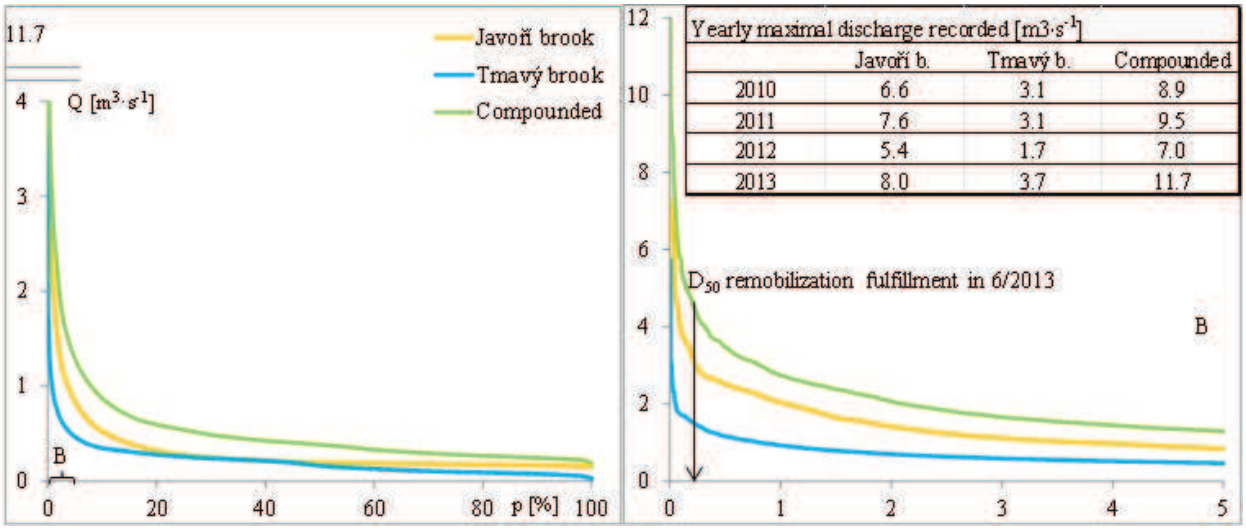

Fig. 3 Compounded discharge downstream the confluence for the period from 2010 - 2013 at Javoří and Tmavý brooks . On the left is the whole range of exceeding probability on the right is the range covering highest discharges (exceeded in less than 5 % of the cases)

Course of curves represents the frequency distribution of individually recorded discharges exceedingly (Fig 3) served for the frequency of causal discharges evaluation. The construction of the frequency curves was based at hourly intervals, averaged values in order to eliminate random fluctuations. The flood event in June 2013 was the largest recorded with the culmination discharge value of 11.7 $m^3 \cdot s^{-1}$ thus the discharges analysed within the study dispose the lowest probability of exceeding. The second highest flood event with the peak value of 9.5 $m^3 \cdot s^{-1}$ was recorded in July 2011.

Hydrodynamic and sediment transport modelling

In order to understand and relate the flow parameters to the movement initialization the numerical two dimensional (2D) hydrodynamic modelling (HD) tool MIKE 21C (Curvilinear) was used for the objective design set up and parameterization. The average cell size was 0.5 x 0.5 m however the curvilinear grid size is varying in both the x and y direction according the degree of curvature applied (DHI, 2012). The simulations were based on the fully dynamic unsteady solution of the depth averaged shallow water equations that in the case of highly variable channel characteristics and fast runoff conditions required the time step reduction on 0.15 s. The velocities at normal flow conditions were verified by field measurement with ultrasonic flow-meter (Flow-tracker). Nevertheless due to the lacking observations at higher flows the sensitivity analysis of the riverbed roughness involving both the hydrodynamic and sediment transport modelling was processed and the maximal possible result misevaluation was accepted. The roughness coefficient in the form of Manning's M [$m^{1/3} \cdot s^{-1}$] (Strickler coefficient $K_s = 1/n$) was varied within the range given by Chow (1959) for gravel bed mountain streams chiefly 20 – 33 for non-vegetated channel, 21 – 34 for the accumulation bodies covered by finer than channel material and 14 – 33 for the floodplain vegetated by high dense grass. The sediment transport module MIKE 21 C RM (River Morphology) is based on the flow parameter calculations that represent the variables of the selected transport equations nevertheless by varying topography as result of the sediment balance calculation the module gives feedback to the HD to create the interactive coupled system.

The Smart and Jaeggi (1983) transport theory was used. It represents a modification of Meyer-Peter Müller formula broadly used for gravel bed load evaluation by including the parameter of inequality in the grain diameter distribution ($D_{90} – D_{10}$). The inequality of non-cohesive sediments was further treated in the separate runs of the model in order to establish

the curve of the remobilization potential of individual sediment fractions by site specific flow conditions. The remobilization rating curves were constructed by using the relative statistical distribution of the granulometry and flow properties in order to dismiss the absolute site specific values.

In order to eliminate the transport caused by setting of the adequate flow conditions at the beginning of the runs the initial conditions were based on the hot start calculated by the average flow conditions with sediment transport included. The same procedure was applied by Li et al. (2008) and improved the results notably.

In order to ensure the objectivity of sediment transport initialization result evaluation the remobilization criteria as an arbitrary set threshold was defined based on the bed level change variations (1). The criteria varied with the sediment spatial extend and granulometric curve properties.

$$z_{t+1} - z_t \leq -(D_i) \quad (1)$$

Where z represents bed level [m a. s. l.], D is the grain diameter [m] of the i percentile [%].

RESULTS

First the conventional characteristics of D_{50} grain size were used in order to evaluate the overall remobilization characteristics during the flood event June 2013. The initiation of grain movement arbitrary defined by the remobilization criteria has been observed at three cross sections (A, B, C),located in the most dynamic reach, by comparing the changes in modelled bathymetry (Fig 3). The criteria of exceeding 0.043 m in the case of A and 0.047 m in the case of B and C resulting from the local granulometric curves was fulfilled by the discharge value of 7.7 $m^3 \cdot s^{-1}$ (A), 6.7 $m^3 \cdot s^{-1}$ (B), 9.4 $m^3 \cdot s^{-1}$ (C). The range of 1.7 $m^3 \cdot s^{-1}$ represents 50 minutes at the June 2013 flood wave hydrograph. The depth averaged velocity at the remobilization criteria fulfilment was 1.8±0.1 $m \cdot s^{-1}$. The values of the excess shear stress ($\tau_e = \tau - \tau_c$) at the remobilization criteria varied within 16.3±8.2 $N \cdot m^{-2}$. The bed level change occurred in the substantial part of the channel in the case of all profiles observed.

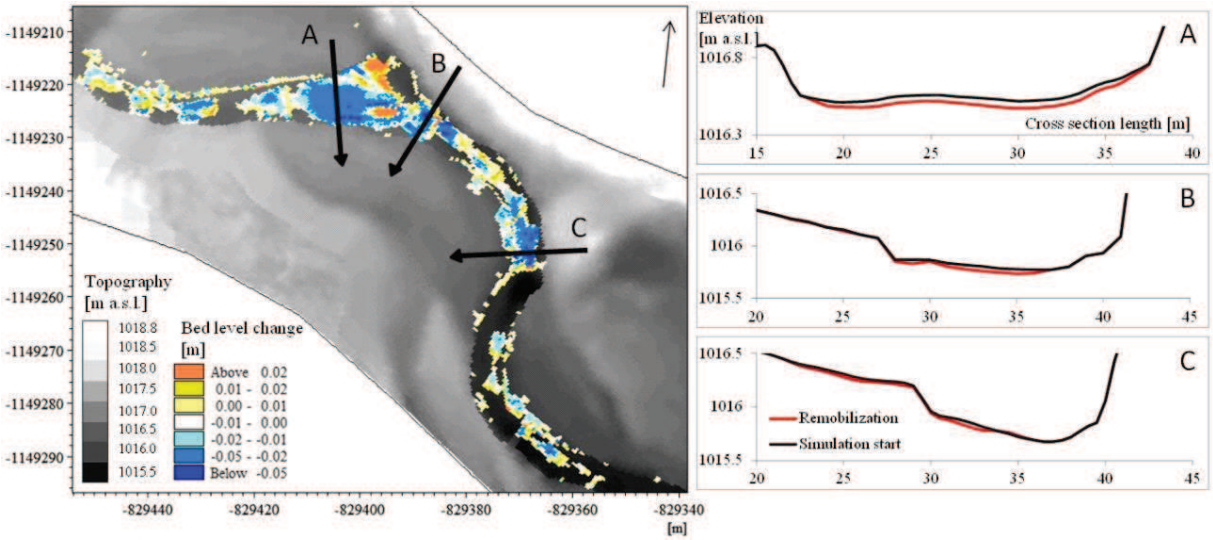

Fig. 4 Remobilization assessment considering the D_{50} parameter as grain size characteristics. Left is the horizontal plan of bed level change at the remobilization criteria fulfilment

Later the grain size was varied in order to describe movement of individual fractions separately. The remobilization of each grain fraction (D_{40} – D_{90}) was evaluated using the remobilization criteria ant the remobilization rating curves were constructed in order to relate the site specific grain characteristics to the causal flow conditions (Fig 5).

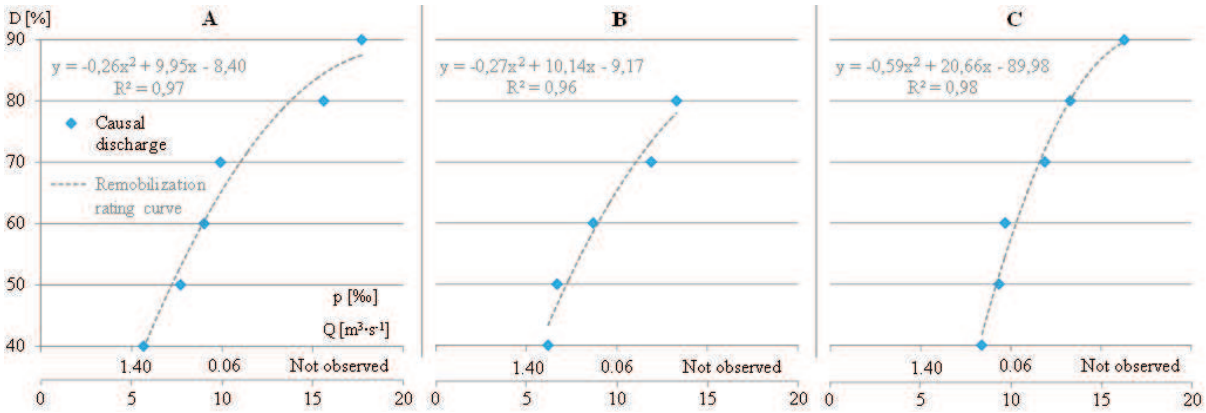

Fig. 5 Remobilization rating curves constructed at the Cross sections localities (A, B, C) base on the frequency of the remobilization causal conditions occurrence

The remobilization of the grain fractions D_{80} and D_{90} occurred after the limits of the hydrograph June 2013 thus it was extended up to 20 $m^3 \cdot s^{-1}$ by retaining the slope of the rising limb. The causal discharges for the smallest regarded D_{40} fraction remobilization were similar (5.7 – 6.2 $m^3 \cdot s^{-1}$) in the case of A and B; meanwhile the remobilization at the C locality occurred later (8.4 $m^3 \cdot s^{-1}$) due to the step backwaters calming. The backwater effect retained for the D_{50} and D_{60} fractions while the D_{70} – D_{90} conditions were more equalized. The fraction D_{90} at the profile B did not fulfil the remobilization criteria and the higher flows were not considered in this study due to the high level of inaccuracy in the hydrography extrapolation. The best fit of the causal conditions related to the sediment fraction was obtained by power functions (Fig 5).

DISCUSSION AND CONCLUSIONS

By comparing the channel morphology before and after flood events, the magnitude of eroded material can be established (e.g. Eaton and Lapointe, 2001). However, flood events are largely unpredictable, thus the data about channel morphology before a flood event is often missing. This study refers to the first observations after the qualitative verification of the model applied on the real case flood event conditions of June 2013 and brings the problem conceptualization.

The study of the most crucial parameter bed roughness was processed in order to understand the inaccuracies caused by lacking of quantitative calibration (Fig 6). The interval of maximum relative possible error was observed ranging from 23±8 % in the case of resulting depth averaged velocity and increased to 30% considering the remobilization causal discharge assessment. As observed by Verhaar et al. (2008) the relative error was smaller for the higher flow conditions than for the low flows at the beginning of the simulation. The roughness coefficient they have obtained by calibration of the gravel cobble bed was M = 23.3 $m^{1/3} \cdot s^{-1}$, not far from the minimum of the roughness interval applied. Nevertheless possible error based on wrong roughness description influence the entire mixture similarly thus according to Wilcock (1993) the skin friction of the particle of each fraction is calculated uniformly resulting in no relative error only the possible shift of the entire remobilization curves towards higher or lower flows.

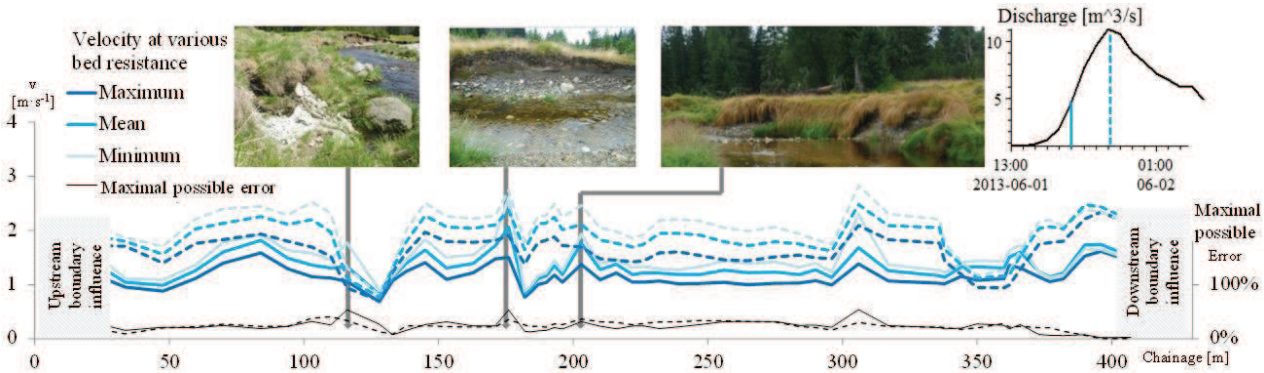

Fig. 6 Velocity longitudinal profiles considering various bed resistance values. The velocity profiles were evaluated at two different time steps. Solid lines are at discharge 3.6 $m^3 \cdot s^{-1}$, the channel capacity. The interrupted lines mark the flow conditions at June 2013 culmination (11.7 $m^3 \cdot s^{-1}$)

The initialization of the grain movement was treated first lumped across the entire granulometric curve. The concept of D_{50} is based on the hiding/exposing effect influencing the small/large particles in the uni-modal mixture (Wilcock, 1993). The result of remobilization assessment pointed at the yearly period of remobilization during the annual largest floods. The flow competence for the particles fractions distributed into characteristic intervals of percentiles $D_{40} – D_{90}$ was later analyzed. The lower percentiles were not included as the hiding effect was regarded to be inalienable. While the sediment transport modelling concept do not allow the particle tracking in general, the simulations distinguishing grain size variations of one site had to be performed in separate runs for each fraction (e.g. Büttner et al., 2006). The study profits from the application of precise topographical data resulting from UAV photogrammetry of the channel morphology and riparian zones during the model schematization (Langhammer et al., 2014) crutial for flow parameters calculation. By using the statistical characteristics of the grain size and causal discharge for the remobilization rating curves construction the absolute values of the both variables were eliminated. Thus this proposed method could later serve for the comparison of remobilization competence all across the geographical scales while considering the approximation that each stream is bedding the sediments adequate to the mean and extreme flow characteristics.

ACKNOWLEDGEMENTS

The study was realized within the research project GAČR P209/12/0997 “The impact of disturbance on the dynamics of fluvial processes in mountain landscapes”

REFERENCES

Abderrezzak, K., Moran, A.,Mosselman, E., Bouchard, J., P., Habersack, H. and Aelbrecht, D., 2013: A physical, movable-bed model for non-uniform sediment transport, fluvial erosion and bank failure in rivers. *Journal of Hydro-environmental research*, In Press, pp.1–20.

Aggett, G. R., and Wilson, J. P., 2009. Creating and coupling a high-resolution DTM with a 1-D hydraulic model in a GIS for scenario-based assessment of avulsion hazard in a gravel-bed river. *Geomorphology*, 113, pp.21–34.

Allen, J., R., L., 1964. A review of the origin and characteristics of recent alluvial sediments. *Sedimentology*, 5, pp.89 – 191.

Breusers, H., N., C., 1986. *Lecture notes on sediment transport problem*. Delft: International course of hydraulic engineering.

Bunte, K., Abt, R., 2001. *Sampling surface and subsurface particle-size distributions in wadable*

gravel- and cobble-bed streams for analyses in sediment transport, hydraulics, and streambed monitoring. Fort Collins: Rocky Mountain Research Station. 428 pp.

Büttner, O., Otte-Witte, K., Krüger, F., Meon, G. and Rode, M., 2006. Numerical modelling of floodplain hydraulics and suspended sediment transport and deposition at the event scale in the middle river Elbe, Germany. *Acta hydrochim. hydrobiol*., 34, pp.265–278.

Dade, W. B., 2000. Grain size, sediment transport and alluvial channel pattern. *Geomorphology*, 35, pp.119–126.

DHI, 2012: *MIKE 21 & MIKE 3 flow model - Scientific documentations*. Horstholm.

Eaton, B., C., and Lapointe, M., F., 2001. Effects of large floods on sediment transport and reach morphology in the cobble-bed Sainte Marguerite River. *Geomorphology*, 40, pp.291–309.

Fang, H., Chen, M. and Chen, Q., 2008. One-dimensional numerical simulation of non-uniform sediment transport under unsteady flows. *International journal of sediment research*, 23, pp.315–328.

Galapatti, R., 1983. *A depth-integrated model for suspended transport*, Delft: Delft Univ. of Technology,

Grabowski, R. C., Droppo, I. G., and Wharton, G., 2011. Erodibility of cohesive sediment: The importance of sediment properties. *Earth-Science Reviews*, 105(3-4), pp.101–120.

Guerrero, M., and Lamberti, A., 2013. Bed-roughness investigation for a 2-D model calibration: the San Martín case study at Lower Paranà. *International Journal of Sediment Research*, 28(4), pp.458–469.

Hardy, R. J., 2013. Process-Based Sediment Transport Modeling. In J., F., Shroder, ed. 2013. *Treatise on Geomorphology*. Elsevier.

Huang, J., Hilldale, R. C., and Greimann, B. P., 2006. Chapter 4: Cohesive sediment transport. In: *Erosion and Sedimentation Manual*. U.S. Department of the Interior Bureau of Reclamation. 55 p.

Chow. V., T., 1959. *Open-Channel Hydraulics*. New York: McGraw-Hill. 680 p.

Kiat, C. C., Ghani, A. A., Abdullah, R., and Zakaria, N. A., 2008. Sediment transport modeling for Kulim River – A case study. *Journal of Hydro-Environment Research*, 2(1), pp.47–59.

Langhammer, J., Miřejovický, J., Hartvich, F., & Kaiglová, J., (2014). Water Remote Sensing and Sensor Technology. In: J. Kacprzyk, ed. 2014. *Computational Inteligence in Hydroinformatics: Current Trends and Problems. Springer*. (In review)

Li, S. S., Millar, R. G., and Islam, S., 2008. Modelling gravel transport and morphology for the Fraser River Gravel Reach, British Columbia. *Geomorphology*, 95(3-4), pp.206–222.

LUEL, (2005). *Sedimetrics 1.0 Digital Gravelometr*. [computer program] Loughborough University Enterprises Limited.

Meyer-Peter, E., Müller, R., 1948: *Formulas for bed load transport*, Proc. 2nd Congr. Stockholm: IAHR

Simpson, G. and Castelltort, S., 2006. Coupled model of surface water flow, sediment transport and morphological evolution. *Computers & Geosciences*, 32, pp.1600-1614.

Smart, G., M. and Jaeggi, M., N., R., 1983. *Sediment transport on steep slopes*. Mitteilung nr. 64 of the laboratory for Hydraulics, Zurich: Hydrology and glaciology at the Federal Technical University.

Vanoni, V., A., 1984: Fifty Years of Sedimentation. *Journal of Hydraul. Engineering*, 110, pp.1021–1057.

Verhaar, P. M., Biron, P. M., Ferguson, R. I., and Hoey, T., 2008. A modified morphodynamic model for investigating the response of rivers to short-term climate change. *Geomorphology*, 101, pp.674–682.

Wilcock, P., 1993. Critical shear stress of natural sediments. *Journal of Hydraulic Engineering*, 119(4), pp.491–505.

Wyrick, J.R., Senter, A.E., and Pasternack, G.B., 2014. Revealing the natural complexity of fluvial morphology through 2D hydrodynamic delineation of river landforms, *Geomorphology*, 210, pp.14–22.

Yang, C.T., J. Huang, and Greimann, B., P., 2004, 2005. *User's manual fbr GSTAR-ID, version 1 .O*, Denver: U.S. Bureau of Reclamation.

Yu, G., Wang, Z., Zhang, K., Chang, T. and Lui, H., 2009. Effect of incoming sediment on the stream transport rate of bed load in mountain streams. *Int. journal of sediment research*, 24, pp.260–273.

7.3 NON-STATIONARITY OF CAUSAL FLOW CONDITIONS BASED ON LONG-TERM OBSERVATIONS (CASE STUDY III)

Bernsteinová, J., Bässler, C., Zimmermann, L., Langhammer, J., Beudert, B., 2015. Changes in runoff of two neighbored catchments in the Bohemian Forest related to climate and land cover changes. Journal of Hydrology and Hydromechanics. In Review.

Langhammer, J., Ye, S., **Bernsteinová, J.**, 2015. Runoff response to climate warming and forest disturbance in a mid-mountain basin, Water. In Review.

vegetation data. Remote Sensing of Environment, 113, 835-845.

Hidalgo, H.G., Das, T., Dettinger, M.D., Cayan, D.R., Pierce, D.W., Barnett, T.P. et al., 2009. Detection and attribution of streamflow timing changes to climate change in the Western United States. Journal of Climate, 22, 3838-3855.

Hirsch, R. M., Slack, J. R. Smith, R. A., 1982. Techniques of trend analysis for monthly water quality data. Water Resources Research, 18, 107-121.

Hisdal, H., Holmqvist, E., Jonsdottir, J.F., Jonsson, P., Kuusisto, E., Lindstrom, G. Roald, L.A., 2010. Has streamflow changed in the Nordic countries? NVE Report No. 1, Oslo.

IPCC 2013. Climate Change 2013. The Physical Science Basis. In: Stocker, T.F., D. Qin, G.-K. Plattner, M. Tignor, S.K. Allen, J. Boschung, A. Nauels, Y. Xia, V. Bex P.M. Midgley (Eds.): Contribution of Working Group I to the Fifth Assessment Report of the Intergovernmental Panel on Climate Change. Cambridge University Press, Cambridge, United Kingdom and New York.

Kliment, Z. Matouskova, M., 2008. Long-term trends of rainfall and runoff regime in Upper Otava river basin. Soil Water Res., 3, 155-167.

Klöcking, B., Schwarze, R., Beudert, B., Suckow, F. Lasch, P., Badeck, F. Pfützner, B., 2005. Auswirkungen des Borkenkäferbefalls auf den Wasser- und Stoffhaushalt zweier Gewässereinzugsgebiete im Nationalpark Bayerischer Wald. Schriftenreihe Wasserhaushalt und Stoffbilanzen im naturnahen Einzugsgebiet Große Ohe. Nationalparkverwaltung Bayerischer Wald, Grafenau.

Määttä, A., Salmi, T., Anttila, P., Ruoho-Airola, T., 2002. MAKESENS 1.0. EXCEL template for the calculation of trend statistics of annual time series. Finnish Meteorological Institute, Helsinki.

Marvel, K., Bonfils, C., 2013. Identifying external influences on global precipitation. Proceedings of the National Academy of Sciences, 110, 19301-19306.

Maurer, E. P., Stewart, T., Bonfils, C., Duffy, P.B., Cayan, D., 2007. Detection, attribution, and sensitivity of trends toward earlier streamflow in the Sierra Nevad. Journal of Geophysical Research, 112, D11118.

McCabe, G.J., Clark, M.P., 2005. Trends and variability in snowmelt runoff in the western United States. Journal of Hydrometeorology, 6, 476-482.

Melloh, R., Hardy, J., Davis, R. Robinson, P., 2001. Spectral albedo/reflectance of littered forest snow during the melt season. Hydrological Processes, 15, 3409–3422.

Mollini, A., Katul, G.G., Porporato, A., 2011. Maximum discharge from snowmelt in a changing climate. Geophysical research Letters, 38, L05402.

Molotch, N.P, Brooks, P.D, Burns, S.P, Litvak, M, Monson, R.K, McConnell, J.R, Musselman, K., 2009. Ecohydrological controls on snowmelt partitioning in mixed-conifer sub-alpine forests. Ecohydrology, 2, 129–142.

Musselman, K., Molotch, N.P, and Brooks, P.D., 2008. Quantifying the effects of forest vegetation on snow accumulation, ablation and potential meltwater inputs, Valles Caldera National Preserve, NM, USA. Hydrological Processes, 22, 2767–76.

Oosterbaan, R.J., 1994. Agricultural Drainage Criteria. In: H.P.Ritzema (Ed.), Drainage Principles and Applications, ILRI Publ. 16, p. 635 – 688, Wageningen, The Netherlands.

Polson, D., Hegerl, G.C., Allan, R.P., Sarojini, B.B., 2013. Have greenhouse gases intensified the contrast between wet and dry regions? Geophysical Research Letters, 40, 4783-4787.

Project team ECA&D, 2013. European Climate Assessment & Dataset (ECA&D), Algorithm Theoretical Basis Document (ATBD). Royal Netherlands Meteorological Institute KNMI, www.ecad.eu/documents/atbd.pdf

Pugh, E., Gordon, E., 2012. A conceptual model of water yield effects from beetle-induced tree death in snow-dominated lodgepole pine forests. Hydrol. Process., 27(14), 2048-2060.

Pugh, E., Small, E., 2012. The impact of pine beetle infestation on snow accumulation and melt in the headwaters of the Colorado River. Ecohydrology, 5, 467–477.

Raffa, K.F., Aukema, B.H., Bentz, B.J., Carroll, A.L., Hicke, J.A., Turner, M.G., Romme, W.H., 2008. Cross-scale drivers of natural disturbances prone to anthropogenic amplification. the dynamics of bark beetle eruptions. Bioscience, 58, 501-517.

Redding, T., Winkler, R., Teti, P., Spittlehouse, D., Boon, S., Chatwin, S., 2008. Mountain pine beetle and watershed hydrology. In Mountain Pine Beetle. From Lessons Learned to Community-based Solutions Conference Proceedings, June 10–11, 2008. BC Journal of Ecosystems and Management, 9, 33–50.

Renner, M., Bernhofer, C., 2011. Long term variability of the annual hydrological regime and sensitivity to temperature phase shifts in Saxony/Germany. Hydrology and Earth System Sciences, 15, 1819-1833.

Seidl, R., Schelhass, M.J., Lexer, M.J., 2011. Unraveling the drivers of intensifying forest disturbance regimes in Europe. Global Change Biology, 17, 2842-2852.

Snedecor, G.W. and Cochran, W.G., 1980. Statistical Methods, 7th edition, Chap. 17.4, p. 401-403. Iowa State University Press.

Stahl, K., Hisdal, H., Hannaford, J., Tallaksen, L.M., van Lanen, H.A.J., Jodar, J., 2010. Streamflow trends in Europe. Evidence from a dataset of near-natural catchments. Hydrol. Earth Syst. Sci. Discuss., 7, 5769–5804.

Stepánek, R., 2005. AnClim – software for time series analysis. Dept. of Geography, Faculty of Sciences, Masaryk University Brno, http://www.sci.muni.cz/~pest/AnClim.html.

Stewart, I.T., Cayan, D.R., Dettinger, M.D., 2005. Changes toward earlier streamflow timing across western North America. Journal of Climate, 18, 1136-1155.

Wessa P., 2014. Paired and Unpaired Two Samples Tests about the Mean (v1.0.5) in Free Statistics Software (v1.1.23-r7), Office for Research Development and Education, URL http://www.wessa.net/rwasp_twosampletests_mean.wasp/

Wilson, D., Hisdal, H., Lawrence, D., 2010. Has streamflow changed in the Nordic countries? – Recent trends and comparisons to hydrological projections. Journal of Hydrology, 394, 334-346.

Winkler, R., Boon, S., Zimonick, B., Baleshta, K., 2010. Assessing the effects of post-pine beetle forest litter on snow albedo. Hydrological Processes, 24. 803–812.

Water **2015**, *7*, 1-x manuscripts; doi:10.3390/w70x000x

OPEN ACCESS

water

ISSN 2073-4441

www.mdpi.com/journal/water

Type of the Paper (Article)

Runoff response to climate warming and forest disturbance in a mid-mountain basin

Jakub Langhammer [1,*], Ye Su [1,†] and Jana Bernsteinová [1,2,†]

[1] Address: Charles University in Prague, Faculty of Science, Albertov 6, Prague 2, 128 43, Czech Republic, ye.su@natur.cuni.cz

[2] Address: DHI a.s., Na Vrsich 5, Prague 10, 100 00, Czech Republic; E-Mail: jana.bernsteinova@gmail.com

† These authors contributed equally to this work.

***** Author to whom correspondence should be addressed; E-Mail: jakub.langhammer@natur.cuni.cz; Tel.: +420-221951415; Fax: +420-221951415

Academic Editor:

Received: / Accepted: / Published:

Abstract: A headwater basin in the Sumava Mountains (Czech Republic), the upper Vydra basin, has undergone forest disturbance as a result of repeated windstorms, bark beetle outbreak, and forest management. This study analyzed the long-term (1961-2010) hydro-climatic changes by using a combination of statistical analyses, including Mann-Kendall test, CUSUM analysis, Buishand's and Petitt´s homogeneity tests, and Kriging. Although the runoff balance over the study period had no apparent change under climate-warming and forest disturbance, there were detected significant changes in share of direct runoff and baseflow, intra-annual variability of runoff regime, runoff seasonal patterns, as well as the distribution of peak flow and low flow. The seasonal runoff shares substantial shifted from summers (decreased from 40% to 28%) to springs (increased by 10%). The occurrence of peak flow events doubled since the 1980s with a seasonal shift from late spring towards the early spring, while, the occurrence of low flow days experienced a triple decrease, and in 1990 followed by an increase a seasonal shift from autumn to mid-winter. The changes in hydrological regime in the mid-mountain basin indicate the sensitivity of its hydrological system and the complexity of the feedback to the changing environment.

Keywords: Runoff variability; baseflow; peak flows; low flows; climate warming; forest disturbance

1. Introduction

In montane regions, both long-term and abrupt changes of climate and/or land cover may result in significant shifts in the hydrological regime, especially in relation to extreme hydrological events such as floods and droughts.

In the past decades, climate change, including changes in precipitation, temperature, vapor pressure, and wind speed, has directly or indirectly altered the hydrological regimes [1-4], and studies on identifying the linkage between the warmer air temperature and occurrence of extreme hydrological events or basin's water yield have accelerated decision-makers' attention concerning natural resource management [5-8]. On the other hand, consistent studies have stated that changes in land cover/land use and climatic changes significantly govern the hydrological regimes (i.e. pattern, magnitude, frequency, timing, duration, and rate of change [9-14]. Forest disturbance as one of the causes driving severe land cover change has strong impacts on interception, evapotranspiration, surface soil hydraulic conductivity, and soil storage, which may lead to changes in the water yield [15,16], runoff formation process [17,18], snow hydrology [19,20], floods [9,21], and low flow regime [22,23]. The effects of different forest disturbances caused or triggered by wildfire, insect infestation, windstorm, logging, pollution, urbanization, agricultural activities, and management interventions on the streamflow have been widely studied at multiple temporal and spatial scales [24-28]. Appropriate environmental policy towards basin management requires an integrated understanding on the hydrological responses to both above-mentioned drivers, especially in montane areas of high vulnerability to both climatic and land forest changes [25,29].

The headwater of the Sumava Mountains, located in Central Europe at the border between Czech Republic and Germany has undergone a significant forest disturbance in past two decades as a result of repeated windstorms and bark beetle infestation. In the core zone of the disturbance, the upper Vydra basin, the extent of forest decay reached almost 60 % of the basin [28]. In the same time period this area is undergoing significant rise of the observed air temperatures. As a National Park with restricted management, the area serves as natural laboratory enabling to study the effects of these environmental changes on hydrological processes in the mid-mountain environment.

This paper aims to assess the hydro-climatic changes in the upper Vydra basin in the period 1961-2010, covering the observed changes in air temperature as well as the forest disturbance. The objectives of the study are: i) to analyze the effect of rising air temperatures and extensive forest disturbance on the hydrological response of the mid-mountain basin, and ii) to assess the hydro-climatic indicators that suitable for detecting such their changes, extent, and timing.

The study applies a set of methods, analyzing various aspects of hydro-climatic variability including baseflow separation by recursive digital filter, CUSUM analysis, analysis of changes in discharge variability and seasonality including Mann-Kendall test, analysis of changing frequency and seasonality of peak flows and low flows, the Buishand's and Petitt´s homogeneity tests and Kriging.

2. Materials and Methods

2.1 Study area

The upper Vydra basin in this study is defined as the upper part of Vydra basin, ending at the Modrava gauging station (49° 1' 30.0216" N, 13° 29' 47.1624" E), which covers 90.1 km^2 (Figure 1). The studied basin is a headwater and located at the top of the Sumava Mountain range with an average altitude of 1112 m (Table 1), in the south-western part of the Czech Republic, along the border of Germany in Central Europe. The bedrock consists mainly of gneisses with locally-permeating granitic rocks [3]. The climate of the study area has typical montane features with moderately warm, distinct summer seasons, and relatively higher precipitation (1232 mm) among the Czech Republic (700 mm) [30,31]. Approximately 40% of the precipitation is in the form of snow and the snow cover lasts an average 143 days per year [32]. The basin is dominated by small streams with fast hydrological response to precipitation events, and the basin's annual mean discharge is 3.34 m^3 s^{-1}.

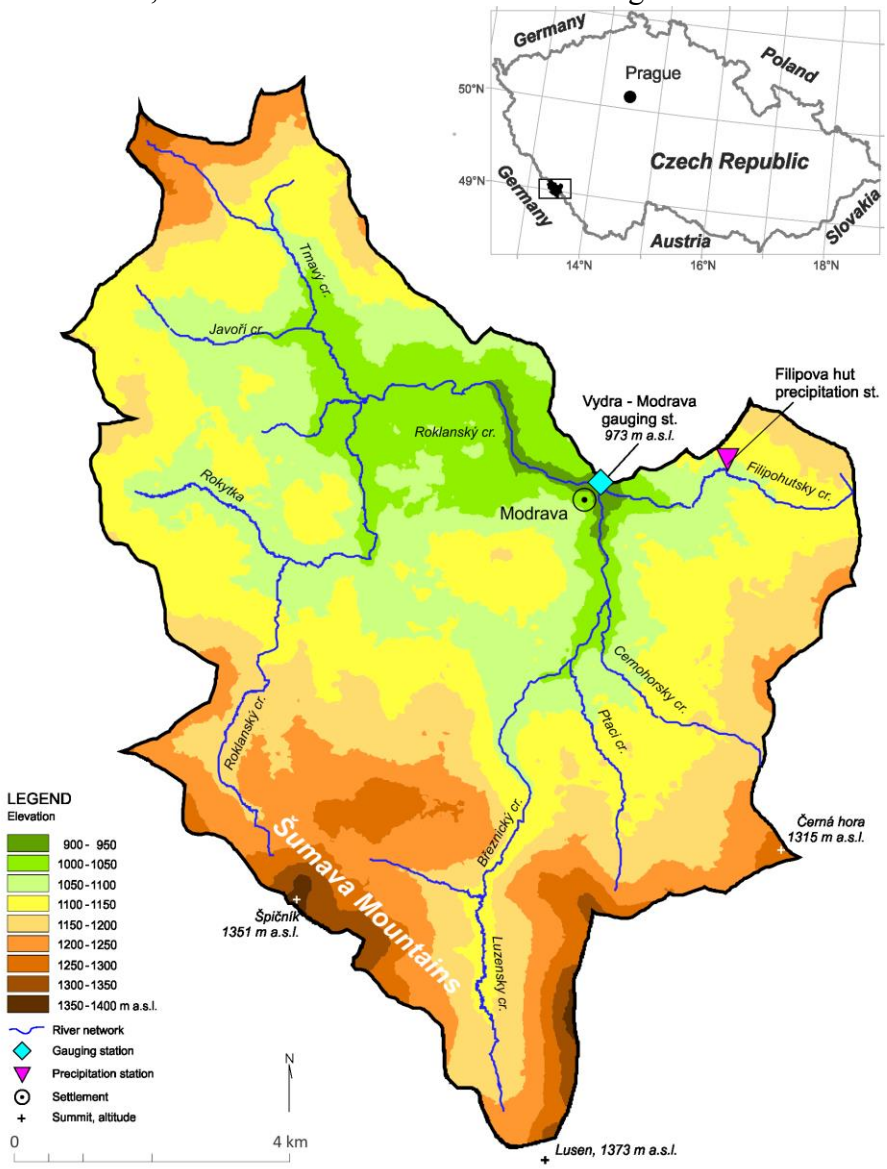

Figure 1. Study area. Location of the upper Vydra basin with river networks and gauging stations.

The land use in the Sumava Mountain was dominated by the original virgin forest, and replaced in the 18th century by a Norway spruce (Picea abies [L.] Karst.) monoculture for the wood industry [33]. Before the 1980s, 86% of the land cover in the upper Vydra basin was consist of coniferous forests and stable. Bark beetle outbreaks in the upper Vydra basin started after windstorms in Bavarian forest in 1984, reaching the peak in the mid of 1990s [26] and again accelerating after the windstorms, Kyrill and Emma, in 2007 and 2008 [28,30]. Between 1984 and 2010, the area of healthy forest decreased from 48% to 13% of the basin area, and the areas of damaged and decayed forest and no forest increased by 22% and 34% to the basin area (Figure 2). The affected areas were left as non-intervention zones as a Sumava National Park management strategy, where the bottom layer of vegetation is undergoing a quick recovery.

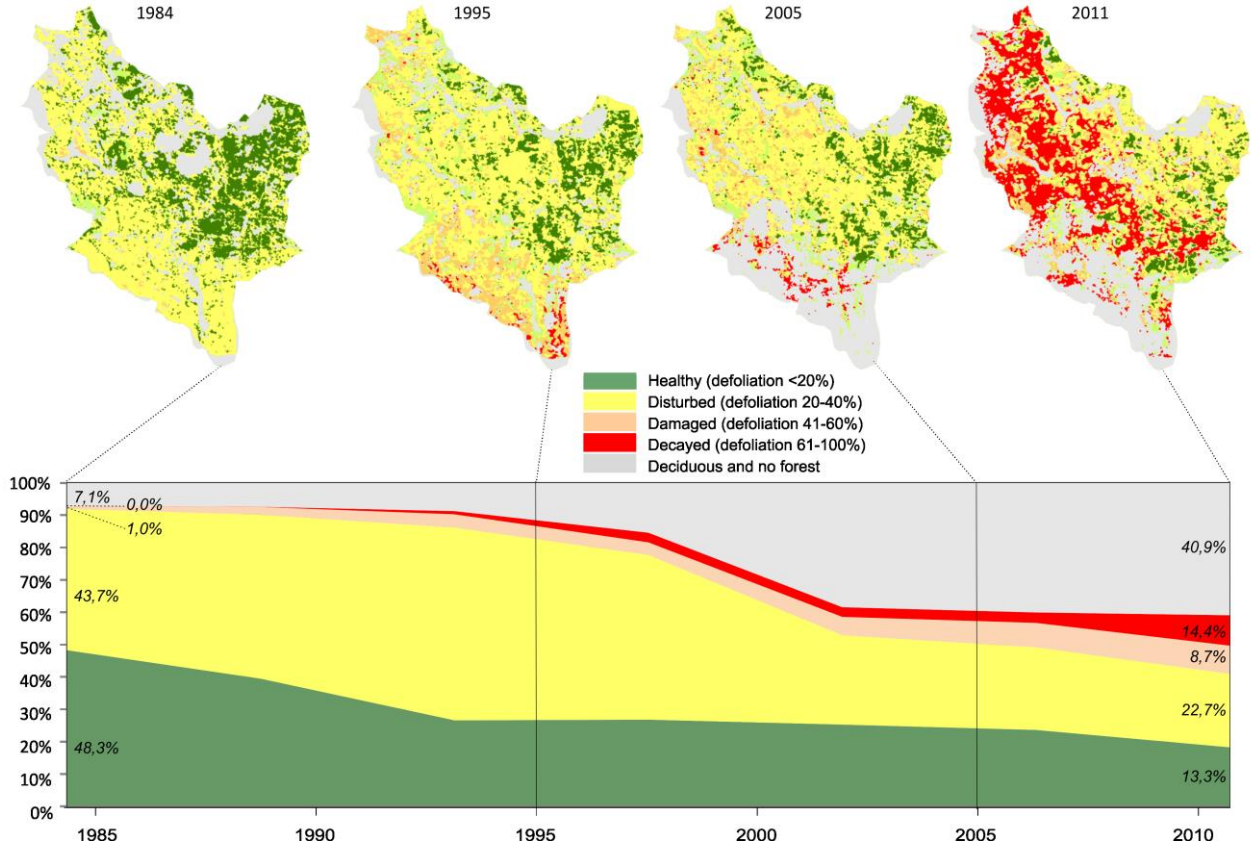

Figure 2. Key stages of the forest disturbance progress in the upper Vydra basin, and the change of forest status between 1984 and 2011.

Table 1. Physiographic characteristics of the upper Vydra basin

Basin/ Unit	A [km^2]	D [$km\ km^{-2}$]	H_{mean} [m]	H_{min} [m]	H_{max} [m]	S_{mean} [^{o}]	S_{max} [^{o}]	T [^{o}C]	P [mm]	Q [$m^3\ s^{-1}$]
Upper Vydra	90.1	2.3	1112	935	1373	7	55	3.6	1232	3.34

Notation: A: area; D: density of river network; H_{mean}, H_{min}, H_{max}: mean, minimum and maximum of altitude; S_{mean}, S_{max}: mean and maximum of slope; T, P, and Q: mean annual air temperature, precipitation, and discharge during 1961-2010.

2.2 Data sources

Daily and monthly long-term observations of precipitation, air temperature, and discharge were obtained from the various Czech Hydrometeorological Institution (CHMI) stations [34], and the period of 1961-2010 were used for the analysis. The air temperature for the study area was estimated according to the elevation gradient by using the observations from two stations: Churanov and Kasperske Hory, and the correction factor in elevation is decreasing $0.6^{o}C\ (100m)^{-1}$. Precipitation for the upper Vydra basin was estimated by using the orographic regression based on the neighboring five stations: Filipova Hut, Churanov, Hartmanice, Kasperske Hory, and Srni, and the interpolated precipitation in elevation is increasing $6.4mm\ (100m)^{-1}$. The daily discharges were measured at the outlet of the upper Vydra basin, Modrava station.

The regional monthly air temperatures with a $2^{o}\times2^{o}$ grid cell corresponding to the study area, including uncertainty assessment, were derived from the 20^{th} century reanalysis of the NOAA Global Climate Model [35] by using the IDV tool [36].

The topographic information, a 5m×5m Digital Elevation Model (DEM), was acquired from the State Administration of Land Surveying and Cadastre [37]. The topographic layers from the digital water management database DIBAVOD were used in this study [38]. Data on forest cover changes were derived from the map layers of defoliation and mortality of forests [39].

2.3 Applied method

A combined approach of statistical and analytical methods, including double-mass curve analysis, recursive digital filter, Mann-Kendall test, CUSUM analysis, Buishand's and Petitt´s homogeneity tests, agglomerative hierarchical clustering, and the ordinary Kriging was applied.

The double-mass curve was used to illustrate the precipitation-discharge relationship in the upper Vydra basin [3]. Precipitation data and discharge data were used a Mann-Kendall non-parametric test to detect the trend at different temporal scales: monthly, seasonally, and yearly [40]. The test was performed by accepting or rejecting a null hypothesis of no trend existence at four stations, and two levels of significance of the alternative hypothesis, two p-values ($p \leq 0.01$ and $p \leq 0.05$) were considered.

The two parameter recursive digital filter [41] was applied for separation of direct flow and baseflow signal from continuous daily discharge data. The algorithm is aimed to partition the streamflow hydrograph in two components -"high frequency" corresponding to direct runoff and "low frequency" corresponding to baseflow [42]. The baseflow separation is calculated according relationship proposed by Eckardt [41] (Equation 1).

$$B_{k+1} = \frac{(1 - BFI_{max}) \cdot \propto \cdot B_k + (1-\propto) \cdot BFI_{max} \cdot Q_{k+1}}{(1-\propto) \cdot BFI_{max}} \quad (1)$$

Where B_k is baseflow at time step k, Q is streamflow at time step k, α is baseflow filter parameter and BFI_{max} is the maximum value of long term ration of baseflow to total streamflow. The baseflow filter parameter α was set to 0.98 and BFI_{max} to 0.80 in the web based WHAT model [43], corresponding to perennial streams with porous aquifers [41].

The actual evapotranspiration (AET) was calculated using empirical relationship [44] (Equation 2).

$$AET = \frac{P}{\sqrt{(0.9 + \frac{P^2}{PET^2})}} \quad (2)$$

where P is precipitation (in mm) and PET is potential evapotranspiration (in mm). PET can be further estimated by Langbein [45]'s empirical relationship in Equation 3.

$$PET = 325 + (21 \cdot T) + (0.9 \cdot T^2) \quad (3)$$

where T is temperature (in °C).

The calculated long-term AET provides the basic information on one component of water balance that is only driven by climatic parameters, T and P.

CUSUM analysis (i.e. cumulative sum, [46,47]) was employed to assess the course of cumulative discharge differences, relative to the whole assessed period's mean discharge. The cumulative sums are calculated as the accumulated differences to the constant target value, in this case represented by the mean value of the applied time series (Equation 4).

$$S_i = \sum_{j=1}^{i} (x_j - c) \quad (4)$$

where S_i is the cumulative sum, x value in time series and c the constant target value.

The daily discharge (Q_d) was used to define the low flows (Q_{330d}), high flows (Q_{30d}), and standard deviation, which were applied as a measure of intra-annual runoff variability. The value of the peak flows over threshold (POT) was set as the minimal value of the yearly maximum discharge in the reference period of 1961-2010 (POT is equivalent to 12.2 m^3 s^{-1}), which secured a selection of at least one event per year in the time series. The low-flow events under a given threshold (LOF) were identified according to a long-term Q_{330d} value (LOF is equivalent to 1.02 m^3 s^{-1}). The analysis of frequency, duration, and magnitude of annual POT events was performed from the resulting dataset. Analysis of changes in frequency and seasonality of events with POT and LOF was made by an aggregation of selected events into a ten-year temporal scale and monthly period in accordance with the days in the year of events. Additionally, ordinary Kriging was used as the interpolation method to derive the patterns of frequency distribution across time and seasonality.

Homogeneity of the time series has been tested by Buishand's and Petitt´s tests [48,49] in order to detect the potential points of change in the assessed time series. The null hypothesis (H_o: data are homogeneous) and an alternative hypothesis (H_a: there is a date at which there is a change in the data) were tested. The non-parametric Petitt's test is a modified Mann-Whitney test that, similar to Buishand´s range test, allows identifying the time at which the shift occurs. Both of the tests are distribution-free and applicable to time series with not known position of the point of change [50]. The p-value has been computed using 10000 Monte Carlo simulations and the significance level alpha setup as 0.05 (α=0.05, i.e. the risk of rejecting the hypothesis is equivalent to 5%). Theoretically, two types of tests tend to be more sensitive to breaks in the middle of time series [51] and report similar results, despite their different nature [52].

The statistical software packages Knime 2.11, XLStat 2014 and Surfer 10 were used for statistical calculations, Grapher 10 for calculating the trend lines, and the ArcGIS 10 was used for GIS analysis and spatial data integration.

3. Results

3.1 Variability of climatic conditions

The annual air temperature from the NOAA reanalysis model at regional scale indicates a sharp rising trend relative to the annual mean value of the 1951-1980 since the 1980s (Figure 3). A 1.5°C rise of the air temperature since the 1980s was also proven by the local observed data at the basin scale (Figure 3). In contrast, the observed annual total precipitation is slightly fluctuated between 1100 and 1300 mm during 1961-2010. The estimated annual actual evapotranspiration (AET) held around 400 mm, correspondingly, a gentle increase since the 1980s.

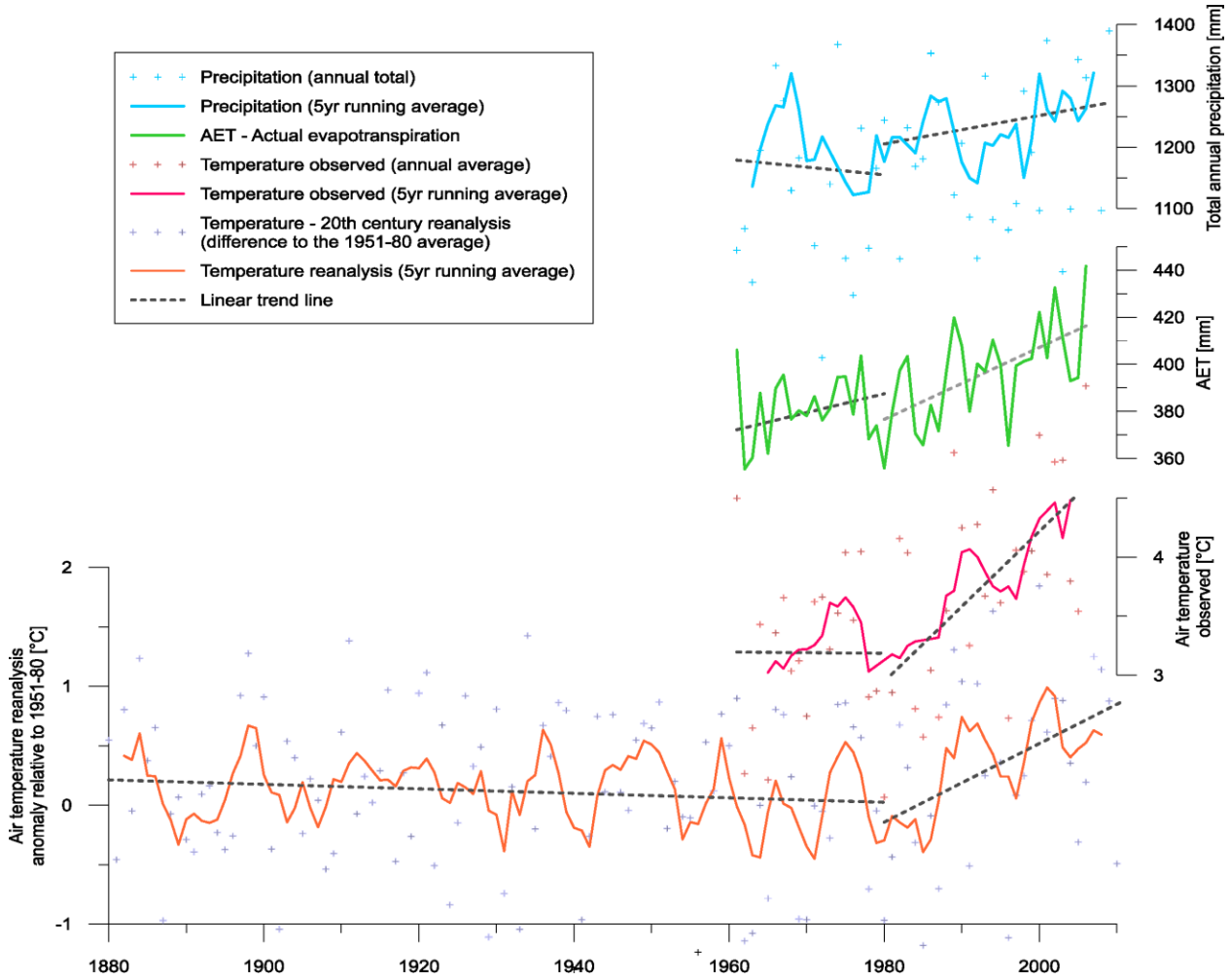

Figure 3. Annual air temperature relative to the average of 1951-1980 resulting from reanalysis since 1880 at the regional scale, and observed annual climatic condition during 1961-2010 at basin scale,

Although the annual precipitation was stable, a significant shift in the seasonal distribution of precipitation has been detected using the Mann-Kendall test at three neighboring precipitation stations, Filipova Hut (1110 m.a.s.l.), Kvilda (1059 m.a.s.l.), and Churanov (1122 m.a.s.l.) (Table 2). The precipitation in three stations varied spatially, but still held a similar tendency. Precipitation has a significant rising trend (with $p \leq 0.01$ or $p \leq 0.05$) in winter (month of XI-I) from the seasonal differences, while the significant decline of precipitation (with $p \leq 0.01$ or $p \leq 0.05$) was found in two

stations in early spring (II-IV) and fall (VIII-X), with the monthly difference mostly occurring in April (IV).

The Mann-Kendall test detected that the rising trend of the basin's discharge was in March ($p \leq 0.05$) and April ($p \leq 0.01$), which corresponded with the rising precipitation in April and with the earlier snowmelt.

Table 2. Mann-Kendall test of seasonal and monthly precipitation (P) and discharge (Q) trends during 1969-2010.

Parameter	Station	XI-I	II-IV	V-VII	VIII-X	I	II	III	IV	V	VI	VII	VIII	IX	X	XI	XII
P	Filipova Hut																
P	Churanov																
P	Kvilda																
Q	Modrava																

Color legend. Blue – increasing trend, red – decreasing trend. Darker color indicate more significant trend:

- $p \leq 0.01$
- $p \leq 0.05$
- non-significant trend
- no trend

3.2 Variability of runoff regime

Double-mass curve (Figure 4) shows no apparent change of rainfall-runoff relationships: neither in the 1990s, when the most intensive forest disturbance occurred (in 1995 and 1996), nor in the 1980s when the air temperature rose significantly.

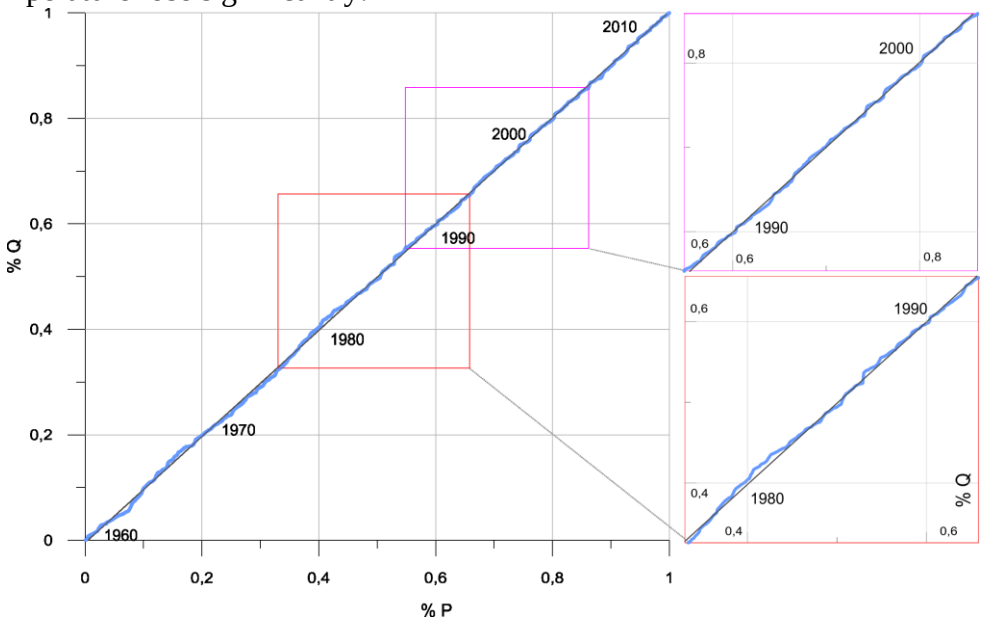

Figure 4. Double-mass curve of accumulated monthly values of discharge (Q) and precipitation (P) during 1961-2010, and two magnified periods of the 1980s and the 1990s

Daily baseflow and direct runoff identified notable change in the two key runoff components since the 1980s (Figure 5). The baseflow index (BFI) has an apparent rise from around 0.86 in decades of

1951-1980 continuously to 0.93 in decade of 2001-2010. As a counterpart, there is notable decrease of direct runoff values since 1980 (Figure 5).

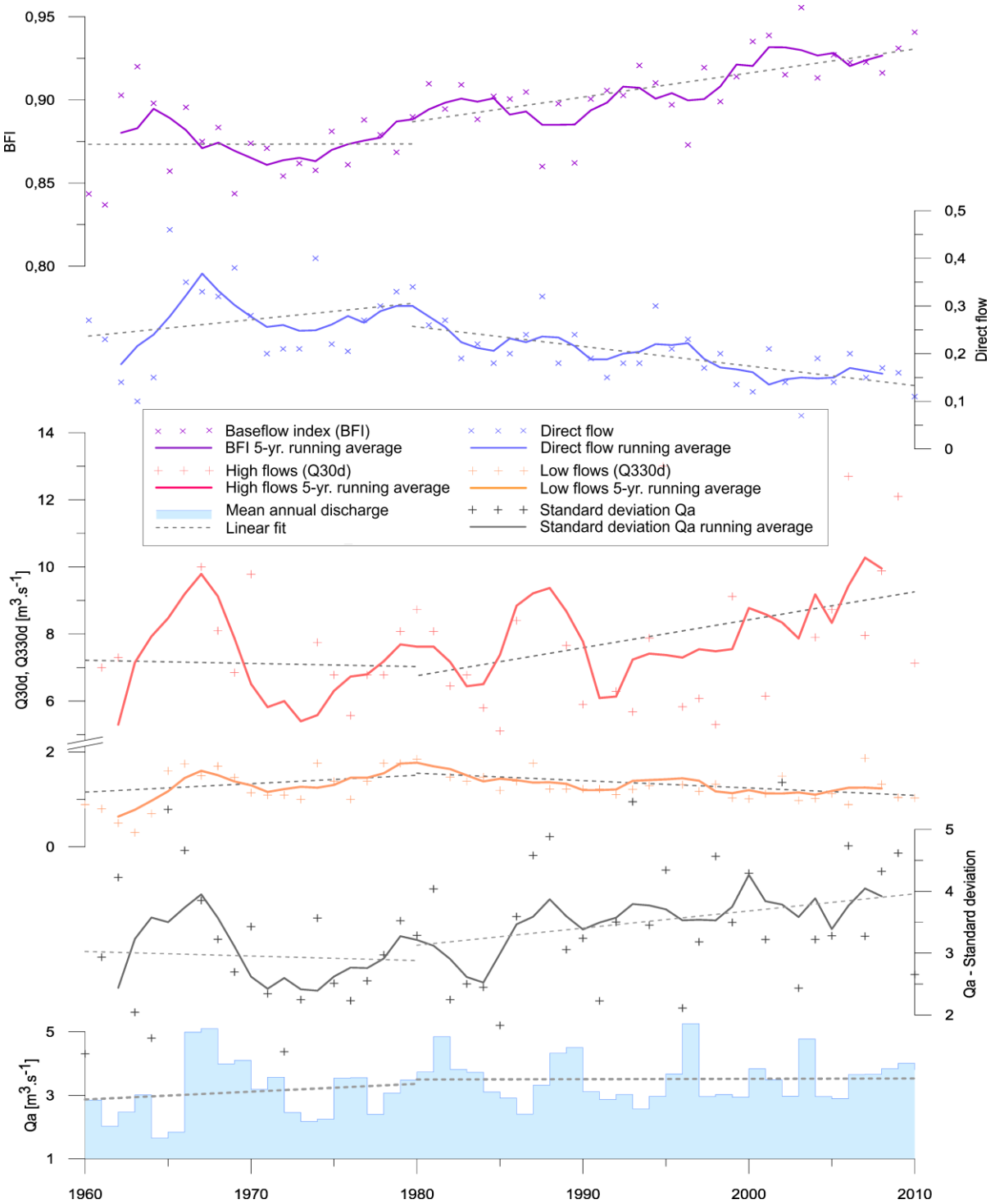

Figure 5. Annual mean values of the direct flow and baseflow index (BFI), high flow (Q_{30d}) and low flow (Q_{330d}), mean annual discharge (Q_a) and its standard deviation in the period of 1961-2010.

Same changing points starting at the 1980s were found for the intra-annual variability of discharge, namely the high flows (Q_{30d}), low flows (Q_{330d}), and the mean annual discharge standard deviation (Figure 5). Specifically, the low flows show a decrease since the 1980s, after a rise in the preceding

decades, both with slight variations within a $1m^3\ s^{-1}$ difference. The high flow's trend indicates, however, an opposite direction. A slight decline before the 1980s is followed by a significant rise since the break point in the 1980s, with large variations ranging from approximately $5m^3\ s^{-1}$ to $12m^3\ s^{-1}$. The rising standard deviation of discharge demonstrates the rising intra-annual volatility of the runoff process since the 1980s, which corresponds to the detected time period of changes in air temperature as well as forest disturbance in the basin.

The CUSUM analysis identified cumulative differences in daily discharges during 1961-2010 relevant to the mean discharge (Figure 6), which indicates repeatedly large fluctuations before the 1980s. CUSUM values continuously jumped from negative towards positive values in the 1980s with a significant reduce in variability, and a steep rise of positive values found since the mid of the 1990s. The position of the turning point in the CUSUM daily discharge data has been located to 4 May 1995 in the case of Buishand´s test and to 5 April 2002 using Petitt´s test (Figure 6).

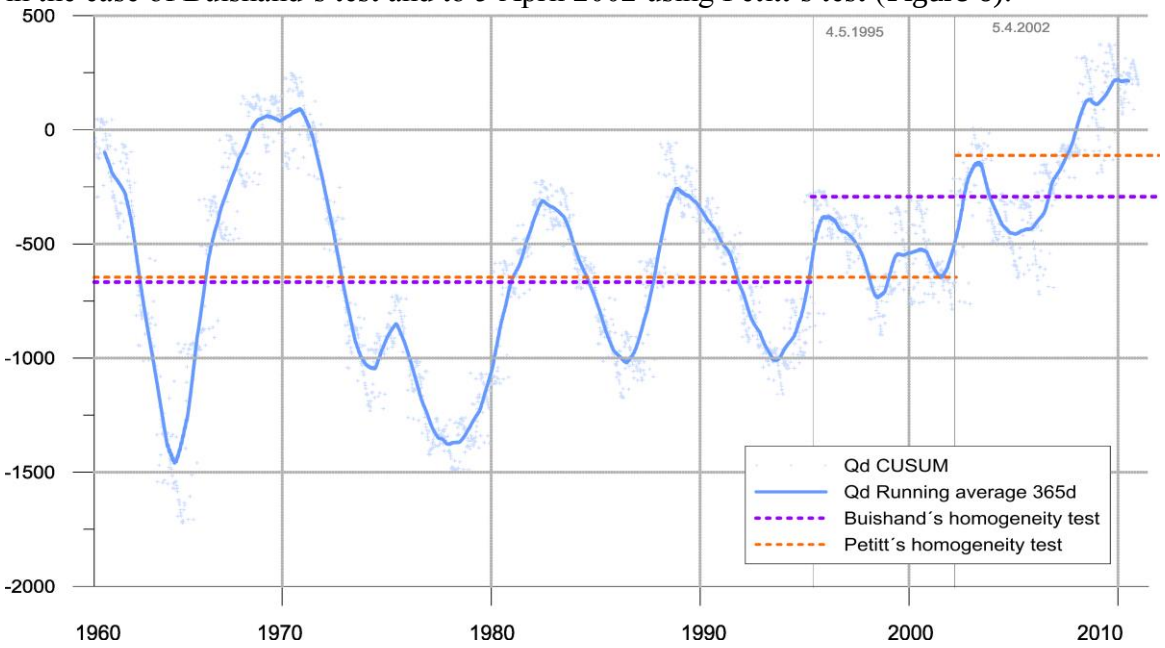

Figure 6. CUSUM analysis of daily discharge (Q_d) during 1961-2010; and the change points are detected by Buishand´s and Petitt´s test, indicating at 4 May 1995 and 5 April 2002 respectively.

A substantial shift in seasonal distribution of the monthly discharge among the seasons was identified (Figure 7). The summer season (VII-IX), which was dominant in the long-term share of runoff, was replaced by the spring season (IV-VI) in 1980. The runoff share for the springs (IV-VI) rose by more than 5% from 22% in the late 1960s to 33% in 2010 (Figure 7a), while the share of the summers (VII-IX) dropped from more than 42% in the 1960s to 27% in 2010 (Figure 7b).

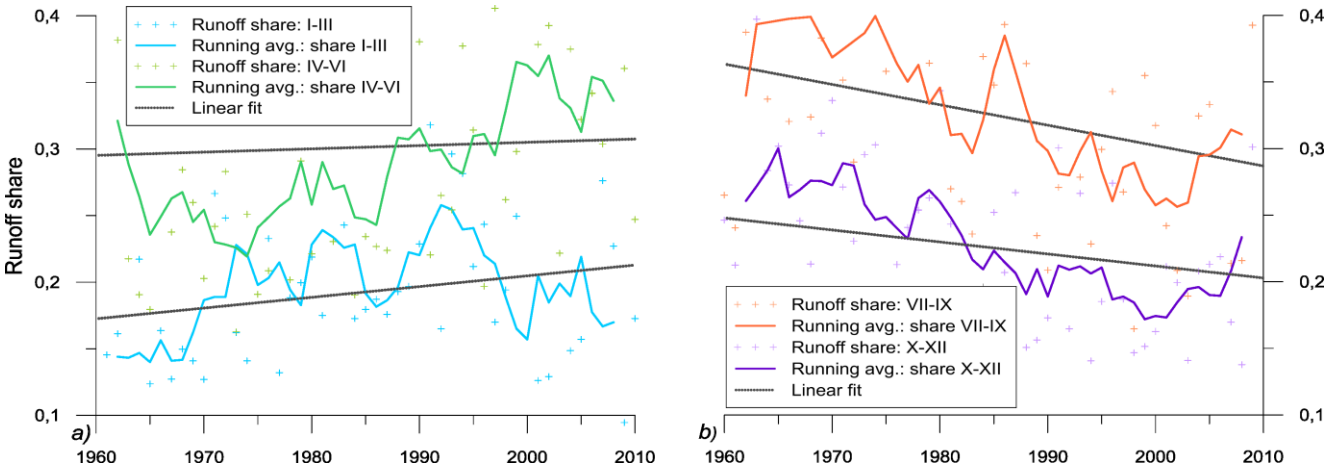

Figure 7. Changes in seasonal distribution of runoff in period 1961-2010 expressed as shares on total yearly balance: (**a**) shares of winter (I-III) and spring (IV-VI); and (**b**) shares of summer (VII-IX) and fall (IX-XII).

3.3 Variability and seasonality of peak flows and low flows

The peak flow (POT) and low flow (LOF) events were evaluated within the assessed period in order to understand the frequency of extreme flow events and the seasonality of their occurrences.

3.1.1. Peak flows

Concerning the regime of the POT event, the average number of days with POT was around 10 days per year (Figure 8a). Before the 1980s, the number of days with POT had a sharp decline; while afterwards, the number of days with POT had a continuous rising trend. The POT events increased from around 4 events (1961-1980) to 5 events (1981-2010) per year, and after 2000, the frequency has almost doubled to 7 events compared to the average events during 1961-1980. Furthermore, the average duration of POT over time has slightly decreased (the average duration of each POT event decreased from 2.5 days in 1961-1980 to 2.2 days in 1981-2010, supplementary material, Figure S1), although the average frequency of POT has increased. Such change in peak flow regime implies that the increasing number of days with POT in the last 30 years was generated by a rising number of short peak flow events.

The changes of peak flow frequency have a counterpart in shifts of seasonality of their occurrences. The pattern of peak flows is indicated in Figure 8b and the majority of POT events were related to the late winter (round Day of the Year (DoY) 90 in March), and the spring snow melting season (around DoY 120 in April and DoY 150 in May). However, there is a clear shift in seasonality from mid-spring (around DoY 150) towards early spring (around DoY 90- DoY 120) since the 1980s (Figure 8b). Specifically, in 1961-1970, there were 98 days with POT recorded in May, occupying 64% of the total 136 POT days. Since the 1980s, the shift in seasonality is distinctly apparent, and during 2001-2010, the average number of POT days in May was occupying just 20% of a total of 161 POT days. The POT events thus tend to occur earlier in the spring season, which corresponds with findings on changes in air temperature seasonal distribution.

3.1.1. Low flows

The substantial change of low flow regimes have been found (Figure 8a). In the 1960s, there were 42 LOF events with total duration of 527 days. Since the 1970s, there were only 11 LOF events with total duration of 138 days and only 11 LOF events with total duration of 57 days in the 1980s (supplementary material, Figure S2). However, at the end of the 1990s, there has been an apparent rise in low flow frequency, as in 2001-2010. There were detected 27 LOF events covering the period of 250 days.

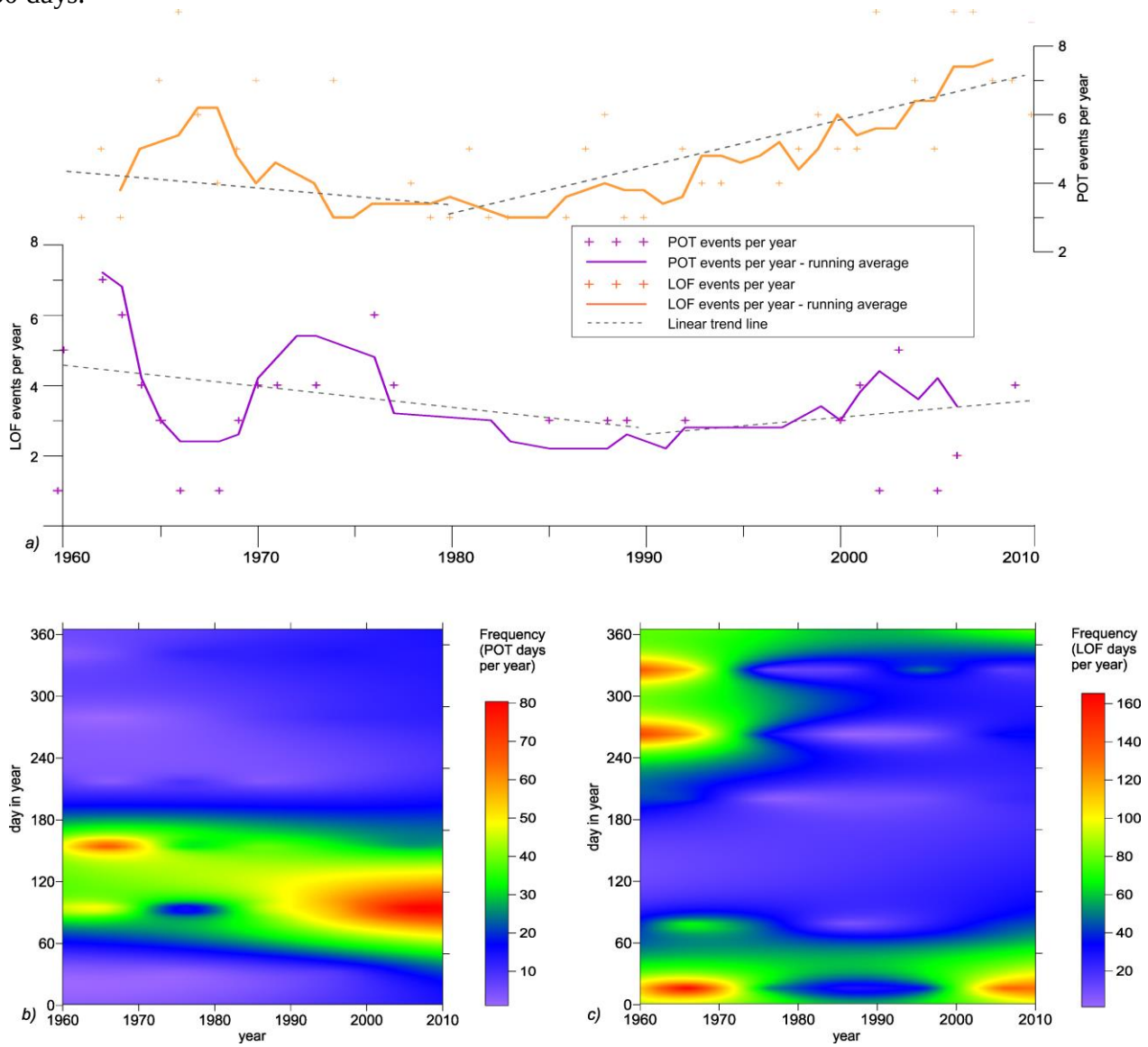

Figure 8. Patterns of frequency and seasonality of peak and low flows during 1961-2010: (**a**) Occurrence of peak flows events, (**b**) Changes in frequency and seasonality of days with POT; and (**c**) Changes in frequency and seasonality of days with LOF. The detailed duration, days, events of POT and LOF are given in the supplementary materials Figure S1 and Figure S2.

There has been observed two trends in LOF events duration (supplementary material, Figure S2): first, the decrease in the LOF event duration from an average of 14 days in the 1960s to 6 days in the 1980s; secondly, an apparent growth after 1990 in both the frequency and the average duration of LOF periods. Since 2000, the average duration of LOF events rose to around 12 days (Figure 8a) while this

decade includes the third-longest continuous LOF period of 77 days, recorded from January to March 2006.

The LOF occurrence has undergone a significant seasonal shift from autumn to mid-winter during 1960-2010 (Figure 8c). The three periods of LOF in the 1960s were typically distributed in early (DoY 330) and late (DoY 30) winters, and late summers (around DoY 270) and this LOF pattern has disappeared since the 1980s. After the 1990s, a new seasonal distribution pattern of low flows was concentrated in a single period during early winter (DoY 30), and the frequency of LOT was lower than in the 1960s.

3.4 The change points of hydro-climatic variables

For finding the points of change in time series of the hydro-climatic conditions, the Buishand´s and Petitt´s tests were applied. Both tests delivered very similar results when the points of change were detected for the same indicator at the same year, although with different levels of significance. Table 3 listed indicators with detected point of change in time series (the rest of the assessed variables is provided in the supplementary materials Table S1 and Figure S3), where the calculated p-values were smaller than 0.05.

For the driving forces of hydro-climatic changes, the inhomogeneity in the observed time series was detected for air temperature and forest disturbance (Table 3). Both tests identified the point of change for air temperature to 1988, although the continuous rise is apparent since the 1980s (Figure 5). Time series of precipitation as the second key driver of hydro climatic properties is, conversely, identified as homogeneous (Table S1). The forest disturbance as third of the driving forces of changes started at the beginning of the 1990s and around 1995 reaches the peak. The point of change was identified differently by the two tests while Petitt´s test find the inhomogeneity at the beginning of the decisive phase of disturbance in 1987 and Buishand´s in its end in 1993 (Table 3).

Most of the indicators of runoff response, where the inhomogeneity was identified, have the point of change located in the 1980s, although there are some exceptions.

Among the indicators reflecting runoff balance, there is no apparent change in the mean or median yearly discharge values (Table S1). Significant inhomogeneity is, however, detected for the separated runoff components – the direct flow (in 1988) and baseflow index (in 1990) with p-value equal to 0,0001 (Table 3). The runoff variability, expressed as standard deviation of yearly mean discharge, has a change point located in 1985. The low flows (Q_{330d} and Q_{355d}) have turn point in time series in 1964, however with p-value slightly exceeding threshold of 0,05 (Table S1).

Among the indicators of runoff seasonality there is apparent inhomogeneity for the share of spring and fall season on yearly runoff. The spring share has a point of change earlier than other indicators - 1974, and the fall share in 1981 (Table 3).

Large inhomogeneity was detected in series of LOF days and POT events. Number of LOF days has significant turn point in 1964. To the contrary, number of POT events has the turn point in 1994. In both indicators, the p-values were lower than 0,01. For other indicators of peak flows and low flows the time series were assessed as homogeneous although for some (POT days, LOF events) the p-values were close to the threshold.

Table 3. Inhomogeneities in the assessed hydro-climatic variables and their driving forces with change points identified by Buishand´s and Petitt´s tests.

	Buishand´s test			**Petitt´s test**		
Variables	Year of change	p-value	Δ	Year of change	p-value	Δ
Air temperature [^{o}C]	1988	0,0001	+ 0, 94	1988	0,0001	+ 0, 94
Deforested area [%]	1993	0,008	+0,31	1987	0,0001	+0,22
Direct runoff [$m^3 s^{-1}$]	1988	0,0001	- 0,09	1988	0,0001	- 0,09
Baseflow index [-]	1990	0,0001	+ 0,04	1990	0,0001	+ 0,04
Qd stand. deviation [-]	1985	0,016	+ 0,85	1985	0,025	+ 0,85
Runoff share-spring [%]	1974	0,030	+ 0,06	1974	0,016	+ 0,06
Runoff share-fall [%]	1981	0,002	- 0,06	1981	0,001	- 0,06
POT events [-]	1994	0,007	+ 2,30	1991	0,011	+ 2,08
LOF days [days]	1964	0,0001	- 82,03	1964	0,049	- 82,03

Note: Δ = mean value after change – mean value before change ("+" denotes positve change and "–" denotes negative change).

4. Discussion

The observed trends and variations of runoff response in the assessed basin can be discussed in the view of the key driving forces altering the hydrological processes in the area which are climate changes and forest disturbance as well the effect of spatial scale of observation, which is vital for understanding and interpretation of changes.

The analysis of historical climate parameters, stemming from the reanalysis of the 20th century by the global climate model, and the observed long-term data together showed the same trend of increasing air temperature in the study region since the 1980s (Figure 2) and the identified change year is 1988 (Table 3). However, the warming climate have not altered the upper Vydra basin's annual water balance based on the double mass curve in Figure 4 and the annual mean discharge in Table 2.

The seasonal and monthly precipitation and runoff trends were detected by the Mann-Kendall test (Table 2), and found the precipitation in winters (month of XI-I) had an increase, while a decrease in springs, especially in April. However, the runoff in April experienced an increase trend because of the seasonal runoff share substantially shifted from summer to spring (Figure 7). Such seasonal runoff shifts can be attributed to the rise in air temperature as the detected change of spring runoff share is located in 1974 corresponding to the climate pre-warmer window (Table 3). Since the warmer air in later winter triggers the snow melting process becoming earlier. The earlier melt could also explain the inconsistence of precipitation-runoff relation in April, and reconfirm the impact of the increasing temperature on the early spring hydrological regime. The decreased direct runoff (Figure 5) has been targeted at its changing year in 1988 (Table 3), which lies at the same time as the observed rise of air temperature.

Forest disturbance changes the functionality of the vegetation as well as the land cover, which could alter the runoff generation process and the runoff regimes. Especially, the study area is covered by the

coniferous forest, the canopy of which can efficiently intercept precipitation, especially in the form of snow. The intercepted rainwater or snow directly control water losses through sublimation governed by radiation fluxes [53,54]. Therefore, during a snow-melting period, forest decline or forest disturbance led to an increase in the frequency and magnitude of high flows [18,54]. In the studied basin, after the forest disturbance a similar winter runoff regime has been detected that the days of the POT has increased and shifted in the same periods (Figure 8a and Table S1).

The disturbed forest could decrease water losses from vegetation evapotranspiration, and increase the groundwater storage [55]. However, those two indicators are the most uncertain components of the water balance because they are difficult to measure and quantify in space and time. The impact of the forest canopy loss after insect-induced disturbance on the significant decrease of evaporation and the rise of the soil moisture, groundwater storage and groundwater recharge were identified by studies at the stand-level as well as at the level of watersheds [56,57]. Bearup et al. [58] used a three-component isotope hydrograph separation techniques identified a significant increase of the runoff contribution was from groundwater storage in the growing season, however, they concluded that the mechanism on basin-scale effect of the bark beetle infestation on the hydrological cycle still remains relatively unknown. The rising trend of baseflow index gained from a two parameter recursive digital filter hydrograph separation technique (Figure 5) has been targeted at its changing year in 1990 (Table 3), which coincides with the period when the forest disturbance occurred in the basin (Figure 2). The sharp increase of the baseflow since the 2000 might be attributed to the loss of evaporation of forest cover resulting from the extensive forest disturbance since the mid of the 1990s.

On the other hand, different changes of high flows and low flows in deforested or forest cover decline basins have been found in many studies. One type of response claimed that high flows may be enhanced by deforestation/ forest cover decline [14,16,21,59], while other studies suggest that high flow may be reduced by reforestation [60,61]. In this studied basin, along with the severe declining of the forest cover induced by bark beetle infestation from 1980 to 2010, apparent changes in high flow were found from in many aspects: more days and events with POT, higher frequency of the short high flow days, and larger variability of the POT event duration (Figure 7a and supplementary material, Figure S1).

The impacts of the natural forest disturbance on hydrological regimes have been widely studied in different regions with different spatial scales. The spatial scale of the assessment is apparently one of the key factors affecting interpretation of the underlying processes. A number of studies have been done to analyze the impact of forest harvesting and clear-cutting on annual runoff and most of them agreed that the runoff will be impacted less by increasing the size of the basin [9,25]. At different scales of observation, there can be different importance of individual driving processes and factors identified. In small homogeneous catchments, the effect of forces acting in large-scale can be overridden by local factors. This has been demonstrated at the study of runoff changes at three experimental micro-catchments in the Bohemian Massif [62] where the diverging trends in runoff response in the period of 1990-2007 was attributed rather to highly diverging physiographic conditions than to forest disturbance. This may result in missing the “big picture” by being focused on the high level of spatial detail. By contrast, in complex and heterogeneous basins the mixture of drivers, which have often undergone a contradictory effect that may hinder the identification of leading forces in the process of change.

5. Conclusions

The study analyzed runoff changes in the montane mid-latitude environment in the example of a mid-montane basin of the upper Vydra in the Sumava Mountains, Central Europe. The study area has undergone significant rise of the observed air temperatures since the 1980s and the extensive forest disturbance and decay since the 1990s.

The observed changes in hydrological response are complex and are apparent in different aspects of the runoff regime. The runoff balance has no apparent change over the assessed period. However, there was detected diverging trend of the baseflow and direct runoff share on the total flow. The rise of baseflow index since 1980s and accelerated in 2000 is followed by the rise of intra-annual runoff variability in the same time scale. Furthermore, there was detected substantial seasonal shift in the share of total runoff from the summers (decreasing from nearly 40% to 28%) to springs (with a 10% increase, as well as in the distribution and frequency of peak and low flows. The occurrence of peak flow events doubled since the 1980s with a shift of frequency from late spring towards the early spring/late winter. The occurrence of low flow days has a seasonal shift from autumn to mid-winter, and experienced a decrease (from 60 days per year down to 20 days), and followed by an increase in both days durations since 1990.

The extent of changes and correspondence of their timing with observed air temperature rise and forest disturbance implies a relationship with the identified changes and the changing environment. Despite the unchanged annual runoff balance the substantial shifts in runoff variability and seasonal distribution as well as the changes in frequency and seasonal patterns of peak ad low flows are notable and are indicating substantial changes in the hydrological behavior of the basin. The environment of the mid-latitude montane basin proved to be very sensitive to climate changes as well as to the changes in land cover. The scope and extent of changes, apparent at the basin scale, are also vital information for efficient water management and conservation of montane catchments.

Acknowledgments

The research was supported by Czech Science Foundation, the research project GAČR P209/12/0997 "The impact of landscape disturbance on the dynamics of fluvial processes".

Author Contributions

Jakub Langhammer has designed the study, selected data and performed analyses of runoff balance and variability, baseflow separation, and patterns of changes in runoff seasonality and peak/low flow distribution. Ye Su prepared methodology, analyzed hydro-climatic parameters, AET and runoff variability. Jana Bernsteinová analyzed peak and low flows distribution and seasonality. The authors have equally contributed to data interpretation and formulation of conclusions.

Conflicts of Interest

The authors declare no conflict of interest.

References

1. Burn, D.H.; Elnur, M.A.H. Detection of hydrologic trends and variability. *Journal of Hydrology* **2002**, *255*, 107-122.
2. IPCC. *Summary for policymakers*; Cambridge University Press: Cambridge, United Kingdom and New York, NY, USA, 2013; pp 19-23.
3. Kliment, Z.; Matouskova, M. Runoff changes in the Sumava mountains (Black Forest) and the foothill regions: Extent of influence by human impact and climate change. *Water Resour Manag* **2009**, *23*, 1813-1834.
4. Wei, X.; Liu, W.; Zhou, P. Quantifying the relative contributions of forest change and climatic variability to hydrology in large watersheds: A critical review of research methods. *Water* **2013**, *5*, 728-746.
5. Al-Faraj, F.A.; Scholz, M.; Tigkas, D. Sensitivity of surface runoff to drought and climate change: Application for shared river basins. *Water* **2014**, *6*, 3033-3048.
6. Dam, J.C. *Impacts of climate change and variability on hydrological regimes*. Cambridge Univeristy Press: Cambridge, U. K., 1999.
7. Dvorak, V.; Hladny, J.; Kasparek, L. Climate change hydrology and water resources impact and adaptation for selected river basins in the Czech republic. *Climatic Change* **1997**, *36*, 93-106.
8. Li, F.; Zhang, G.; Xu, Y. Separating the impacts of climate variation and human activities on runoff in the Songhua River basin, northeast China. *Water* **2014**, *6*, 3320-3338.
9. Blöschl, G.; Ardoin-Bardin, S.; Bonell, M.; Dorninger, M.; Goodrich, D.; Gutknecht, D.; Matamoros, D.; Merz, B.; Shand, P.; Szolgay, J. At what scales do climate variability and land cover change impact on flooding and low flows? *Hydrological Processes* **2007**, *21*, 1241-1247.
10. Tomer, M.D.; Schilling, K.E. A simple approach to distinguish land-use and climate-change effects on watershed hydrology. *Journal of Hydrology* **2009**, *376*, 24-33.
11. Zheng, H.; Zhang, L.; Zhu, R.; Liu, C.; Sato, Y.; Fukushima, Y. Responses of streamflow to climate and land surface change in the headwaters of the yellow river basin. *Water Resources Research* **2009**, *45*, W00A19.
12. Palamuleni, L.; Ndomba, P.; Annegarn, H. Evaluating land cover change and its impact on hydrological regime in upper Shire River catchment, Malawi. *Reg Environ Change* **2011**, *11*, 845-855.
13. Ma, X.; Xu, J.; van Noordwijk, M. Sensitivity of streamflow from a himalayan catchment to plausible changes in land cover and climate. *Hydrological Processes* **2010**, *24*, 1379-1390.
14. Dung, B.X.; Gomi, T.; Miyata, S.; Sidle, R.C.; Kosugi, K.; Onda, Y. Runoff responses to forest thinning at plot and catchment scales in a headwater catchment draining japanese cypress forest. *Journal of Hydrology* **2012**, *444*, 51-62.
15. Bosch, J.M.; Hewlett, J.D. A review of catchment experiments to determine the effect of vegetation changes on water yield and evapotranspiration. *Journal of Hydrology* **1982**, *55*, 3-23.
16. Ide, J.; Finer, L.; Lauren, A.; Piirainen, S.; Launiainen, S. Effects of clear-cutting on annual and seasonal runoff from a boreal forest catchment in eastern Finland. *Forest Ecology and Management* **2013**, *304*, 482-491.

17. Buttle, J.M.; Metcalfe, R.A. Boreal forest disturbance and streamflow response, northeastern Ontario. *Canadian Journal of Fisheries and Aquatic Sciences* **2000**, *57*, 5-18.
18. Beudert, B.; Klöcking, B.; Marcq, B.; Niederberger, J.; Puhlmann, H.; Schwarze, R.; Wilpert, K.-H.v. *Forest hydrology-results of research in germany and russia*; ihp.hwrp Germany: Koblenz, 2007; p 131.
19. Pomeroy, J.; Fang, X.; Ellis, C. Sensitivity of snowmelt hydrology in Marmot creek, Alberta, to forest cover disturbance. *Hydrological Processes* **2012**, *26*, 1891-1904.
20. Troendle, C.A.; Reuss, J.O. Effect of clearcutting on snow accumulation and water outflow at Fraser, Colorado. *Hydrol Earth Syst Sc* **1997**, *I* 325-332.
21. Kuraś, P.K.; Alila, Y.; Weiler, M. Forest harvesting effects on the magnitude and frequency of peak flows can increase with return period. *Water Resources Research* **2012**, *48*, W01544.
22. Robinson, M.; Cognard-Plancq, A.-L.; Cosandey, C.; David, J.; Durand, P.; Führer, H.-W.; Hall, R.; Hendriques, M.; Marc, V.; McCarthy, R. Studies of the impact of forests on peak flows and baseflows: A European perspective. *Forest Ecology and Management* **2003**, *186*, 85-97.
23. Brown, A.E.; Western, A.W.; McMahon, T.A.; Zhang, L. Impact of forest cover changes on annual streamflow and flow duration curves. *Journal of Hydrology* **2013**, *483*, 39-50.
24. Rex, J.; Dubé, S.; Foord, V. Mountain pine beetles, salvage logging, and hydrologic change: Predicting wet ground areas. *Water* **2013**, *5*, 443-461.
25. Zhang, M.; Wei, X. The effects of cumulative forest disturbance on streamflow in a large watershed in the central interior of British Columbia, Canada. *Hydrol Earth Syst Sc* **2012**, *16*, 2021-2034.
26. Zemek, F.; Herman, M. Bark beetle - a stress factor of spruce forests in the Bohemian Forest. *Ekologia-Bratislava* **2001**, *20*, 95-107.
27. Stednick, J.D. Monitoring the effects of timber harvest on annual water yield. *Journal of Hydrology* **1996**, *176*, 79-95.
28. Hais, M.; Jonášová, M.; Langhammer, J.; Kučera, T. Comparison of two types of forest disturbance using multitemporal landsat tm/etm+ imagery and field vegetation data. *Remote Sensing of Environment* **2009**, *113*, 835-845.
29. Birsan, M.-V.; Molnar, P.; Burlando, P.; Pfaundler, M. Streamflow trends in switzerland. *Journal of Hydrology* **2005**, *314*, 312-329.
30. Vacek, S.; Podrazsky, V. Forest ecosystems of the Sumava mts. and their management. *Journal of Forest Science* **2003**, *49*, 291-301.
31. ČHMÚ. *Climatic atlas of czechia*. ČHMÚ: Prague, 2007; p256.
32. Čurda, J.; Janský, B.; Kocum, J. The effects of physical-geographic factors on flood episodes extremity in the Vydra river basin. *Geografie* **2011**, *116*, 335-353.
33. Křenová, Z.; Hruška, J. Proper zonation – an essential tool for the future conservation of the Sumava national park. *European Journal of Environmental Sciences* **2012**, *2*, 62-72.
34. CHMI. *Precipitation and runoff database*. CHMI: Prague, 2013.
35. NOAA. CM2.X model datasets. http://nomads.gfdl.noaa.gov/CM2.X/ (accessed on 05.12.2014)
36. UNCAR. *IDV data viewer*; http://www.unidata.ucar.edu/software/idv/index.html (accessed on 05.12.2014
37. CUZK. *4G digital elevation model*. CUZK: Prague, 2013.

38. WRI. DIBAVOD. *Digital Water Management Map, Prague, VUV TGM*. http://www.dibavod.cz/ (accessed on 05.10.2014)
39. UHUL. Maps of the health condition of Czech Republic forests based on satellite images. *Map of defoliation and mortality of coniferous forests*. http://geoportal2.uhul.cz/cgi-bin/landsat.asp (accessed on 15.11.2014)
40. Hamed, K.H. Trend detection in hydrologic data: The mann–kendall trend test under the scaling hypothesis. *Journal of Hydrology* **2008**, *349*, 350-363.
41. Eckhardt, K. How to construct recursive digital filters for baseflow separation. *Hydrological Processes* **2005**, *19*, 507-515.
42. Nathan, R.; McMahon, T. Evaluation of automated techniques for base flow and recession analyses. *Water Resources Research* **1990**, *26*, 1465-1473.
43. Lim, K.J.; Engel, B.A.; Tang, Z.; Choi, J.; Kim, K.S.; Muthukrishnan, S.; Tripathy, D. Automated web GIS based hydrograph analysis tool, WHAT1. Wiley Online Library: 2005.
44. Turc, L. The water balance of soils, relation between precipitation evaporation and flow. *Ann. Agron.* **1954**, *5*, 491–569.
45. Langbein, W.B. Annual runoff in the United States. *US Geological Survey Circular* **1949**, *52*, 14.
46. Chen, X.C.; Steinhaeuser, K.; Boriah, S.; Chatterjee, S.; Kumar, V. In *Contextual time series change detection*, SDM, 2013; SIAM: pp 503-511.
47. Jessop, B.M.; Harvie, C.J. A CUSUM analysis of discharge patterns by a hydroelectric dam and discussion of potential effects on the upstream migration of american eel elvers. **2003**.
48. Buishand, T.A. Some methods for testing the homogeneity of rainfall records. *Journal of Hydrology* **1982**, *58*, 11-27.
49. Machiwal, D.; Jha, M. Efficacy of time series tests: A critical assessment. In *Hydrologic time series analysis: Theory and practice*, Springer Netherlands: 2012; pp 139-164.
50. Taxak, A.K.; Murumkar, A.; Arya, D. Long term spatial and temporal rainfall trends and homogeneity analysis in Wainganga basin, central India. *Weather and Climate Extremes* **2014**, *4*, 50-61.
51. Costa, A.C.; Soares, A. Homogenization of climate data: Review and new perspectives using geostatistics. *Mathematical Geosciences* **2009**, *41*, 291-305.
52. Kang, H.M.; Yusof, F. Homogeneity tests on daily rainfall series. *Int. J. Contemp. Math. Sciences* **2012**, *7*, 9-22.
53. Lundberg, A.; Nakai, Y.; Thunehed, H.; Halldin, S. Snow accumulation in forests from ground and remote-sensing data. *Hydrological Processes* **2004**, *18*, 1941-1955.
54. Schnorbus, M.; Werner, A.; Bennett, K. *Quantifying the water resource impacts of mountain pine beetle and associated salvage harvest operations across a range of watershed scales: Hydrologic modeling of the fraser river basin*. Pacific Forestry Centre: 2010; 423.
55. Ogden, F.L.; Crouch, T.D.; Stallard, R.F.; Hall, J.S. Effect of land cover and use on dry season river runoff, runoff efficiency, and peak storm runoff in the seasonal tropics of central Panama. *Water Resources Research* **2013**, *49*, 8443-8462.
56. Redding, T.; Lapp, S.; Leach, J. Natural disturbance and post-disturbance management effects on selected watershed values. *Journal of Ecosystems and Management* **2012**, *13*.

57. Smerdon, B.D.; Redding, T.; Beckers, J. An overview of the effects of forest management on groundwater hydrology. *Journal of Ecosystems and Management* **2009**, *10*.
58. Bearup, L.A.; Maxwell, R.M.; Clow, D.W.; McCray, J.E. Hydrological effects of forest transpiration loss in bark beetle-impacted watersheds. *Nature Clim. Change* **2014**, *4*, 481-486.
59. Jones, J.A. Hydrologic processes and peak discharge response to forest removal, regrowth, and roads in 10 small experimental basins, Western Cascades, Oregon. *Water Resources Research* **2000**, *36*, 2621-2642.
60. Waterloo, M.J.; Schellekens, J. ; Bruijnzeel, L.A.; T., R.T. Changes in catchment runoff after harvesting and burning of a Pinus Caribaea plantation in Viti Levu, Fiji. . *Ecological Management* **2007**, *251*, 31-44.
61. Ogden, F.L.; Crouch, T.D.; Stallard, R.F.; Hall, J.S. Effect of land cover and use on dry season river runoff, runoff efficiency, and peak storm runoff in the seasonal tropics of central Panama. *Water Resources Research* **2013**, 49,8443–8462.
62. Krám, P., Beudert, B., Červenková, J., Čech, J., Váňa, M., Fottová, D., Dieffenbach-Fries, H. . Daily streamwater runoff characteristics of the ICP IM catchments (CZ01, CZ02, DE01) in the Bohemian massif. *The Finnish Environment* **2008**, *28*, 39-46.

Supplementary materials

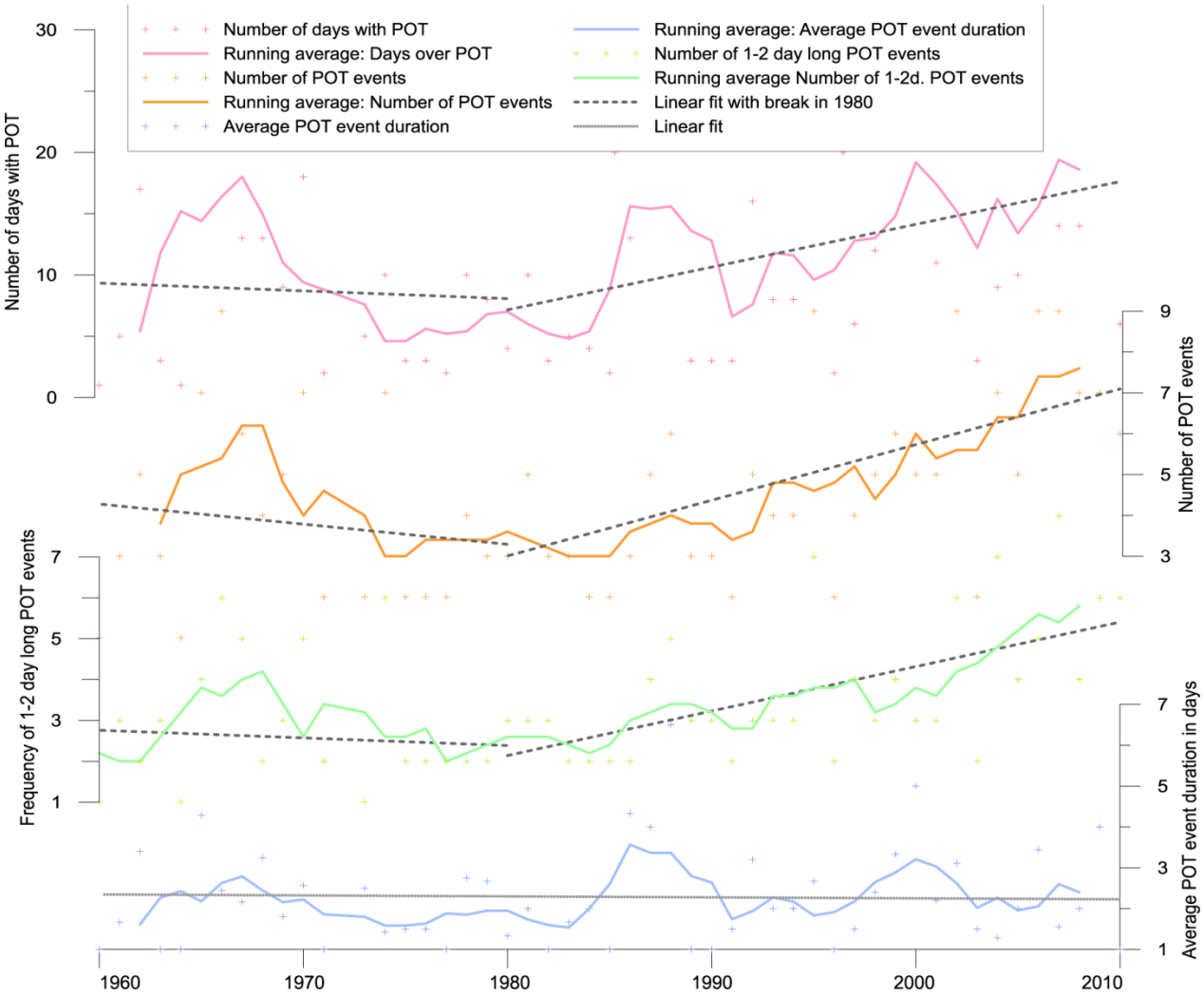

Figure S1 Changing frequency and duration of peak flow events.

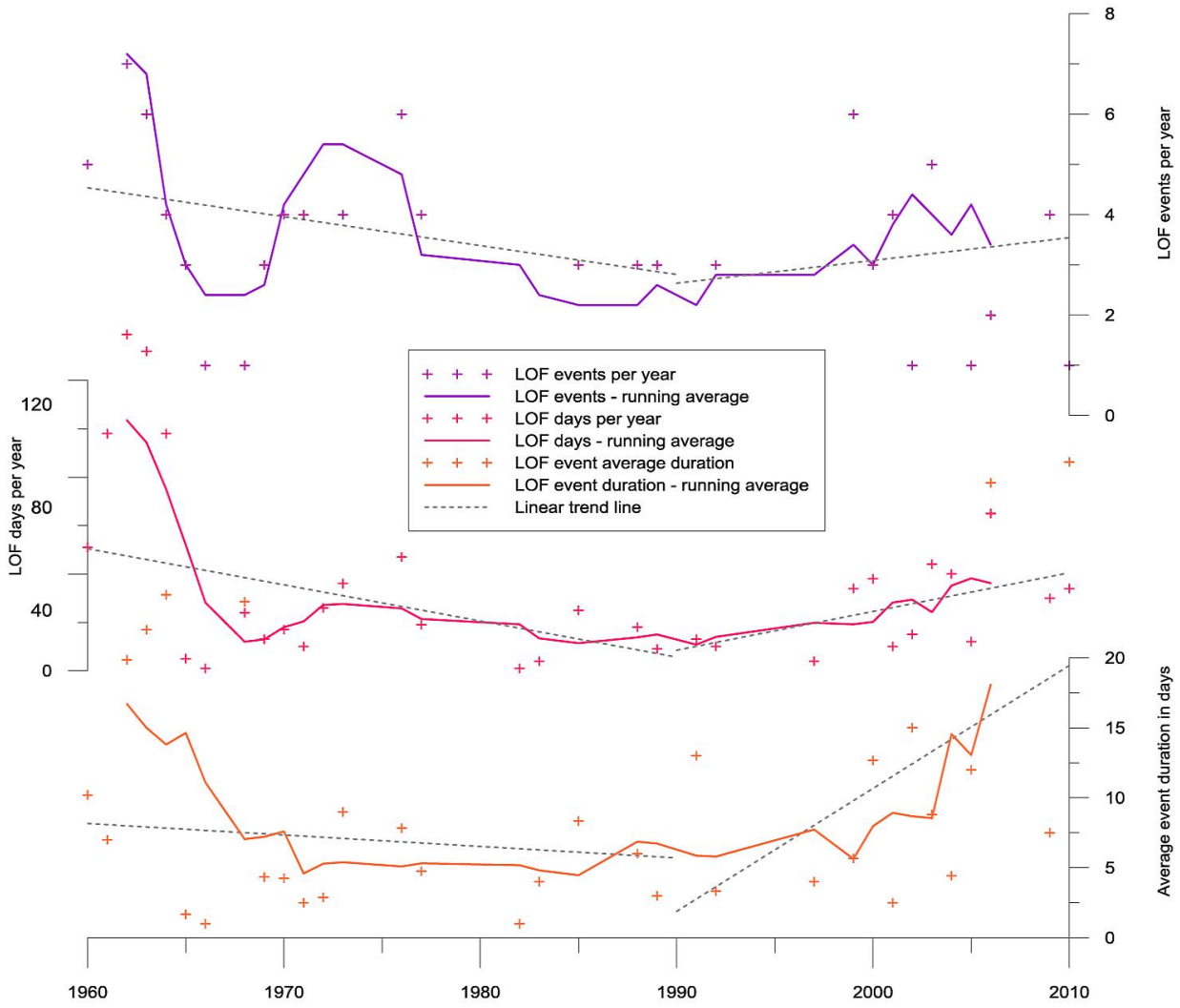

Figure S2 Changing frequency and duration of low flow events.

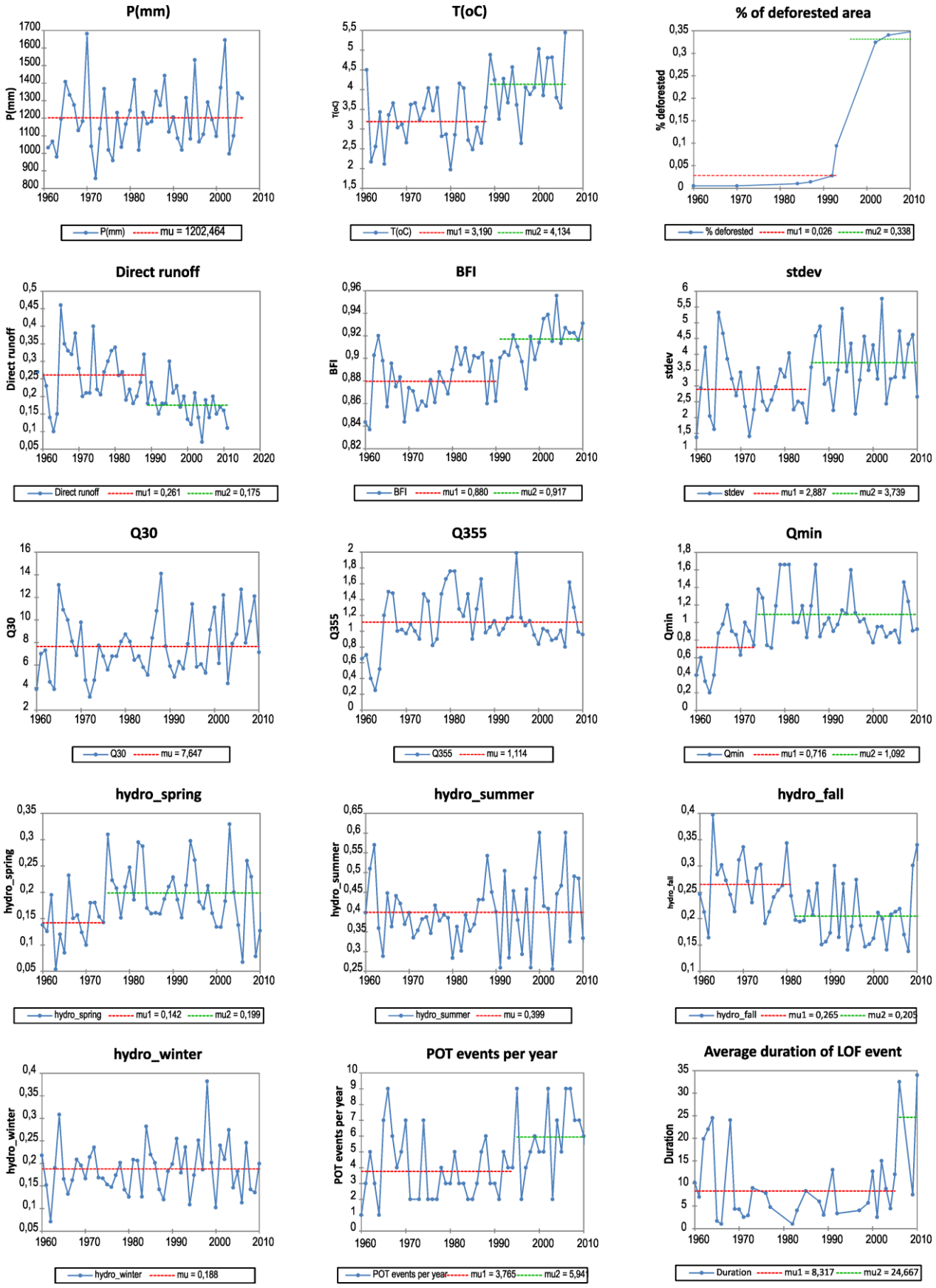

Figure S3 Test of homogeneity. Plots of variables with marked points of changes and lines of mean values for pre-change (mu1) and post-change (mu2) period according the Buishand´s test.

Table S1 Homogeneity tests and detection of change points in the assessed indicators using Buishands´s and Petitt´s tests.

		Buishand´s test						**Petitt´s test**					
	Variable	*p-value*	*test result*	*t date of change*	*risk of H0 rejection*	*mu1*	*mu2*	*p-value*	*test result*	*t date of change*	*risk of H0 rejection*	*mu1*	*mu2*
driving forces	Precipitation	0,714	H0	1974	71,4%			0,583	H0	1979	58,3%		
	Air temperature	**0,0001**	**Ha**	**1988**	**0,01%**	**3,19**	**4,134**	**0,0001**	**Ha**	**1988**	**0,01%**	**3,19**	**4,134**
	Deforested area	**0,008**	**Ha**	**1993**	**0,8%**	**0,026**	**0,338**	**0,0001**	**Ha**	**1987**	**0,01%**	**0,008**	**0,227**
runoff balance	Qy	0,152	H0	1965	15,2%			0,161	H0	1965	16,1%		
	Qmedian	0,38	H0	1964	38,0%			0,202	H0	1964	20,2%		
	Direct runoff	**0,0001**	**Ha**	**1988**	**0,0%**	**0,261**	**0,175**	**0,0001**		**1988**	**0,01%**	**0,261**	**0,175**
	Baseflow index (BFI)	**0,0001**	**Ha**	**1990**	**0,0%**	**0,88**	**0,917**	**0,0001**	**Ha**	**1990**	**0,01%**	**0,88**	**0,917**
runoff variability	Q30	0,202	H0	1985	20,2%			0,205	H0	1998	20,5%		
	Q330	0,064	H0	1964	6,4%			0,134	H0	1964	13,4%		
	Q355	*0,055*	*H0*	*1964*	*5,5%*			0,134	H0	1964	13,4%		
	SD	**0,016**	**Ha**	**1985**	**1,6%**	**2,887**	**3,739**	**0,025**	**Ha**	**1985**	**2,5%**	**2,887**	**3,739**
runoff seasonality	**Spring share**	**0,03**	**Ha**	**1974**	**3,0%**	**0,142**	**0,199**	**0,016**	**Ha**	**1974**	**1,6%**	**0,142**	**0,199**
	Summer share	0,594	H0	1998	59,4%			0,513	H0	1985	51,3%	-	-
	Fall share	**0,002**	**Ha**	**1981**	**0,2%**	**0,265**	**0,205**	**0,001**	**Ha**	**1981**	**0,1%**	**0,265**	**0,205**
	Winter share	0,693	H0	1983	69,3%			0,655	H0	1983	65,5%		
peak flows and low flows	**POT events**	**0,007**	**Ha**	**1994**	**0,7%**	**3,765**	**6,063**	**0,011**	**Ha**	**1991**	**1,1%**	**3,71**	**5,789**
	POT days	0,125	H0	1985	12,5%			*0,08*	*H0*	*1985*	*8,0%*		
	POT event duration	0,277	H0	1985	27,7%			0,492	H0	1985	49,2%		
	LOF events	0,128	H0	1977	12,8%			*0,069*	*H0*	*1977*	*6,9%*		
	LOF days	**0,0001**	**Ha**	**1964**	**0,0%**	**103,6**	**21,571**	**0,049**	**H0**	**1964**	**4,9%**	**103,6**	**21,571**
	LOF event duration	0,251	H0	2004	25,1%			0,294	H0	2001	29,4%		